BIOPHYSICS AND BIOCHEMISTRY OF RECEPTOR-LIGAND MEDIATED ADHESION TO THE ENDOTHELIUM

A dissertation presented to

the faculty of

the Russ College of Engineering and Technology of Ohio University

In partial fulfillment

of the requirements for the degree

Doctor of Philosophy

Vivek R. Shinde Patil

June 2002

This dissertation entitled

BIOPHYSICS AND BIOCHEMISTRY OF RECEPTOR-LIGAND MEDIATED ADHESION TO THE ENDOTHELIUM

BY

VIVEK R. SHINDE PATIL

has been approved for

the Department of Chemical Engineering

and the Russ College of Engineering and Technology by

Douglas J. Goetz

Assistant Professor of Chemical Engineering

Jerrel R. Mitchell

Interim Dean, Russ College of Engineering and Technology

SHINDE PATIL, VIVEK R. Ph.D. June 2002. Chemical Engineering

Biophysics and Biochemistry of Receptor-Ligand Mediated Adhesion to the Endothelium

(188 pp.)

Director of Dissertation: Douglas J. Goetz

The circulatory system consists of blood flowing through an intricate network of blood vessels, whose inner lining is composed of endothelial cells, collectively known as the vascular endothelium. Blood is composed of formed elements (blood cells and platelets) suspended in a saline solution containing dissolved proteins and other solutes. Molecular interactions between *receptors* expressed on the vascular endothelium and *ligands* expressed on the formed elements play a critical role in a variety of physiological and pathological processes. Well-known examples include, leukocyte recruitment and platelet deposition at sites of tissue injury, tumor metastasis and atherosclerosis. Since this adhesion occurs in the fluid dynamic environment of circulation, it is paramount to study vascular adhesion from both a biological and an engineering standpoint.

There is a distinct possibility that differences in the diameters of formed elements affect their adhesion and consequently, their function. This motivates a study into the role of particle diameter in receptor-ligand mediated adhesion. Our results clearly demonstrate that adhesion is strongly dependent on particle size and provide experimental proof for mathematical models linking particle size to adhesion.

The *selectin* and *integrin* families of cell adhesion molecules play a key role in orchestrating leukocyte recruitment to sites of inflammation. In a separate study, we examine molecular interactions between the leukocyte *integrin* Mac-1 (CD11b/CD18), and endothelial cells under flow. Our results reveal that Mac-1 coated microspheres adhere to endothelial cells via E-selectin and an additional mechanism that perhaps involves a yet unidentified endothelial receptor.

Motivated by a desire to further the understanding of leukocyte recruitment and hematopoietic progenitor cell (HPC) entry into bone marrow, numerous studies have focused on identifying ligands for E-selectin on a specific HPC cell line, namely HL60 cells. These previous reports both support and refute the ability of HL60 cell expressed P-selectin glycoprotein ligand (PSGL-1) to serve as an E-selectin ligand. Our third study provides evidence that PSGL-1 can, in fact, support attachment of HL60 cells to endothelial E-selectin under flow.

Taken together, these three studies contribute to the understanding of the biochemistry and biophysics of receptor-ligand mediated adhesion to the endothelium.

Approved: Douglas J. Goetz

Assistant Professor of Chemical Engineering

To my parents

Acknowledgments

I would like to thank my advisor Dr. Douglas J. Goetz, for his guidance, patience and help. I would like to thank the other committee members, Drs. Kendree Sampson, Darin Ridgway and Frank Horodyski for their insightful comments and assistance. I would like to thank my parents, Ranjit and Mrunalini Shinde Patil, for their moral support and encouragement. I would also like to thank Lee Smith, Chris Lloyd and Maureen Wargo for their help with some of the experimentation. Finally, I would like to thank Terry and Michael Marovich for their advice and never ending words of encouragement.

Table of Contents

List of Tables

Table Page

List of Figures

CHAPTER 1

AN OVERVIEW OF CELL ADHESION

The adhesive interactions between cells and interactions between cells and proteins within the extracellular matrix are crucial to cellular organization, structure, proliferation, metabolism and gene expression (1-5). From directing the migration of cells (6) involved in modeling the embryo during early embryological development (7, 8), to maintaining homeostasis (physiological balance) (9) and regulating host defenses in multicellular organisms (10), cell adhesion plays a pivotal role in numerous physiological and pathological processes.

Extensive research in the last few decades has highlighted the importance of the inner vascular (endothelial) lining (Figure 1.1) as an active participant in a variety of pathological and physiological processes. The human circulatory system consists of blood flowing through an intricate network of blood vessels such as arteries, capillaries, veins and venules, each with a distinct physiology and vessel diameter. The wide spectrum of wall shear stresses that are prevalent in the vascular network are attributed to differences in vessel cross-section and material properties of these vessels (Table 1) (11). Blood, may be loosely defined as a suspension of formed elements (blood cells and platelets) in a saline solution containing dissolved proteins and other solutes. The formed elements comprising of erythrocytes (red blood cells), leukocytes (white blood cells) and platelets, constitute around 45% of whole blood, while plasma (proteins and solutes)

accounts for the remaining 55% (Figure 1.1). A detailed listing of the cellular constituents of blood and its physical and chemical properties can be found at http://www.ent.ohiou.edu/~adhesion/

Vessel Type	**Vessel Diameter (cm)**	**Volumetric Flow rate (cm^3/sec)**	**Reynolds Number Re**	**Wall Shear Rate (s^{-1})**	**Wall Shear Stress ($dyne/cm^2$)**
Ascending aorta	2.3 - 4.5	100	800 - 1600	50 - 300	2 - 10
Femoral artery	0.5	4	280	325	11
Common carotid	0.6	5	300	235	8
Small arteries	0.03	4×10^{-3}	5	1500	53
Arterioles	3×10^{-3}	5×10^{-6}	4×10^{-2}	1900	60
Capillaries	6×10^{-4}	$0.8 - 6 \times 10^{-8}$	$0.4 - 3 \times 10^{-3}$	370 - 2800	-
Post capillary venules				35-560	1-20

Table 1.1. Physiological Flow Parameters of Human Circulation (11)

Any deviation from homeostasis, such as tissue injury or infection, precipitates an inflammatory response by the host (12, 13). Initial events in this inflammatory response include the recruitment (and stimulation) of polymorphonuclear leukocytes (PMNs) and platelets to sites of infection or tissue damage; their primary function being to localize and eradicate the irritant or source of infection and subsequently induce restoration of damaged tissue to its normal physiological state. In the event that this does not occur, the inflammation progresses to a chronic state. Chronic inflammation is

characterized by the recruitment of other leukocyte sub-types (e.g. lymphocytes and mononuclear phagocytic cells) that essentially continue where the PMNs left off and ensure complete eradication of the irritant (or pathogenic agent) and induction of tissue repair and restoration. Critical steps in the host's inflammatory response, including recruitment of PMNs and platelets during acute inflammation and subsequent trafficking of lymphocytes and macrophages during chronic inflammation, are all mediated through adhesive interactions between these respective cell types and the endothelium.

Aside from numerous physiological processes, a variety of pathological processes including cancer (14, 15) and atherosclerosis involve cell adhesion events. The occurrence of cancer is characterized by tumor invasion and metastasis, often attributed to a decrease in cell-cell and/or cell-matrix adhesion in tumors (16). This loss of adhesion results in the detachment of cancer cells from primary tumors. These detached cells might eventually enter the vasculature and travel in the bloodstream until they arrest within the vasculature of a secondary site. Subsequent to arrest, a cancer cell may transmigrate from this intra-vascular compartment into the extravascular space, where the cancer cell undergoes uncontrolled proliferation (16). Almost every aspect of the metastatic process including the development of primary tumors, the detachment of cancer cells from the primary tumor, and their subsequent arrest and transmigration from the vasculature at a secondary site, is mediated by adhesive interactions.

Another illustration of adhesion- mediated pathology includes atherosclerosis (13, 17). Presence of a variety of injurious agents (e.g. free radicals caused by cigarette smoking, modified low density lipoproteins (LDL), infectious organisms, etc.) is known to alter the normal hemostatic properties of the endothelium during the initial stages of atherosclerosis. A physiological inflammatory response to injury mediated by these agents often leads to endothelial dysfunction, causing an increase in the endothelium's adhesiveness for leukocytes (lymphocytes and monocytes) and an alteration of endothelial permeability. This continuing inflammatory response also results in the migration and proliferation of smooth-muscle cells from surrounding tissues to the lesion. This mass of different cell types, lipids and cell debris (necrotic core) is eventually sealed off with a fibrous cap that can either stay stable or undergo rupture. Rupture of this atherosclerotic plaque leads to severe injury of the intact endothelium and precipitates platelet aggregation. Extensive aggregation of platelets (i.e. thrombus formation) causes further intrusion of the plaque into the lumen and occlusion of the artery. This rupture of the plaque and eventual thrombosis accounts for as many as 50 percent of all acute coronary syndromes and heart attacks. It is clearly evident, that an interplay of adhesive interactions between different cell types and the endothelium mediates crucial events in the pathogenesis of atherosclerosis.

As mentioned in the above discussion, the recruitment of leukocytes and deposition of platelets at sites of tissue injury occurs largely through adhesive interactions between these respective cell types and the endothelial cell lining of the blood vessels. A

leukocyte, platelet, or for that matter any cell type adherent to the endothelium under physiological flow conditions is subjected to a *disruptive* fluid force and torque that is exerted by the flowing fluid on an adherent cell (18). For the cell adherent on the endothelium to be in mechanical equilibrium, this disruptive force and torque must be balanced by an opposing counteractive force, which in fact turns out to be an adhesive force mediated by bonds formed between adhesive *ligand* molecules on the adhering cell and complementary *receptor* molecules expressed on the endothelium.

Arguably, the two most important issues in studying cell adhesion are: (1) identifying the relevant endothelial receptors and cell ligands involved in different adhesion processes and (2) characterizing the biophysical attributes underlying these adhesion phenomena, some of which are outlined in Figure 1.2.

For the sake of simplicity, assume that the receptor-ligand pair(s) mediating a cellular-endothelial interaction is known. Having fixed the receptor-ligand chemistry, a simplified approach to studying biophysical attributes and their effect on adhesive mechanics would be to alter the *system parameters* (that are receptive to external control) outlined in Figure 1.2 and then study the *measurable adhesion response*. Inherent to this identified receptor-ligand pair are certain *biophysical parameters* including receptor-ligand kinetics, bond strength and response of the bonds to stress that are not susceptible to alteration. One could, however, alter *system parameters* that are prone to modulation such as ligand and receptor densities, radius of the particle, substrate type, degree of

disruptive force on the system and, material properties of the particle. Varying these parameters and studying their effect on rates of attachment, strength of adhesion and rolling velocities provide vital insights into the adhesive dynamics underlying the receptor-ligand mediated adhesion event.

A primary focus of this doctoral study is to investigate the role of one such system parameter, namely particle size, in receptor-ligand mediated adhesion. The motivation to undertake such a study (described in Chapter 2) on the role of particle diameter in adhesion stems from the following: (1) the relevant size range of cells which may adhere to the endothelium in the vasculature is quite broad (Figure 1.1), ranging from 2 μm (platelets) to 20 μm in diameter (the size of some metastasizing cancer cells), with leukocytes (7 - 20 μm) falling within this range. There is a distinct possibility that the size of these different cells affects their adhesion in the vasculature and consequently, their functionality. (b) Various theoretical models of adhesion have also predicted a relationship between particle size and adhesion (19, 20). In spite of these two compelling observations, there have been few experimental studies aimed at investigating the relationship between cell diameter and adhesion. Of most relevance is an initial study demonstrating that the adhesion of 5μm diameter ligand coated microspheres is different from 10 μm diameter microspheres under flow (21). In this dissertation, we sought to generalize this specific result by studying a range of particle sizes that span the spectrum of cell diameters that could be present in the vasculature. The results of this more

comprehensive study provide experimental proof for theoretical models that indicate a role for particle size in cell adhesion under flow.

Equally important to the study of cell adhesion is the identification of the repertoire of receptor-ligand pairs involved in mediating different adhesion processes discussed in the first few paragraphs of this chapter. This dissertation seeks to examine the roles played by two of these receptor-ligand pairs in mediating *one* specific well-characterized adhesion phenomena: the adhesion of leukocytes to the endothelium in the fluid dynamic environment of the circulatory system (22-25). During the past 15 years, it has been revealed that leukocyte adhesion to the endothelium occurs through a cascade of adhesive events (23, 25-29). A well-studied specific example is polymorphonuclear leukocyte (neutrophil) adhesion to the endothelium in the post-capillary venules during emigration. (Figure 1.3) Initially, neutrophils circulating in the blood attach to the endothelium from the free stream and begin to translate with a low velocity (roll) on the apical surface of the endothelium. Subsequent to attachment and rolling, the neutrophil may detach and release back into the bloodstream or the neutrophil may stop translating (arrest), spread and migrate between adjacent endothelial cells to reach the extravascular space (extravasate).

This entire process is orchestrated by a series of molecular interactions between the neutrophil and the endothelium. Taking cues from fundamental chemistry, researchers have modeled molecular interactions between receptors (R) on the endothelium and

ligands (L) on the neutrophil as reversible interactions of the type $L + R \leftrightarrow C$, where C is the receptor-ligand complex representing a non-covalent bond (30). Gaining an insight into the molecular attributes underlying neutrophil recruitment to the endothelium would not only require identification of the receptors (R) and ligands (L) involved, but also require estimating whether the bond formed between these molecular species has sufficient biophysical properties to mediate and sustain the adhesion under physiological flow.

Consequently, identification of the key (molecular) players in the neutrophil recruitment process (Figure 1.3) and their roles has been the major focus of a number of studies in the last two decades (23, 25-29). It is now well understood that the *selectin* family of cell adhesion molecules, namely E-selectin, P-selectin (expressed on endothelial cells) and L-selectin (expressed on leukocytes), are found to play a major role in mediating initial events in the neutrophil adhesion cascade, namely, neutrophil attachment and rolling. Subsequent to this, the neutrophil undergoes activation by sensing chemokines on the endothelium that causes upregulation and activation of an entirely separate family of adhesion molecules known as *integrins* on the neutrophil. The *integrins*, presented to endothelial counter-receptors in a functionally active 'able to bind' conformation (31), have been implicated in the latter steps of the neutrophil recruitment process, namely firm arrest, spreading and eventual extravasation. As stated previously, this dissertation seeks to highlight the role played by a member of the *integrin* family,

Mac-1 (CD11b/CD18; $\alpha_m\beta_2$) in mediating various aspects of the neutrophil adhesion cascade.

Using leukocyte-sized microspheres coated with the leukocyte β_2-integrin Mac-1, our laboratory has previously shown that the Mac-1-E-selectin bond has sufficient biophysical properties to mediate *attachment* of Mac-1 coated microspheres to E-selectin expressing cellular monolayers. Consistent with previous reports in the literature (32-35), subsequent studies in our laboratory suggested the presence of an additional mechanism via which Mac-1 mediates *firm adhesion* of these microspheres to activated endothelium. We therefore hypothesized that leukocyte-sized microspheres coated with Mac-1 could adhere to activated endothelial cells via two distinct mechanisms: one mediating attachment and rolling, and the other firm adhesion. We probed this hypothesis (described in Chapter 3) by studying the adhesion of Mac-1 coated microspheres to activated human umbilical vein endothelial cells in a physiologically relevant fluid dynamic environment.

In addition to mediating initial steps in neutrophil recruitment to sites of inflammation, selectins are also involved in the homing of hematopoietic progenitor cells (HPC) to bone marrow via interactions with corresponding ligands. Although, P-selectin glycoprotein ligand-1 (PSGL-1) is well established as a physiological ligand for P-selectin, its ability to serve as a corresponding ligand for E-selectin is still open to debate. There have been a number of studies, motivated by a desire to further our understanding

of HPC entry into bone marrow and leukocyte recruitment to a site of tissue injury that have focused on identifying counter-receptors for E-selectin on a specific HPC cell line, namely HL60 cells. This body of work has resulted in data both supporting and refuting the hypothesis that PSGL-1 is involved in HL60 cell adhesion to endothelial expressed E-selectin under flow (36-40). In Chapter 4, we probe the role of P-selectin-glycoprotein ligand-1 (PSGL-1) on HL60 cells in serving as a physiological ligand for E-selectin expressed on activated endothelium.

References

1. Parsons, J.T., K.H. Martin, J.K. Slack, J.M. Taylor, and S.A. Weed. 2000. Focal adhesion kinase: a regulator of focal adhesion dynamics and cell movement. *Oncogene*. 19: 5606-13.

2. Streuli, C.H., and A.P. Gilmore. 1999. Adhesion-mediated signaling in the regulation of mammary epithelial cell survival. *J Mammary Gland Biol Neoplasia*. 4:183-91.

3. Buckley, C.D., G.E. Rainger, P.F. Bradfield, G.B. Nash, and D.L. Simmons. 1998. Cell adhesion: more than just glue (review). *Mol Membr Biol*. 15:167-76.

4. Hynes, R.O. 1999. Cell adhesion: old and new questions. *Trends Cell Biol*. 9:M33-7.

5. Hynes, R.O., and A.D. Lander. 1992. Contact and adhesive specificities in the associations, migrations, and targeting of cells and axons. *Cell*. 68:303-22.

6. Madri, J.A., and D. Graesser. 2000. Cell migration in the immune system: the evolving inter-related roles of adhesion molecules and proteinases. *Dev Immunol*. 7:103-16.

7. Perantoni, A.O. 1999. Cell adhesion molecules in the kidney: from embryo to adult. *Exp Nephrol*. 7:80-102.

8. Darribere, T., M. Skalski, H.L. Cousin, A. Gaultier, C. Montmory, and D. Alfandari. 2000. Integrins: regulators of embryogenesis. *Biol Cell*. 92:5-25.

9. Butcher, E.C., and L.J. Picker. 1996. Lymphocyte homing and homeostasis. *Science*. 272:60-6.

10. Pfeilschifter, J. 2000. [Adhesion molecules]. *Schweiz Rundsch Med Prax*. 89:439-42.

11. Slack, S.M. and Turitto, V.T. 1993. Fluid dynamics and hemorheologic considerations. *Cardiovasc Pathol*. 2:11S-21S.

12. Ley, K. 2001. Physiology of inflammation. Oxford University Press.

13. Rubin, E. and Farber, J. 1988. Pathology. J.B. Lippincott Company, Philadelphia.

14. Giavazzi, R. 1996. Cytokine-mediated tumor-endothelial cell interaction in metastasis. *Curr. Top. Microbiol. Immunol.* 213:13-30.

15. Goetz, D.J., H. Ding, W.J. Atkinson, G. Vachino, R.T. Camphausen, D.A. Cumming, and F.W. Luscinskas. 1996. A human colon carcinoma cell line exhibits adhesive interactions with P-selectin under fluid flow via a PSGL-1-Independent mechanism. *Am. J. Path.* 149:1661-1673.

16. Cavallaro, U., and G. Christofori. 2001. Cell adhesion in tumor invasion and metastasis: loss of the glue is not enough. *Biochim Biophys Acta.* 1552:39-45.

17. Ross, R. 1999. Atherosclerosis - an inflammatory disease. *N. Engl. J. Med.* 340:115-126.

18. Goldman, A.J., R.G. Cox, and H. Brenner. 1967. Slow viscous motion of a sphere parallel to a plane wall. II. Couette flow. *Chem. Eng. Sci.* 22:635-660.

19. Cozens-Roberts, C., J.A. Quinn, and D.A. Lauffenburger. 1990. Receptor-mediated adhesion phenomena: model studies with the radial flow detachment assay. *Biophys. J.* 58:107-125.

20. Hammer, D.A., and S.M. Apte. 1992. Simulation of cell rolling and adhesion on surfaces in shear flow: general results and analysis of selectin-mediated neutrophil adhesion. *Biophys. J.* 62:35-57.

21. Shinde Patil, V.R. 1999. Particle size influences adhesion under flow. *In* Biomedical Engineering. University of Memphis, Memphis TN. 67.

22. Kansas, G.S. 1996. Selectins and their ligands: current concepts and controversies. *Blood*. 88:3259-3287.

23. Luscinskas, F.W., and M.A. Gimbrone. 1996. Endothelial-dependent mechanisms in chronic inflammatory leukocyte recruitment. *Annu. Rev. Med.* 47:413-421.

24. Carlos, T.M., and J.M. Harlan. 1994. Leukocyte-endothelial adhesion molecules. *Blood*. 84:2068-2101.

25. Springer, T.A. 1994. Traffic signals for lymphocyte recirculation and leukocyte emigration: the multistep paradigm. *Cell*. 76:301-314.

26. Lawrence, M.B., and T.A. Springer. 1991. Leukocytes roll on a selectin at physiologic flow rates: distinction from and prerequisite for adhesion through integrins. *Cell*. 65:859-873.

27. von Andrian, U.H., J.D. Chambers, L.M. McEvoy, R.F. Bargatze, K.E. Arfors, and E.C. Butcher. 1991. Two-step model of leukocyte-endothelial cell interactions in inflammation: distinct roles for LECAM-1 and the leukocyte ß$_2$ integrins in vivo. *Proc. Natl. Acad. Sci. USA*. 88:7538-7542.

28. Lawrence, M.B., C.W. Smith, S.G. Eskin, and L.V. McIntire. 1990. Effect of venous shear stress on CD18-mediated neutrophil adhesion to cultured endothelium. *Blood*. 75:227-237.

29. Ebnet, K., and D. Vestweber. 1999. Molecular mechanisms that control leukocyte extravasation: the selectins and the chemokines. *Histochem. Cell Biol.* 112:1-23.

30. Lauffenburger, D.A., and J.J. Linderman. 1993. Receptors. Oxford University Press, New York.

31. Diamond, M.S., and T.A. Springer. 1994. The dynamic regulation of integrin adhesiveness. *Current Biology*. 4:506-517.

32. Diamond, M.S., and T.A. Springer. 1993. A subpopulation of Mac-1 (CD11b/CD18) molecules mediates neutrophil adhesion to ICAM-1 and fibrinogen. *J. Cell Biol.* 120:545-556.

33. Diamond, M.S., D.E. Staunton, S.D. Marlin, and T.A. Springer. 1991. Binding of the integrin Mac-1 (CD11b/CD18) to the third immunoglobulin- like domain of ICAM-1 (CD54) and its regulation by glycosylation. *Cell*. 65:961-71.

34. Diamond, M.S., D.E. Staunton, A.R. de Fougerolles, S.A. Stacker, J. Garcia-Aguilar, M.L. Hibbs, and T.A. Springer. 1990. ICAM-1 (CD54): A counter-receptor for Mac-1 (CD11b/CD18). *J. Cell Biol.* 111:3129-3139.

35. Ding, Z.M., J.E. Babensee, S.I. Simon, H. Lu, J.L. Perrard, D.C. Bullard, X.Y. Dai, S.K. Bromley, M.L. Dustin, M.L. Entman, C.W. Smith, and C.M. Ballantyne. 1999. Relative contribution of LFA-1 and Mac-1 to neutrophil adhesion and migration. *J Immunol*. 163:5029-38.

36. Dimitroff, C.J., J.Y. Lee, S. Rafii, R.C. Fuhlbrigge, and R. Sackstein. 2001. CD44 is a major E-selectin ligand on human hematopoietic progenitor cells. *J Cell Biol*. 153:1277-86.

37. Patel, K.D., K.L. Moore, M.U. Nollert, and R.P. McEver. 1995. Neutrophils use both shared and distinct mechanisms to adhere to selectins under static and flow conditions. *J. Clin. Invest.* 96:1887-1896.

38. Goetz, D.J., D.M. Greif, R.T. Camphausen, S. Howes, K.M. Comess, K.R. Snapp, G.S. Kansas, and F.W. Luscinskas. 1997. Isolated P-selectin glycoprotein-1 dynamic adhesion to P- and E-selectin. *J. Cell Biol.* 137:509-519.

39. Norman, K.E., A.G. Katopodis, G. Thoma, F. Kolbinger, A.E. Hicks, M.J. Cotter, A.G. Pockley, and P.G. Hellewell. 2000. P-selectin glycoprotein ligand-1 supports rolling on E- and P-selectin in vivo. *Blood*. 96:3585-91.

40. Snapp, K.R., H. Ding, K. Atkins, R. Warnke, F.W. Luscinskas, and G.S. Kansas. 1998. A novel P-selectin glycoprotein ligand-1 monoclonal antibody recognizes an epitope within the tyrosine sulfate motif of human PSGL-1 and blocks recognition of both P- and L-selectin. *Blood*. 91:154-164.

Figures

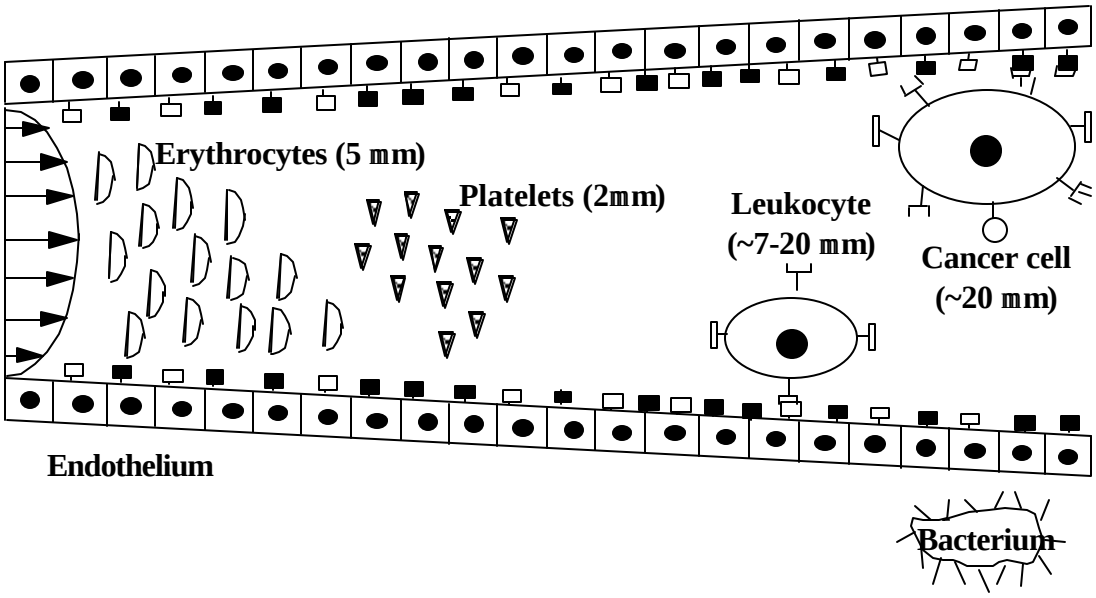

Figure 1.1 Adhesion in the vasculature

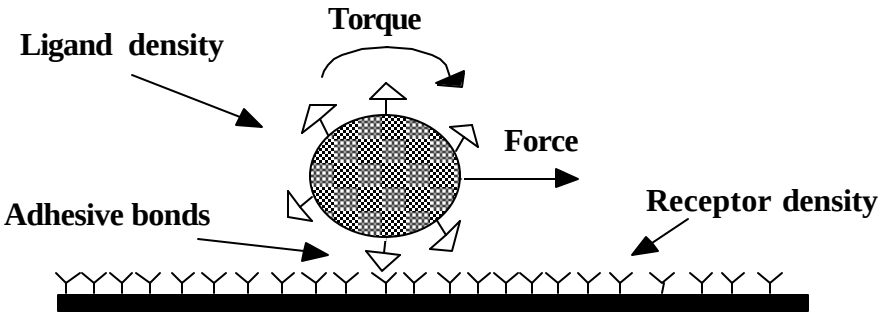

System Parameters	+	*Biophysical Bond Properties*	→	*Measurable Adhesion Response*
Ligand density		**Receptor-ligand kinetics**		**Rate of attachment**
Receptor density		**Strength of bond**		**Strength of adhesion**
Radius of particle		**Response of bonds to stress**		**Rolling velocity**
Disruptive force				
Substrate				
Material properties of particle				

Figure 1.2. Biophysics of cell adhesion under flow

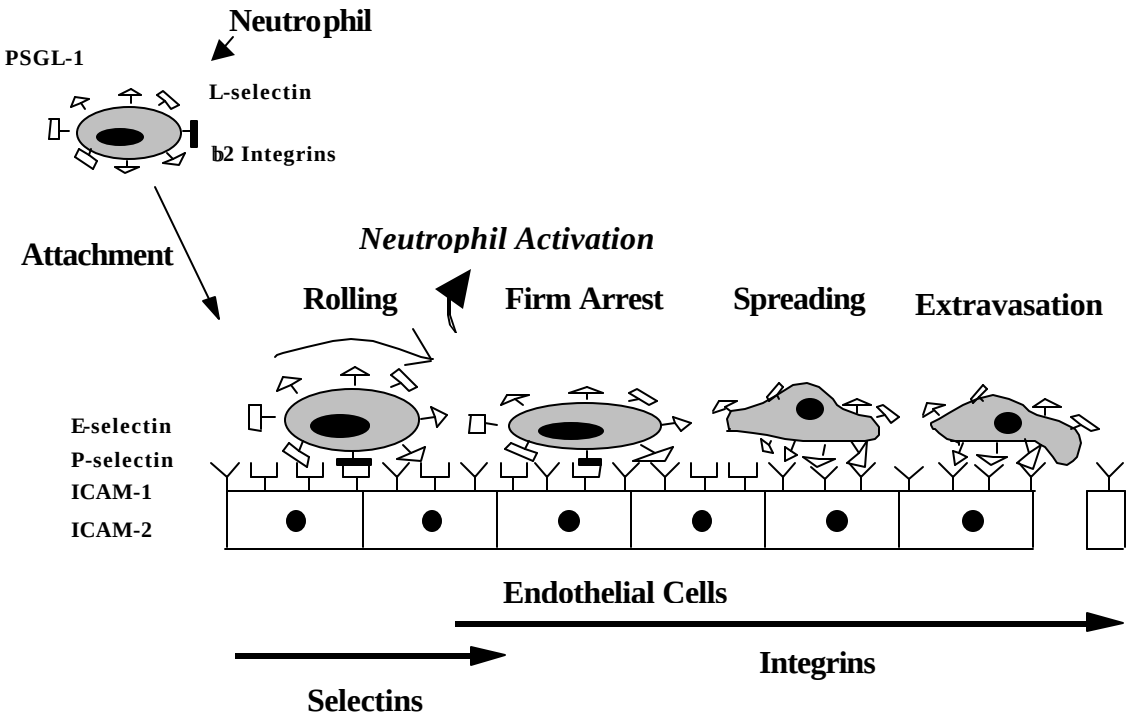

Figure 1.3. Neutrophil adhesion cascade

CHAPTER 2

PARTICLE DIAMETER INFLUENCES ADHESION UNDER FLOW[1]

Introduction

Cellular adhesion to the vascular endothelium in the fluid dynamic environment of blood circulation is an important aspect of many physiological and pathological processes. Examples include platelet adhesion during the later stages of atherosclerosis (1), leukocyte adhesion during recruitment to a site of tissue injury (2), and cancer cell adhesion during metastasis (3). The diameters of these various adhering cells span an order of magnitude from 2 μm (the approximate size of a platelet) to 20 μm (the size of some metastasizing cells) with leukocytes (7 - 10 μm) falling within this range. It is important to recognize that the adhesion exhibited by a cell may be a function of the diameter of the cell. Examples of where a clear understanding of the role of cell diameter in adhesion is necessary include (a) comparing platelet adhesion (4) to leukocyte adhesion (5), (b) experimental adhesion assays with ligand transfectants (e.g. using a ~10 μm diameter mammalian cell line transfected with a platelet ligand (6)) and (c) elucidating the relative importance of mechanical trapping verses specific adhesion in cancer cell arrest in a secondary organ (7-11).

[1] Previously published as: **Particle Diameter Influences Adhesion Under Flow**. Shinde Patil V.R., Campbell C.J., Yun Y.H., Slack S.M., and Goetz D.J. *Biophys. J.* 80: 1733-1743. (2001)

In considering the role of cell diameter in adhesion it is helpful to realize that adhesion under flow is a rather broad term, encompassing several adhesive states (10, 12). The initial attachment of the cell from the free stream to the endothelium is often referred to as attachment (10), capture (13), or initial tethering (14). Subsequent to attachment, the cell may remain stationary on the endothelium (exhibit firm adhesion), may release back into the free stream (detachment) or may continue to move in the direction of flow at a low velocity (roll). Thus, cell adhesion can be categorized into several types of adhesive behavior including attachment, rolling, and firm adhesion.

Mathematical models of firm adhesion strongly suggest that the diameter of an adhering cell will significantly influence the adhesion of the cell to the endothelium. In the ideal case of a non-deformable spherical cell firmly adherent to an adhesive substrate under Couette flow, the force and torque exerted on the cell by the flow of the fluid will be proportional to the square and the cube of the cell diameter respectively (15). For the cell to remain firmly adherent, this disruptive force and torque must be balanced by an adhesive force mediated by receptor-ligand bonds occurring in the area of contact between the adherent cell and the adhesive substrate. It is reasonable to argue that the adhesive force will be a function of the size of the contact area. Since the size of the contact area is a function of the diameter of the cell (16), it appears that both the disruptive and adhesive forces acting on the adherent cell will be a function of the diameter of the cell.

Using these ideas and the model by Hammer and Lauffenburger (17), Cozens-Roberts et al. (16) derived an expression for the shear stress required to remove an adherent particle from an adhesive substrate. They termed this parameter the critical shear stress, Sc, and deduced that Sc can be estimated by the relationship $K (\sin \Theta)^3$. Here, K accounts for the thermodynamic properties of the receptor-ligand pair, the temperature and the surface densities of the receptor and ligand. Θ is the angle of the contact area over which a receptor-ligand bond can form. Since Θ is a function of the diameter of the particle (16), the analysis of Cozens-Roberts et al. (16) suggests that Sc will be a function of the diameter of the cell.

Clearly then, it is reasonable to suspect that cell diameter affects firm adhesion. A review of mathematical models of cell attachment and rolling also suggests that cell diameter will affect attachment and rolling (12, 17, 18). In addition to the direct effect cell diameter may have on adhesion (i.e. the direct effect on the adhesive mechanics just described), cell diameter will also affect the transport of the cell by influencing the diffusion of the cell (19) and the hydrodynamic effect of the vessel wall on the cell velocity (15).

Although theory clearly predicts that cell diameter will affect adhesion and the size range of cells which may bind to the endothelium is quite broad, there have been few experimental studies aimed at investigating the relationship between cell diameter and adhesion. Wattenbarger et al. (20), studied the adhesion of glycophorin liposomes to

lectin-coated surfaces in shear flow. Although this study was not intended to be a thorough investigation into the relationship between cell diameter and adhesion, the results did suggest that particle diameter affects adhesion. In particular, Wattenbarger et al. found that the larger diameter glycophorin liposomes had a greater propensity to detach from the lectin-coated substrate compared to the smaller diameter glycophorin liposomes. It should be noted that they did not know if the surface density of glycophorin on the liposomes was similar for each diameter liposome and they did not probe all adhesive states (e.g. attachment and rolling).

In summary, it is reasonable to postulate, and indeed mathematical models predict, that the observed adhesion between a cell and an adhesive substrate will be a function of the diameter of the cell. The experimental data investigating this issue is limited. Thus, in this study we used *in vitro* flow assays to probe the role of cell diameter in adhesion. Since cells have attributes, in addition to diameter, which vary from one cell type to another and may significantly affect the adhesion of the cell, we investigated the role of cell diameter using ligand-coated microspheres. We have previously employed this approach (21) to investigate the role of particle diameter in the adhesion of two different sized microspheres. Expanding on that prior study, we generated 5, 10, 15 and 20 μm diameter microspheres (22) coated with equivalent surface densities of a recombinant P-selectin glycoprotein ligand-1 (PSGL-1) construct termed 19.ek.Fc. We then compared the adhesion of the different sized 19.ek.Fc microspheres to P-selectin under *in vitro* flow conditions which mimic, in part, flow conditions present *in vivo*.

Materials and Methods

Materials and preparation of 19.ek.Fc microspheres: Hanks balanced salt solution (HBSS) with Ca^{2+} and Mg^{2+} (HBSS+), was from BioWhittaker (Walkersville, MD). Human IgG_1 and bovine serum albumin (BSA) were from Sigma (St. Louis, MO). Protein A was from Zymed (San Francisco, CA). Leukocyte function blocking murine anti-P-selectin mAb, HPDG2/3 (IgG_1) (23), non-blocking murine anti-P-selectin mAb, HPDG2/1 (IgG_1) (23), murine blocking anti-PSGL-1 (Pharmigen, San Diego, CA) were used as purified IgG_1. Recombinant P-selectin consisting of the full extracellular region of P-selectin has been previously described (23, 24). The PSGL-1 molecule used in this study is a chimera consisting of a truncated extracellular region of mature PSGL-1 (the first 19 amino acids of mature PSGL-1) linked to an enterokinase cleavage site which in turn is linked to the heavy chain CH2-CH3 (Fc) region of human IgG_1. This construct is referred to as 19.ek.Fc and has been previously described (22, 24). The approximate molecular weight of 19.ek.Fc is 72 kDa (24). The 19.ek.Fc construct was coupled to 5, 10, 15 and 20 μm diameter polystyrene microspheres (Bangs Laboratories Inc.; Fishers, IN) via protein A as previously described (22). Briefly, the microspheres were incubated overnight at room temperature (RT) in protein A. Following one wash, they were held in 19 ek.Fc for 1 hour at RT. The 19 ek.Fc coated microspheres were then washed and resuspended to $1x10^{8}$ microspheres/ml until use in the adhesion assays. The coating concentration of the 19.ek.Fc solution was 20 μg/ml. Note that when coupling the 19.ek.Fc to the microspheres, the amount of 19.ek.Fc added per protein A microsphere

surface area was the same for each sized microsphere. Thus, per 5 µl of the 19.ek.Fc coating solution, $4x10^6$ 5 µm microspheres were coated, $1x10^6$ 10 µm microspheres were coated, $4.44x10^5$ 15 µm microspheres were coated and $2.5x10^5$ 20 µm microspheres were coated. Coating in this manner resulted in microspheres that had similar surface densities of 19.ek.Fc, as corroborated experimentally (21). BSA coated microspheres were prepared by incubating the microspheres in HBSS+, 1% BSA at least 1 hr. prior to use in an adhesion assay. Note that, standard deviations in the diameters of the 5µm, 10µm, 15µm and 20µm microspheres were 0.07µm, 0.1µm, 0.42µm and 0.33µm respectively. The mAbs to P-selectin, 19.ek.Fc construct and soluble P-selectin were a generous gift from Dr. Raymond T. Camphausen (Genetics Institute; Cambridge, MA).

Parallel plate flow chamber: The parallel plate flow chamber (Glycotech; Rockville, MD) is similar to that used by McIntire, Smith and colleagues (25) and consists of a plexiglass flow deck that fits inside a 35 mm tissue culture dish. Our particular flow set-up described previously (26), consists of a flow field defined by a gasket which sits between the flow deck and the 35 mm dish (Appendix A-2). The shear stress at the bottom surface of the flow chamber is given by $\tau = 3Q\mu/2wh^2$ where Q is the volumetric flow rate, μ is the viscosity, h is half the height (0.1 mm) of the flow field, and w is the width (0.5 cm) of the flow field. The volumetric flow rate was adjusted to obtain the desired shear stress. After assembly, the flow chamber was placed on an inverted microscope connected to a CCD videocamera, VCR and monitor. The 35 mm dish was

rinsed with buffer and the flow of the microspheres ($1x10^6$ / ml in HBSS+, 0.5% BSA) initiated. Experiments were carried out at room temperature (24 ^{0}C).

Preparation of P-selectin substrates for use in the adhesion assay: A silicon ring (Unisyn Technologies, Hopkinton, MA) with an inner diameter of 6 mm was placed on 35 mm tissue culture dishes (Corning, Corning, NY). The inner region of the ring was outlined on the reverse side of the tissue culture dishes. 35 µl of soluble P-selectin (diluted to 20 µg/ml in HBSS) or HBSS alone (negative control) was placed inside the rings. The dishes were incubated at 4 ^{0}C overnight (in a humidified chamber to avoid buffer evaporation), washed and the entire dish flooded with HBSS+, 1% BSA. The dishes were incubated in HBSS+, 1% BSA at least 30 minutes prior to the adhesion assay. BSA coated dishes (negative controls) were prepared by adding 1 ml of HBSS+, 1% BSA to the bottom surface of 35 mm tissue culture dishes at least 30 minutes prior to the adhesion assay.

mAb blocking: In certain experiments, the P-selectin coated surface was treated with mAbs to P-selectin (10 µg/ml) 15 minutes prior to the adhesion assays. For these experiments, the 19.ek.Fc microspheres were incubated in 200 µg/ml human IgG_1 prior to use in the adhesion assay. This prevents microsphere bound protein A from binding to the Fc region of the mAb bound to P-selectin on the substrate. In certain experiments, the 19.ek.Fc microspheres were pretreated with mAb KPL1 (anti-PSGL-1) 15 minutes prior to the adhesion assay. In all cases, the number of microspheres present after 2 minutes of

flow was determined in eight different fields of view. These values were averaged and divided by the area of the field of view to give the number of microspheres present/ mm^2. This represented an n = 1. The entire experiment was done at least 3 times and the results averaged to give the presented data.

Measuring microsphere attachment: After assembling the flow chamber, the microscope objective was positioned at the first field of view (the one closest to the inlet) coated with P-selectin. After a short rinse, the flow of 19.ek.Fc microspheres was initiated. The number of 19.ek.Fc microspheres adherent to the surface in the field of view was determined as a function of time. Plots of the number of 19.ek.Fc microspheres bound per unit surface area versus time resulted in curves which were initially linear. As the experiment progressed, the rate of increase in the number of adherent 19.ek.Fc microspheres decreased, apparently due to the surface becoming saturated with microspheres. The initial portion of this curve (i.e. where the rate of attachment appeared to be independent of bound microspheres) was used along with linear regression to determine the effective rate of attachment, k_e. The effective rate of attachment is the rate at which microspheres attach to the P-selectin surface, i.e. go from the free stream velocity to being in an adhesive state (either rolling or firmly adherent) on the P-selectin surface. To correct k_e for the effect of microsphere diameter on delivery to the bottom surface of the flow chamber, the number of microspheres which passed through the field of view "near" the bottom surface of the flow chamber (as indicated by their lower velocity) was determined. For the 75 s^{-1} data, this number was used along with k_e to

calculate a percent adhesion. Since the microspheres were moving too fast at $400s^{-1}$ and $600s^{-1}$ to allow an accurate determination of the number of microspheres near the surface, the attachment data could not be corrected for transport at these higher shear rates. Thus, k_e values were used rather than percent adhesion at these shear rates.

Determination of percent firmly adherent: Suspensions containing 19.ek.Fc microspheres were perfused over the P-selectin surfaces at 0.5 dynes/cm^2. After 10 minutes of flow, the shear stress was increased in steps. Each level of shear stress was maintained for 1 minute for shear stresses 10 dynes / cm^2 and for thirty seconds for shear stresses > 10 dynes / cm^2. 19.ek.Fc microspheres which did not exhibit any motion in the direction of flow within a 5 second time period selected in the middle of the each shear stress interval, were scored as firmly adherent. In certain control experiments, the detachment of 19.ek.Fc microspheres from BSA coated plastic or the detachment of BSA microspheres from P-selectin coated surfaces was measured. In this case, the microspheres were drawn into the flow chamber and the flow stopped. Following a 10 minute incubation, the flow was slowly and smoothly reinitiated. Prior to reinitiation of the flow, the number of microspheres present on the surface was determined. Immediately after reinitiation of the flow, the number of microspheres firmly adherent was determined.

Determination of the rolling velocity: Recorded data at each shear stress was analyzed for 5 seconds. 19.ek.Fc microspheres which exhibited a motion in the direction of flow

within this time interval were scored as rolling. To evaluate the rolling velocity, the distance traversed by a rolling 19.ek.Fc microsphere in the 5 second interval was determined. This was divided by 5 seconds to yield the microsphere rolling velocity. This procedure was extended to all the 19.ek.Fc microspheres within a field of view.

Statistics: When comparing two means, statistical analyses were done by unpaired Student's *t*-test of the means. In cases of multiple groups, we performed a single factor ANOVA and, if appropriate, subsequently a Dunnett's test for multiple comparisons against a single control. To check for factor interactions (i.e. shear and microsphere diameter) we used a two-factor randomized block design ANOVA. Error bars indicate standard deviations unless otherwise noted.

Results

Microspheres coated with a recombinant PSGL-1 construct, 19.ek.Fc, attach, roll and firmly adhere to P-selectin adsorbed to tissue culture plastic

The leukocyte adhesion molecule P-selectin glycoprotein ligand - 1 (PSGL-1) has been shown to mediate granulocyte attachment and rolling on P-selectin (22, 27). Previously we demonstrated that 10 μm diameter microspheres coated with the recombinant PSGL-1 construct, 19.ek.Fc, attach and roll on cell lines expressing P-selectin (22). The 19.ek.Fc construct consists of the first 19 amino acids of mature PSGL-1, including the binding site for P-selectin, linked to an enterokinase cleavage site which in turn is linked to the Fc region of human IgG_1 (24). We coupled the 19.ek.Fc construct to polystyrene microspheres via protein A as previously described (22). Coupling via protein A allows for the correct orientation of the 19.ek.Fc construct on the microspheres, i.e., the Fc portion bound to the protein A and the PSGL-1 portion of the construct oriented away from the microsphere and available for binding to P-selectin.

In preliminary studies we found that 19.ek.Fc microspheres attach to soluble purified P-selectin adsorbed to tissue culture plastic and subsequent to attachment, the 19.ek.Fc microspheres either rolled or firmly adhered depending on the concentration of 19.ek.Fc on the microspheres and the shear stress (data not shown). Thus, we chose to use the 19.ek.Fc microspheres to investigate the role of particle diameter in adhesion

since this system (a) exhibits a range of adhesive states, (including attachment, rolling and firm adhesion) at physiologically relevant shear stresses, (b) involves a physiologically relevant ligand -receptor pair, (c) contains a minimal level of extraneous factors which could affect adhesion (e.g. cellular surface topology (28), cellular deformation (29)) and (d) contains a minimal number of variables which could vary from experiment to experiment.

As shown in Figure 2.1A, the adhesion of the 19.ek.Fc microspheres to P-selectin adsorbed to tissue culture plastic appears to be specific as: (a) 19.ek.Fc microspheres attached to adsorbed P-selectin, but not to adsorbed BSA (negative control), (b) the attachment to P-selectin was ablated by a function blocking mAb to P-selectin but not by a non-function blocking mAb to P-selectin, (c) the attachment to P-selectin was ablated by a function blocking mAb to PSGL-1 and (d) human IgG_1 coated microspheres did not attach to adsorbed P-selectin. In addition, we found that 19.ek.Fc microspheres which were allowed to settle onto BSA coated plastic under static conditions and BSA microspheres which were allowed to settle onto P-selectin coated plastic under static conditions were immediately removed from the substrate with the onset of flow (Figure 2.1B and 2.1C). Although this experiment was performed initially for two different sized particles (21), it was subsequently repeated with all four different sized microspheres as part of this study.

Microsphere diameter affects the rate of attachment under flow

We would ultimately like to understand the role of particle diameter in adhesion *in vivo.* However, the *in vivo* flow environment is rather complex (19). These complexities include the facts that (a) blood is not a dilute suspension and the transport of a particular cell is influenced by the presence of other cells in the suspension (e.g. leukocyte and platelet transport to the vessel wall is influenced by the presence of red blood cells (19, 30, 31)); and (b) the blood vessels are of finite size and the ratio of vessel diameter to particle diameter can affect the drag force on a particle near the wall (32-34). As a first step towards understanding the role of particle size in adhesion, we sought to investigate the role of particle diameter in adhesion under well-defined and controlled *in vitro* fluid flow conditions. To do this, we studied the adhesion of the 19.ek.Fc microspheres using a dilute suspension of microspheres in an *in vitro* parallel plate flow chamber. While such an *in vitro* model does have its limitations (i.e. it clearly does not recreate all of the complexities of the *in vivo* environment discussed above), it is routinely used to gain insight into adhesion events, which occur *in vivo* (5, 26, 27, 35, 36). In addition, our group (22, 26) and Hammer's group (37-39) have shown that key features of cellular adhesion can be recreated using ligand coated microspheres in a two-dimensional Poiseuille flow adhesion assay.

The initial step of particle adhesion to a substrate under flow is the attachment of the particle to the substrate from the fluid stream. To investigate attachment, 5, 10, 15

and 20 μm 19.ek.Fc microspheres were perfused over P-selectin substrates at three different shear rates. At 75 s^{-1}, the percentage of 5, 10, 15 and 20 μm diameter microspheres which attached to the P-selectin surface were similar (Figure 2.2A). In contrast, at higher shear rates there was a distinct dependence of the rate of attachment on the microsphere diameter. At the highest shear investigated, 600 s^{-1} (Figure 2.2C), only the 5μm diameter microspheres consistently exhibited appreciable attachment. Occasionally a 10μm microsphere would attach to the P-selectin surface at this shear rate. We never observed a 15μm or 20 μm microsphere attach at this shear rate. ANOVA indicated that the rate of attachment was a function of the diameter of the microsphere at this shear rate. We next tested an intermediate shear rate. At 400 s^{-1} (Figure 2.2B), we did observe attachment of the 10 μm and 15 μm microspheres as well as the 5μm microspheres. The 20 μm microspheres, however, did not attach at this shear rate. ANOVA indicated that the rate of attachment appeared to be a function of microsphere diameter at this shear rate ($p = 0.07$). Note that the microspheres were moving too fast at $400s^{-1}$ and $600s^{-1}$ to allow an accurate determination of the number of microspheres near the surface. Thus, we did not correct for the rate of delivery of the microspheres to the P-selectin substrate at these shear rates. Since the Stoke's settling velocity for a microsphere is proportional to the square of the diameter of the microsphere (40), it is reasonable to assume that the rate of delivery of the 19.ek.Fc microspheres to the P-selectin substrate increases with increasing microsphere diameter (e.g. the rate of delivery of the 20 μm microspheres is greater than the 5 μm microspheres). This consideration suggests that the trends observed at 400 and 600 s^{-1} (Figures 2.2B and 2.2C) would be

more pronounced if the rate of delivery were taken into account. Combined, the data in Figure 2.2 clearly indicate that the microsphere diameter can affect the rate of attachment and that this effect appears to be coupled to the level of fluid shear.

The shear stress required to set in motion a firmly adherent 19.ek.Fc microsphere decreases with increasing microsphere diameter

At the high concentrations of 19.ek.Fc and P-selectin used in this study, the majority of the 19.ek.Fc microspheres were firmly adherent at the lowest shear stress tested. As the shear stress was increased, a portion of the 19.ek.Fc microspheres would begin to roll (i.e. they would move in the direction of flow while remaining in contact with the substrate). To assess the role of particle diameter in firm adhesion, we allowed the 19.ek.Fc microspheres to attach to the P-selectin coated surface at 0.5 dynes/cm^2. Subsequently, the shear stress was increased in a stepwise fashion and the percentage of microspheres which continued to remain firmly adherent determined. In general, the smaller microspheres were more likely to be firmly adherent compared to the larger microspheres (Figure 2.3). For example at 2 dynes/cm^2, 100% of the 5 μm microspheres, ~49% of the 10 μm microspheres, ~29% of the 15 μm microspheres and only ~5% of the 20 μm microspheres were firmly adherent. Multiple factor ANOVA indicated that the percent firmly adherent was a function of microsphere diameter and this effect was coupled to the level of fluid shear. Cozens-Roberts et al. (16) defined the critical shear stress, Sc, as the shear stress required to remove 50% of a population of adherent

particles. From the data presented in Figure 2.3, we estimate Sc for the 20 μm microspheres to be ~0.9 dynes/cm^2, for the 15 μm microspheres to be ~1.2 dynes/cm^2 for the 10 μm microspheres to be ~2 dynes/cm^2 and for the 5 μm microspheres to be ~5 dynes/cm^2. These Sc values are plotted as a function of microsphere diameter in Figure 2.4. Please refer to the discussion for an explanation of these values.

The rolling velocity increases with increasing microsphere diameter

We determined the rolling velocity of the 19.ek.Fc microspheres at various shear stresses (Figure 2.5). In general, the larger microspheres rolled faster than the smaller microspheres. Note for example at 3 dynes/cm^2, the rolling velocity of the 20 μm microspheres was ~8.8 μm/sec, the rolling velocity of the 15 μm microspheres was ~3.6 μm/sec, the rolling velocity of the 10 μm microspheres was ~1.7 μm/sec, and the rolling velocity of the 5 μm microspheres was ~0 μm/sec. Multiple factor ANOVA indicated that the rolling velocity was a function of microsphere diameter and this effect was coupled to the level of fluid shear. We also found that the rolling velocity for all of the 19.ek.Fc microspheres increased with increasing shear stress and that the increase was dependent on the microsphere diameter. To illustrate this, for each set of 19.ek.Fc microspheres we performed linear regression on the data presented in Figure 2.5. The slope of the regression lines is the change of the rolling velocity with the shear stress. We then plotted these slopes as a function of microsphere diameter (Figure 2.6). Linear regression of the data in Figure 2.6 indicated that the slope was 0.21 and significantly

different from zero. Thus, it appears that the rolling velocity increases with microsphere diameter, this effect is coupled to the level of fluid shear and the change in the rolling velocity with shear stress is also a function of microsphere diameter.

Discussion

Although theoretical arguments clearly suggest a role for cell diameter in adhesion, there have been very few experimental studies exploring this issue. In this study we probed the role of cell diameter in adhesion by comparing the adhesion of 5, 10, 15 and 20 μm diameter 19.ek.Fc microspheres to P-selectin under *in vitro* flow conditions. We found that for all adhesive states investigated (attachment, rolling and firm adhesion) the adhesion was a function of the microsphere diameter.

We found that the attachment of 19.ek.Fc microspheres to P-selectin was a function of microsphere diameter and this effect was coupled to the fluid shear (Figure 2.2). At high shear (600 s^{-1}), only the 5 μm diameter 19.ek.Fc microspheres consistently exhibited appreciable levels of attachment (Figure 2.2C). At the lowest shear tested, there was little difference in the attachment (Figure 2.2A) and at an intermediate shear the rate of attachment appeared to decrease with increasing microsphere diameter (Figure 2.2B).

This trend could be explained by a variety of arguments including the idea that there are two different adhesion regimes operative over the range of shear rates tested (18, 41). At high shear, the adhesion may take place in a reaction-controlled regime and at low shear the adhesion may be influenced by both transport and kinetics. A key parameter in this analysis is the slip velocity of the microspheres which has been

estimated as ~0.47 U (18) where U is the translational velocity of the microsphere corrected for the wall effect (15). Note that U is proportional to the particle diameter and thus the slip velocity increases with increasing particle diameter (15). In the high shear, reaction-limited regime, a lower slip velocity favors adhesion (18, 41).

Another important parameter may be the contact area which, from the analysis of Cozens-Roberts et al. (16), increases with increasing particle diameter. Although what occurs in the transport-limited regime may be rather complex due to the fact that several factors, in addition to contact area, may have an influence (e.g. particle and receptor diffusion (18, 19)) it could be argued that larger microsphere diameter favors adhesion since the larger microsphere will sample a larger area of the P-selectin substrate for the same length of substrate sampled.

Thus, a plausible explanation for the trend observed in Figure 2.2 is that at high shear the adhesion takes place in a reaction-controlled regime. In this regime, smaller microsphere diameter is favorable for attachment since the smaller microspheres have a lower slip velocity compared to the larger microspheres. As the shear rate is decreased, reaction issues become less dominant and the transport begins to influence the attachment. As the attachment moves towards the transport-limited regime, the probability of a larger microsphere attaching becomes similar to the probability of smaller microsphere attaching since, from a transport standpoint, the larger contact area of the larger microspheres relative to the smaller microspheres favors attachment.

In discussing the results of the firm adhesion data (Figures 2.3 and 2.4), it is insightful to consider the analysis of Cozens-Roberts et al. (16) with respect to the role of particle diameter in adhesion. As discussed in the introduction, increasing the particle diameter increases the disruptive force and torque exerted on an adherent particle by the fluid flow (15) as well as the contact area between the particle and the substrate (16). The latter effect should be pro-adhesive while the former is detrimental to adhesion. Cozens-Roberts et al. (16) defined the critical shear stress, Sc, as the shear stress required to remove 50% of a population of adherent particles and developed a model to predict Sc as a function of a variety of factors including the particle diameter. Their analysis indicates that Sc is given by $K(\sin \Theta)^3$ where Θ is given by $\cos^{-1}[1-(H-h_s)/\rho_B]$, h_s is the separation distance between the 19.ek.Fc microsphere and the P-selectin surface, ρ_B is the radius of the microsphere and H is the maximum separation distance for 19.ek.Fc – P-selectin binding. For a fixed h_s and H, Θ decreases, $\sin \Theta$ decreases and consequently Sc decreases with increasing microsphere diameter. Thus, the net effect of an increase in microsphere diameter is a decrease in the level of shear stress needed to remove an adherent microsphere. Please refer to the appendix (Section A-1) for a detailed calculation of theoretical critical shear stress values.

As would be predicted from this model (16), we observed that the shear stress required to set in motion a firmly adherent microsphere decreased with increasing microsphere diameter (Figures 2.3 and 2.4). Using the analysis of Cozens–Roberts et al. (16), it is possible to predict the change in Sc with particle diameter. We estimated K

from the 5 μm microsphere data using h_s = 10 nm and H = 40 nm. We then plotted Sc vs. microsphere diameter using this value of K and the equation Sc = K $(\sin \Theta)^3$. The resulting curve is given in Figure 2.4 and is shown to closely track the experimental data. The rolling velocity data also indicated that post-attachment adhesion decreased with increasing microsphere diameter (Figure 2.5). In addition, the sensitivity of the rolling velocity to changes in fluid shear increased with increasing microsphere diameter (Figure 2.6).

In summary, we have probed the role of particle diameter in receptor-ligand mediated adhesion under fluid flow and found that for all adhesive states tested, microsphere diameter affected the adhesion and the effect of diameter was coupled to the level of fluid shear. At relatively high shear, smaller microsphere diameter was favorable for attachment. At the lowest shear rate tested, however, there was little difference in the attachment between the different sized microspheres. The effect of an increase in the microsphere diameter on post-attachment adhesion was a decrease in the adhesion as indicated by a decrease in shear stress required to set in motion an adherent microsphere and an increase in the rolling velocity of microspheres which were not firmly adherent.

References

1. Ross, R. 1999. Atherosclerosis - an inflammatory disease. *N. Engl. J. Med.* 340:115-126.

2. Springer, T.A. 1994. Traffic signals for lymphocyte recirculation and leukocyte emigration: the multistep paradigm. *Cell*. 76:301-314.

3. Giavazzi, R. 1996. Cytokine-mediated tumor-endothelial cell interaction in metastasis. *Curr. Top. Microbiol. Immunol.* 213:13-30.

4. Frenette, P.S., R.C. Johnson, R.O. Hynes, and D.D. Wagner. 1995. Platelets roll on stimulated endothelium in vivo: an interaction mediated by endothelial P-selectin. *Proc. Natl. Acad. Sci.* 92:7450-7454.

5. Lawrence, M.B., and T.A. Springer. 1991. Leukocytes roll on a selectin at physiologic flow rates: distinction from and prerequisite for adhesion through integrins. *Cell*. 65:859-873.

6. Fredrickson, B.J., J.F. Dong, L.V. McIntire, and J.A. Lopez. 1998. Shear-dependent rolling on von Willebrand factor of mammalian cells expressing the platelet glycoprotein Ib-IX-V complex. *Blood*. 92:3684-3693.

7. Scherbarth, S., and F.W. Orr. 1997. Intravital videomicroscopic evidence for regulation of metastasis by the hepatic microvasculature: effects of interleukin-1α on metastasis and the location of B16-F1 melanoma cell arrest. *Can. Res.* 57:4105-4110.

8. Chambers, A.F., I.C. MacDonald, E.E. Schmidt, S. Koop, V.L. Morris, R. Khokha, and A.C. Groom. 1995. Steps in tumor metastasis: new concepts from intravital videomicroscopy. *Cancer Metastasis Review*. 14:279-301.

9. Goetz, D.J., H. Ding, W.J. Atkinson, G. Vachino, R.T. Camphausen, D.A. Cumming, and F.W. Luscinskas. 1996. A human colon carcinoma cell line exhibits adhesive interactions with P-selectin under fluid flow via a PSGL-1-Independent mechanism. *Am. J. Path*. 149:1661-1673.

10. Goetz, D.J., B.K. Brandley, and D.A. Hammer. 1996. An E-selectin-IgG chimera supports sialylated moiety dependent adhesion of colon carcinoma cells under fluid flow. *Ann. Biomed. Eng*. 24:87-98.

11. McCarty, O.J., S.A. Mousa, P.F. Bray, and K. Konstantopoulos. 2000. Immobilized platelets support human colon carcinoma cell tethering, rolling, and firm adhesion under dynamic flow conditions. *Blood*. 96:1789-97.

12. Hammer, D.A., and S.M. Apte. 1992. Simulation of cell rolling and adhesion on surfaces in shear flow: general results and analysis of selectin-mediated neutrophil adhesion. *Biophys. J*. 62:35-57.

13. Munn, L.L., R.J. Melder, and R.K. Jain. 1995. Analysis of cell flux in the parallel plate flow chamber: implications for cell capture studies. *Biophys. J*. 67:889-895.

14. Lawrence, M.B., D.F. Bainton, and T.A. Springer. 1994. Neutrophil tethering to and rolling on E-selectin are separable by requirement for L-selectin. *Immunity*. 1:137-145.

15. Goldman, A.J., R.G. Cox, and H. Brenner. 1967. Slow viscous motion of a sphere parallel to a plane wall. II. Couette flow. *Chem. Eng. Sci*. 22:635-660.

16. Cozens-Roberts, C., J.A. Quinn, and D.A. Lauffenburger. 1990. Receptor-mediated adhesion phenomena: model studies with the radial flow detachment assay. *Biophys. J.* 58:107-125.

17. Hammer, D.A., and D.A. Lauffenburger. 1987. A dynamical model for receptor-mediated cell adhesion to surfaces. *Biophys. J.* 52:475-487.

18. Chang, K.C., and D.A. Hammer. 1999. The forward rate of binding of surface-tethered reactants: effect of relative motion between two surfaces. *Biophys. J.* 76:1280-1292.

19. Goldsmith, H.L., and V.T. Turitto. 1986. Rheological Aspects of Thrombosis and Haemostasis: Basic Principles and Applications. *Thrombosis and Haemostasis*. 55:415-435.

20. Wattenbarger, M.R., D.J. Graves, and D.A. Lauffenburger. 1990. Specific adhesion of glycophorin liposomes to a lectin surface in shear flow. *Biophys. J.* 57:765-777.

21. Shinde Patil, V.R. 1999. Particle size influences adhesion under flow. *In* Biomedical Engineering. University of Memphis, Memphis TN. 67.

22. Goetz, D.J., D.M. Greif, R.T. Camphausen, S. Howes, K.M. Comess, K.R. Snapp, G.S. Kansas, and F.W. Luscinskas. 1997. Isolated P-selectin glycoprotein-1 dynamic adhesion to P- and E-selectin. *J. Cell Biol.* 137:509-519.

23. Sako, D., X.J. Chang, K.M. Barone, G. Vachino, H.M. White, G. Shaw, G.M. Veldman, K.M. Bean, T.J. Ahern, B. Furie, D.A. Cumming, and G.R. Larsen. 1993. Expression cloning of a functional glycoprotein ligand for P-selectin. *Cell*. 75:1179-1186.

24. Sako, D., K.M. Comess, K.M. Barone, R.T. Camphausen, D.A. Cumming, and G.D. Shaw. 1995. A sulfated peptide segment at the amino terminus of PSGL-1 is critical for P-selectin binding. *Cell*. 83:323-331.

25. Gopalan, P.K., D.A. Jones, L.V. McIntire, and C.W. Smith. 1996. Cell adhesion under hydrodynamic flow conditions. *In* Current Protocols in Immunology. J.E. Coligan, A.M. Kruisbeek, D.H. Margulies, E.M. Shevach, and W. Strober, editors. J. Wiley, New York. 7.29.1-7.29.23.

26. Crutchfield, K.L., V.R. Shinde Patil, C.J. Campbell, C.A. Parkos, J.R. Allport, and D.J. Goetz. 2000. CD11b/CD18-coated microspheres attach to E-selectin under flow. *J. Leuk. Biol.* 67:196-205.

27. Patel, K.D., and R.P. McEver. 1997. Comparison of tethering and rolling of eosinophils and neutrophils through selectins and P-selectin glycoprotein ligand-1. *J. Immunol.* 159:4555-4565.

28. von Andrian, U.H., S.R. Hasslen, R.D. Nelson, S.L. Erlandsen, and E.C. Butcher. 1995. A central role for microvillous receptor presentation in leukocyte adhesion under flow. *Cell*. 82:989-999.

29. Dong, C., J. Cao, R.J. Struble, and H.H. Lipowsky. 1999. Mechanics of leukocyte deformation and adhesion to endothelium under shear flow. *Annal. Biomed. Eng.* 27:298-312.

30. Melder, R.J., M. L.L., S. Yamada, C. Ohkubo, and R.K. Jain. 1995. Selectin- and integrin-mediated T-lymphocyte rolling and arrest on TNF-a-activated endothelium: Augmentation by erythrocytes. *Biophys. J.* 69:2131-2138.

31. Chien, S. 1982. Rheology in the microcirculation in normal and low flow states. *Adv. in Shock Res.* 8:71-80.

32. Schmid-Schoenbein, G.W., Y.C. Fung, and B.W. Zweifach. 1975. Vascular endothelium-leukocyte interaction; sticking shear force in venules. *Circ Res*. 36:173-84.

33. House, S.D., and H.H. Lipowsky. 1988. In vivo determination of the force of leukocyte-endothelium adhesion in the mesenteric microvasculature of the cat. *Circ Res*. 63:658-68.

34. Chapman, G.B., and G.R. Cokelet. 1998. Flow resistance and drag forces due to multiple adherent leukocytes in postcapillary vessels. *Biophys J*. 74:3292-301.

35. Lawrence, M.B., C.W. Smith, S.G. Eskin, and L.V. McIntire. 1990. Effect of venous shear stress on CD18-mediated neutrophil adhesion to cultured endothelium. *Blood*. 75:227-237.

36. Luscinskas, F.W., G.S. Kansas, H. Ding, P. Pizcueta, B.E. Schleiffenbaum, T.F. Tedder, and M.A. Gimbrone, Jr. 1994. Monocyte rolling, arrest, and spreading on IL-4-activated vascular endothelium under flow is mediated via sequential action of L-selectin, ß1-integrins, and ß2-integrins. *J. Cell Biol.* 125:1417-1427.

37. Brunk, D.K., D.J. Goetz, and D.A. Hammer. 1996. Sialyl Lewisx/E-selectin-mediated rolling in a cell-free system. *Biophys. J.* 71:2902-2908.

38. Brunk, D.K., and D.A. Hammer. 1997. Quantifying rolling adhesion using a cell-free assay: E-selectin and its carbohydrate ligands. *Biophys. J.* 72:2820-2833.

39. Rodgers, S.D., R.T. Camphausen, and D.A. Hammer. 2000. Sialyl Lewis^X-Mediated, PSGL-1-Independent Rolling Adhesion on P-selectin. *Biophys. J.* 79:694-706.

40. Brenner, H. 1961. The slow motion of a sphere through a viscous fluid towards a plane surface. *Chem. Engng. Sci.* 16:242-251.

41. Swift, D.G., R.G. Posner, and D.A. Hammer. 1998. Kinetics of adhesion of IgE-sensitized rat basophilic leukemia cells to surface-immobilized antigen in couette flow. *Biophys. J.* 75:2597-2611.

Figures

Figure 2.1. 19.ek.Fc microspheres exhibit specific adhesion to P-selectin. (A) 10 μm 19.ek.Fc or human IgG_1 microspheres were perfused over 35 mm dishes coated with P-selectin or BSA (negative control). In certain cases the substrate or the microspheres were pretreated with mAbs. Legend: Ligand indicates which molecule was on the microsphere; substrate indicates coating the 35 mm dishes with P-selectin (P) or BSA (B); mAb indicates pretreatment of the microsphere (KPL-1) or substrate (2/3 and 2/1) with the indicated mAb (2/3 = HPDG2/3, 2/1 = HPDG2/1); n = 3; * $p < 0.01$ compared to left most bar. **(B)** 19.ek.Fc microspheres were allowed to settle onto BSA coated 35 mm dishes under no flow conditions for 10 minutes. Following the incubation, the flow was slowly and smoothly reinitiated. Immediately after reinitiation of flow, the number of 19.ek.Fc microspheres remaining bound to the surface was determined. **(C)** BSA microspheres were allowed to settle onto P-selectin under no flow conditions for 10 minutes. Following the incubation, the flow was slowly and smoothly reinitiated. Immediately after reinitiation of flow, the number of BSA microspheres remaining bound to the surface was determined. Legend for (B) and (C): BF = before flow; AF = after flow. n = 3; * indicates $p < 0.01$. All results shown are for 10 μm microspheres. Similar results were obtained with 5, 15 and 20 μm microspheres.

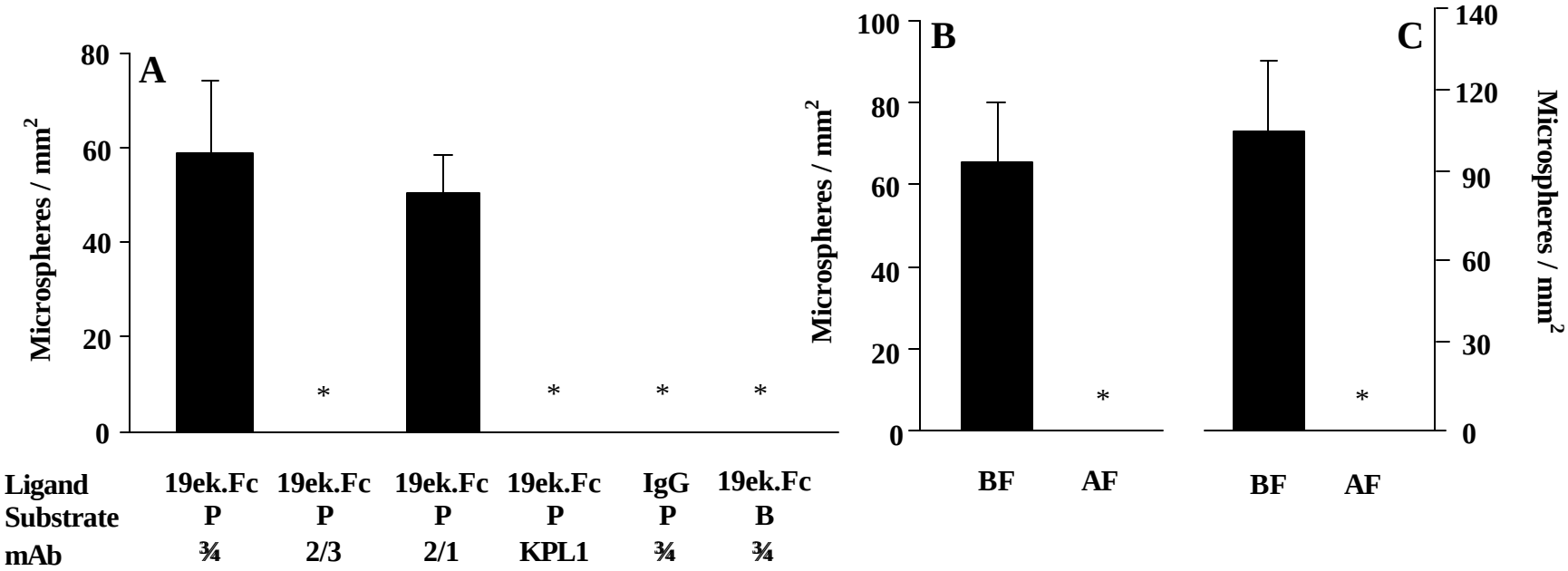
A
B
C
Microspheres / mm2
Microspheres / mm2
Microspheres / mm2
80
60
40
20
0
100
80
60
40
20
0
140
120
90
60
30
0
*
*
*
*
*
*
*
*
Ligand
Substrate
mAb
19ek.Fc
P
¾
19ek.Fc
P
2/3
19ek.Fc
P
2/1
19ek.Fc
P
KPL1
IgG
P
¾
19ek.Fc
B
¾
BF
AF
BF
AF

Figure 2.2. Comparison of the rates of attachment of 5, 10, 15 and 20 mm 19.ek.Fc microspheres to P-selectin. **(A)** The effective rate of attachment of the 19.ek.Fc microspheres to the P-selectin substrate at 75 s^{-1} was determined. This value along with an estimate of the number of 19.ek.Fc microspheres which passed through the field of view near the P-selectin coated surface was used to determine the percentage of 19.ek.Fc microspheres that attached to the P-selectin substrate. At this shear rate, the % attachment did not appear to be a function of the microsphere diameter ($p > 0.1$; $n \geq 4$). **(B)** The effective rate of attachment of the 19.ek.Fc microspheres to the P-selectin substrate at a shear rate of 400 s^{-1} was determined. At this shear, the rate of attachment appeared to be a function of the diameter of the 19.ek.Fc microspheres ($p = 0.07$; $n \geq 2$). **(C)** The effective rate of attachment of the 19.ek.Fc microspheres to the P-selectin substrate at a shear rate of 600 s^{-1} was determined. At this shear, the rate of attachment was a function of the diameter of the 19.ek.Fc microspheres. ($p < 0.05$; $n \geq 3$). Note that in **B** and **C** the data were not corrected for the fact that the delivery of the 19.ek.Fc microspheres to the P-selectin surface is a function of the diameter of the microspheres. Since the Stoke's settling velocity is proportional to the square of the microsphere diameter, it is reasonable to assume that if the delivery were taken into account the trends observed in **B** and **C** would be more pronounced.

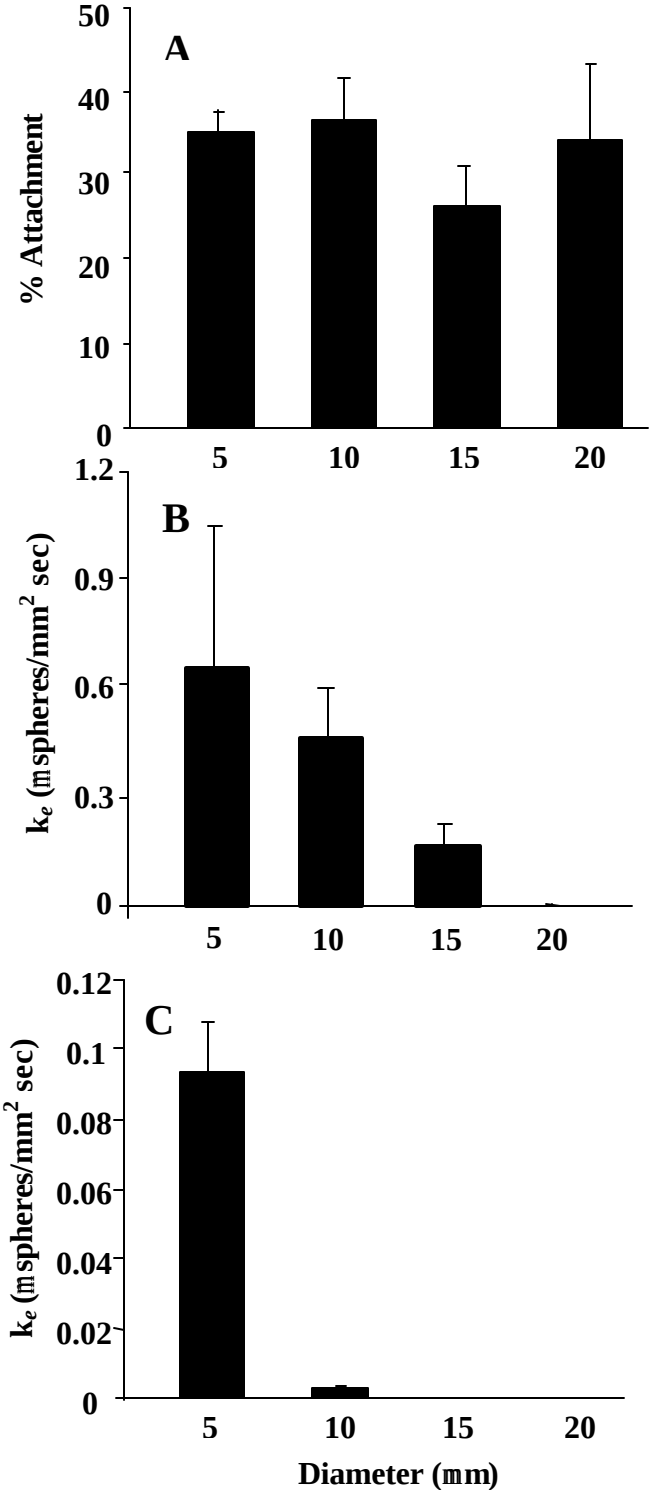
A
% Attachment
50
40
30
20
10
0
5
10
15
20
B
k_e (mspheres/mm^2 sec)
1.2
0.9
0.6
0.3
0
5
10
15
20
C
k_e (mspheres/mm^2 sec)
0.12
0.1
0.08
0.06
0.04
0.02
0
5
10
15
20
Diameter (mm)

Figure 2.3. The shear stress required to set in motion a firmly adherent 19.ek.Fc microsphere decreases with increasing microsphere diameter. 5, 10, 15 and 20 μm 19.ek.Fc microspheres were allowed to attach to the P-selectin substrate for 10 minutes at 0.5 dynes/cm^2. Subsequently, the shear stress was increased in a stepwise fashion. 19.ek.Fc microspheres which did not exhibit motion in the direction of flow were scored as firmly adherent. The percentage of firmly adherent 19.ek.Fc microspheres was plotted as a function of the shear stress. Multiple factor ANOVA indicated that % firmly adherent was a function of microsphere diameter ($p < 0.01$) and this effect was coupled to the level of fluid shear ($p < 0.01$). (Legend: circles represent 5 μm microspheres, boxes represent 10 μm microspheres, triangles represent 15 μm microspheres and crosses represent 20 μm microspheres. $n \geq 5$ replicates shown; Error bars represent SEM).

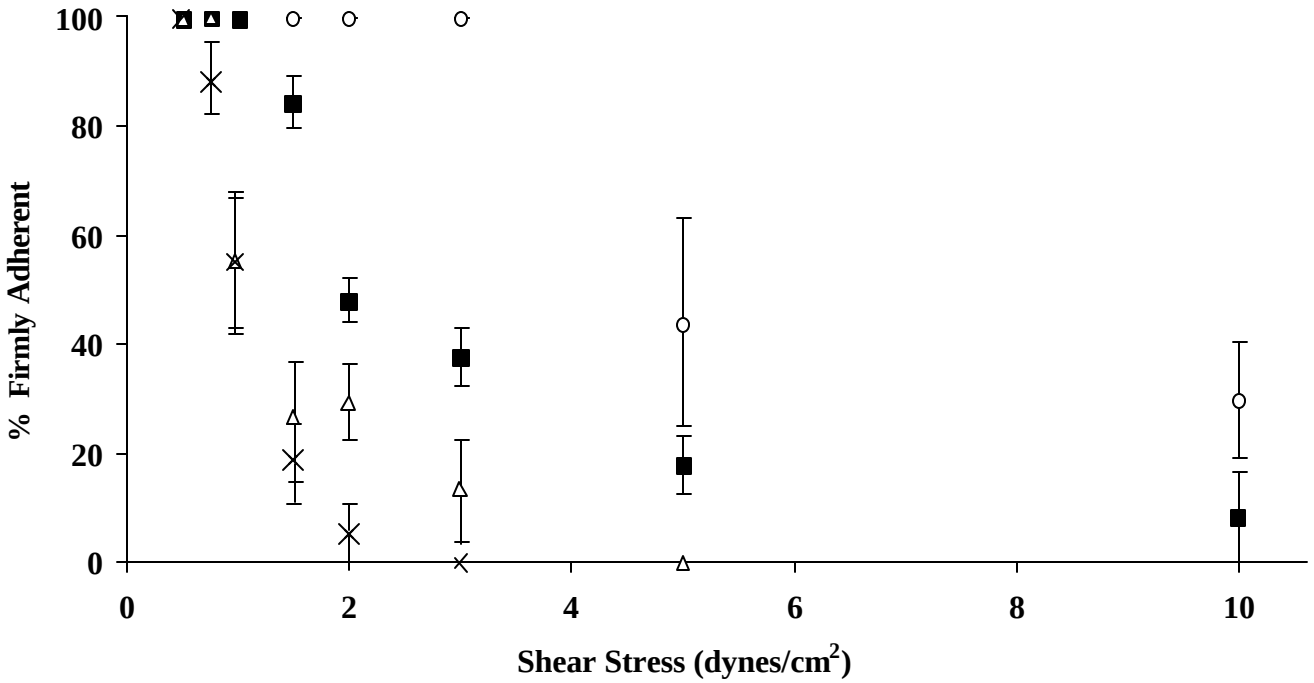
100
80
60
40
20
0
% Firmly Adherent
0
2
4
6
8
10
Shear Stress (dynes/cm2)

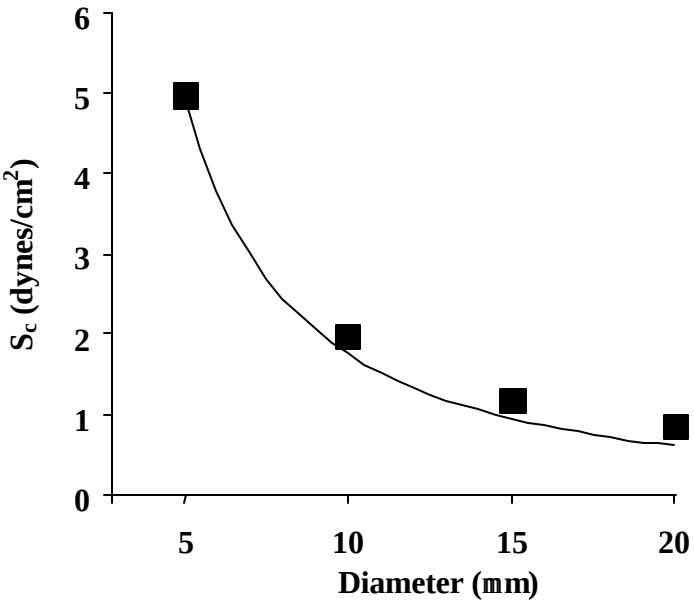

Figure 2.4. A comparison of experimental and critical shear stress Sc values. The critical shear, Sc, was estimated from the data shown in Figure 2.3. These values were than plotted (the black squares) as a function of microsphere diameter. The line depicts a theoretical curve developed as described in the discussion section using the relationship of Cozens-Roberts et al. (17), $Sc = K (\sin \Theta)^3$. Note that the experimental data closely follows the theoretical curve. Please refer to the Appendix section A-1 for more details on the calculation.

Figure 2.5. The rolling velocity of the 19.ek.Fc microspheres increases with increasing microsphere diameter. The rolling velocity of the 19.ek.Fc microspheres which were not firmly adherent to the P-selectin substrate was determined. In general, the rolling velocity appears to increase with microsphere diameter. Multiple factor ANOVA indicated that the rolling velocity was a function of microsphere diameter ($p < 0.01$) and this effect was coupled to the level of fluid shear ($p < 0.01$). (Legend: circles represent 5 μm microspheres, boxes represent 10 μm microspheres, triangles represent 15 μm microspheres and crosses represent 20 μm microspheres. $n \geq 5$ separate experiments with ≥ 6 microspheres analyzed at each shear stress in a given experiment; Error bars represent SEM).

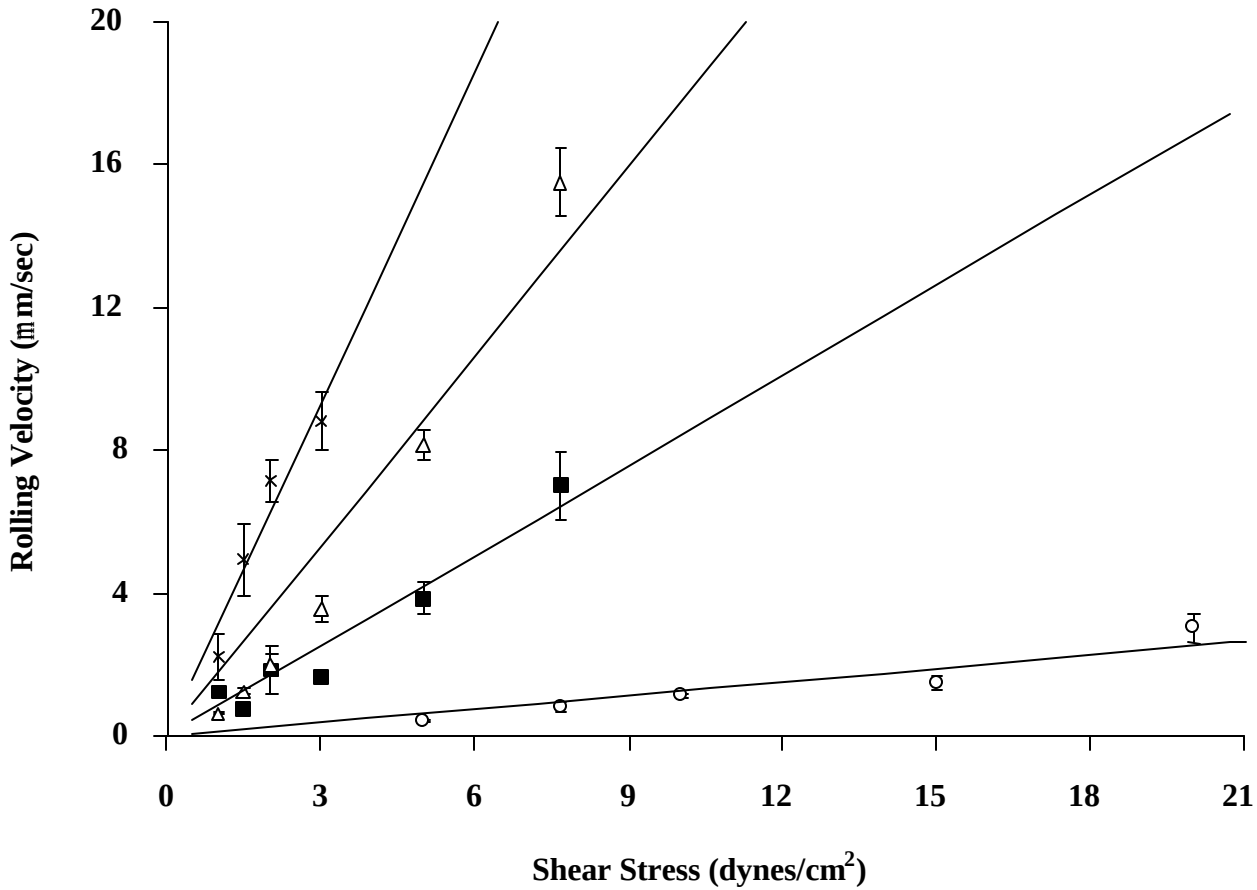
20
16
12
8
4
0
Rolling Velocity (mm/sec)
0
3
6
9
12
15
18
21
Shear Stress (dynes/cm2)

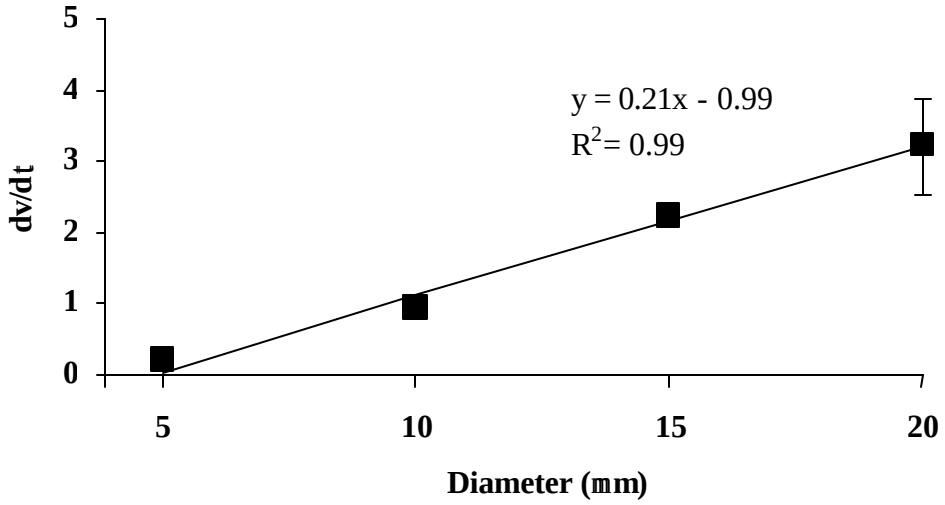

Figure 2.6. The change in the rolling velocity with fluid shear increases with microsphere diameter. Linear regression was performed on the data presented in Figure 2.5. The slopes of these regression lines were plotted as a function of the microsphere diameter. Linear regression was performed on this data. The slope was found to be 0.21 +/-0.15 (slope +/- 95% confidence interval) indicating that the change in the rolling velocity with fluid shear significantly increases with increasing microsphere diameter. (Error bars indicate 95% confidence interval on slopes determined using regression on the data in Figure 2.5.)

CHAPTER 3

MICROSPHERES COATED WITH MAC-1 PURIFIED FROM LEUKOCYTE LYSATES ADHERE TO 4 HR. IL-1 ACTIVATED HUVEC VIA TWO DISTINCT MECHANISMS

Introduction

Broad context: A critical component of many physiological and pathological processes is the adhesion of leukocytes to the endothelium in the fluid dynamic environment of the circulatory system (1-4). During the past 15 years, it has been revealed that leukocyte adhesion to the endothelium occurs through a cascade of adhesive events (2, 4-8) orchestrated by receptor-ligand interactions that cause initial attachment of these cells to the endothelial lining (also known as initial tethering), rolling along the endothelial surface, subsequent firm adhesion or arrest and ultimately, migration of these cells through endothelial spaces into the extravascular space (extravasation or transendothelial migration) (5).

Inducible endothelial cell adhesion molecules are involved in neutrophil recruitment: Central to this adhesion cascade is the concept of endothelial cell activation and inducible endothelial cell adhesion molecules. Using an *in vitro* model of endothelial cells, namely endothelial cells isolated from human umbilical veins (HUVEC), Bevilacqua et al. demonstrated that exposure of HUVEC to inflammatory mediators such as IL-1, TNF-α or certain gram-negative endotoxins results in the surface expression of an endothelial

cell adhesion molecule now termed E-selectin (CD62E) (9, 10). E-selectin expression requires *de novo* protein synthesis and occurs after approximately 2 hours of treatment with activating inflammatory mediators (10). E-selectin expression peaks between 3-5 hours after initial activation and ultimately diminishes to close to the basal (no expression) level by 24 hours after initial activation (10). Other endothelial cell adhesion molecules can also be upregulated by inflammatory mediators. In particular, the expression of intercellular adhesion molecule-1 (ICAM-1, CD54), which is expressed at a low level on unactivated HUVEC, is upregulated in response to inflammatory mediators (4, 11). Similar to E-selectin expression, increased ICAM-1 expression requires *de novo* protein synthesis and occurs after several hours of treatment with activating cytokines (11). In contrast to E-selectin, however, ICAM-1 expression occurs more slowly and remains at close to peak levels 24 hours after initial activation (11). Other endothelial cell adhesion molecules are also involved in leukocyte adhesion to the endothelium and include P-selectin (CD62P) (12), vascular endothelial cell adhesion molecule - 1 (VCAM-1) (3, 11), and ICAM-2 (3, 11).

Adhesion molecules involved in neutrophil attachment and rolling on the endothelium: Both *in vivo* and *in vitro* studies strongly suggest that P-selectin and E-selectin are involved in neutrophil initial attachment and rolling on activated vascular endothelium (5, 13-18). P- and E-selectin are two members of the selectin family of adhesion molecules; the third known member being L-selectin (CD62L). A notable feature of the selectins is their N-terminal, lectin-like domain which binds carbohydrate moieties in a Ca^{2+}

dependent manner (11). Thus, several carbohydrate ligands for P- and E-selectin have been proposed including the sialyl Lewis x (SLe^X) tetrasaccharide and related glycans (19-21).

Recent studies have focused on identifying the underlying proteins that present carbohydrate ligands for binding to E- and P-selectin. P-selectin glycoprotein ligand-1 (PSGL-1) is present on a variety of leukocyte sub-types, carries SLe^x and appears to be the primary leukocyte ligand for P-selectin (13, 15, 22-27). Although several ligands for E-selectin have been proposed, including PSGL-1 (13, 28), L-selectin (CD62L) (13, 29, 30), E-selectin ligand - 1 (ESL-1) (31, 32), CD66 nonspecific cross-reacting antigens (33), CD43 (34), and CD44 (35) to date, no single leukocyte adhesion molecule has been demonstrated to be the primary ligand for E-selectin.

The above listed proposed ligands for E-selectin are similar in that they all express sialylated fucosylated glycans (SLe^X-type glycans). Several lines of evidence suggest that SLe^x alone may be sufficient to mediate adhesion to E-selectin. Indeed, microspheres coated with SLe^x attach and roll on E-selectin (36, 37); transfection of human cell lines with α (1,3) fucosyltransferase (e.g. FucT-VII) confers the ability to recognize and attach to E-selectin under flow (38-40); and cell lines expressing E-selectin attach and roll on planar surfaces coated with glycolipids presenting SLe^X-type glycans (41). Combined, these studies strongly suggest that SLe^X-type glycans alone are sufficient to mediate attachment and rolling on E-selectin.

The integrins are a family of non-covalently associated heterodimeric glycoproteins consisting of an α and a β chain (4, 42). The β_2 integrins are unified in their common β chain, CD18, and have distinct α chains. The leukocyte β_2 integrins include LFA-1 (CD11a/CD18), Mac-1 (CD11b/CD18), p150,95 (CD11c/CD18) (4) and αd/CD18 (CD11d/CD18) (43). Based on the observations described in the above paragraph and the fact that the leukocyte β_2 integrins carry SLe^x (44), it is reasonable to suspect that β_2 integrin - E-selectin molecular interactions are involved in leukocyte adhesion to the endothelium. As argued previously by Crutchfield et al. (45), there are data both refuting and supporting this conjecture.

Data refuting this notion include the observations that neutrophils treated with mAbs to CD18 do not exhibit a reduction in accumulation over IL-1 activated HUVEC (7) or purified E-selectin (46), and neutrophils isolated from patients deficient in β_2 integrins retain the ability to attach to IL-1 activated HUVEC (7) . These findings seem to discount the role of β_2 integrins in mediating adhesion to E-selectin. However, there are several caveats to drawing this conclusion, including the following. First, the lack of inhibition by these mAbs may be due to the mAbs recognizing peptides while the adhesion occurs through a carbohydrate. Second, a variety of neutrophil glycoproteins may in fact bear glycans, that may be able to mediate adhesion to E-selectin. Thus, the number of E-selectin counter-receptors present on the neutrophil may be in significant excess of that which is actually needed to mediate adhesion to E-selectin. In this event, one might anticipate that elimination of any one of these adhesive mechanisms may have

little effect on adhesion. Indeed, as suggested or revealed by a number of biochemical assays, a variety of leukocyte glycoproteins recognize E-selectin. Thus, the elimination assays are somewhat ambiguous and do not rule out the possibility of the involvement of β_2 integrins in adhesion to E-selectin.

Data supporting a role for β_2 integrin - E-selectin molecular interactions include the observations that microspheres coated with Mac-1 attach to E-selectin under *in vitro* flow conditions (45), both Mac-1 and LFA-1 recognize E-selectin in biochemical recognition assays (47), CD18-deficient neutrophils demonstrate elevated rolling velocities over IL-1-stimulated endothelium (49), and leukocytes roll with increased velocities in TNF-α treated CD18 deficient mice (48). While these latter two observations could be attributed to interactions of β_2 integrins with endothelial cell adhesion molecule distinct from E-selectin, these observations are also consistent with the hypothesis that the interactions of β_2 integrins with E-selectin lead to a reduction in rolling velocities of leukocytes on cytokine activated endothelium.

Thus, there are data both refuting and supporting a role for β_2 integrin – E-selectin molecular interactions in leukocyte adhesion to the endothelium. The hypothesis that we have previously investigated is that β_2 integrin – E-selectin molecular interactions do play a role in leukocyte adhesion to the endothelium (45). We probed this hypothesis by coating leukocyte-sized polystyrene microspheres with Mac-1 purified from human leukocytes and studied the adhesion of the resulting Mac-1 microspheres to cellular

substrates under *in vitro* flow conditions. A full discussion of the motivation for using the Mac-1 microspheres to probe this hypothesis has been described in our previous study. In that study (45), we found that Mac-1 microspheres do indeed *attach, i.e. bind from the free stream*, to cellular expressed E-selectin under physiologically relevant shear stress conditions; thus bolstering the above hypothesis.

Molecular mechanisms involved in neutrophil firm arrest on the endothelium: Subsequent to attachment and rolling, the neutrophil may arrest and spread on the endothelium. These steps are mediated in part by integrins on the surface of the neutrophil (5, 6, 50). The transition from rolling to firm adhesion requires neutrophil activation and involves a family of chemotactic cytokines termed chemokines (4, 5, 8, 51, 52). A current working hypothesis is that as the neutrophil rolls along the endothelium it is exposed to chemokines bound to the endothelium (4). Exposure to the chemokines activates the neutrophil that leads to a variety of changes including an increased adhesiveness of the neutrophil for the endothelium. This increased adhesiveness appears to be due, in part, to an up-regulation of LFA-1 and Mac-1 adhesion mechanisms (4, 53). Neutrophil integrin LFA-1 has previously been implicated in neutrophil firm adhesion to the endothelium (54-56) via its interactions with endothelial-expressed ligands ICAM-1, ICAM-2 and ICAM-3 (57), while integrin Mac-1 mediates neutrophil adhesion through interactions with ICAM-1, ICAM-2 and other undefined endothelial ligand(s) (56-59). It has been shown that LFA-1 expression on resting neutrophils, which is high compared to the level of expression of Mac-1, does not change upon neutrophil activation (53). Thus,

the increase in the LFA-1 adhesion mechanism appears to be due to a qualitative change in the adhesiveness of LFA-1 for ICAM-1 rather than a quantitative change in the amount of LFA-1 expressed on the surface of the neutrophil (60, 61). In contrast, Mac-1 exhibits a greater than ten-fold quantitative increase of expression on the cell surface after stimulation (53). This up-regulation occurs through translocation of Mac-1 containing secretory granules to the cell surface (53). However, this change in level of expression of Mac-1 does not appear to coincide with increased adhesion via Mac-1 (53). Thus, it has been hypothesized that Mac-1, similar to LFA-1, can exist in an active (able to bind ligand) and an inactive (not able to bind ligand) conformation (62). Indeed, mAb, CBRM1/5 that recognizes an activation-specific neo-epitope on Mac-1 has been described (53, 62). This mAb recognizes Mac-1 on activated neutrophils but does not recognize Mac-1 on resting myeloid cells (53, 62).

We previously demonstrated that native Mac-1 coated microspheres attach to 4 hr IL-1 activated human umbilical vein endothelial cells (HUVEC) via E-selectin under flow (45). Previous studies have highlighted the role of Mac-1 in mediating neutrophil firm adhesion thorough interactions with ICAM-1, ICAM-2 and other undefined endothelial ligands (56-59). Preliminary studies with Mac-1 in our laboratory not only corroborated this latter observation but when coupled with results of our previous study (45), led us to pose the following hypothesis: leukocyte sized particles coated with native Mac-1 purified from leukocytes adhere to 4 hr. IL-1β activated HUVEC via a multi-step process involving at least two mechanisms with distinct apparent kinetics. We probed this

hypothesis by generating leukocyte sized (10μm) microspheres coated with native Mac-1 (in a functionally active conformation) and recombinant Mac-1, and examining their adhesion to un-activated and 4 hr IL-1 activated HUVEC under two different shear stresses.

Materials and Methods

Materials: Medium199, fetal bovine serum (FBS), L-glutamine, trypsin-versene and penicillin streptomycin were obtained from BioWhittaker (Walkersville, MD). Endothelial mitogen was obtained from Biomedical Technologies Inc. (Stoughton, MA). Gelatin was from Difco Labs (Detroit, MI). Heparin, dimethyl sulfoxide (DMSO), sodium bicarbonate, O-phenylenediamine (OPD) and human IgG_1 were from Sigma Chemical Co. (St. Louis, MO). Interleukin–1β (IL -1β) was from Calbiochem (La Jolla, CA). HBSS (Hanks Balanced Salt Solution) with Ca^+ and Mg^+ ($HBSS^+$) or without ($HBSS^-$) were also from BioWhittaker (Walkersville, MD). Bovine Serum Albumin, BSA (Sigma, St. Louis, MO) was added to $HBSS^+$ to generate HBSS+, 1%BSA blocking buffer that was heated-treated in a water bath at 60^oC for 25 minutes. A *Tris* buffer, pH 7.3, containing 150 mM NaCl, 2mM $MgCl_2$ and 25 mM Trizma base (Sigma, St. Louis, MO) was used to dilute native and recombinant Mac-1 (CD11b/CD18), and LFA-1 (CD11a/CD18). Native Mac-1 purified from leukocyte lysates (56) was generously provided by Dr. Charles A. Parkos (Emory University, Atlanta, GA). Recombinant Mac-1 and LFA-1 were obtained from Genentech Inc. (San Francisco, CA). 10μm polystyrene microspheres [P (S/2%DVB)] with a standard deviation of 0.10μm were purchased from Bangs Laboratories Inc. (Fishers, IN).

Antibodies: The following purified murine monoclonal antibodies (mAbs) were employed against Mac-1 (CD11b/CD18) and LFA-1 (CD11a/CD18): TS1/18 (anti-CD18, IgG_1; Endogen, Woburn MA), 44 (anti - CD11b; IgG_1; R & D Systems, Minneapolis, MN), LM2/1 (anti - CD11b (63); IgG_1), CBRM1/5 (anti-activation-specific neoepitope of CD11b/CD18 (63); IgG_1), CBRM1/29 (anti - CD11b (63); IgG_1) and TS1/22 (anti-CD11a; IgG_1; Endogen). The following purified murine monoclonal antibodies were employed on HUVEC: HEL3/2 (anti-E-selectin; IgG_1: Dr. Raymond Camphausen, Genetics Institute, Cambridge MA), R6.5 (anti-ICAM-1; IgG_{2a}: Boehringer Ingelheim Corp., Ridgefield CT), and B-T1 (anti-ICAM-2; IgG: Serotec, Raleigh NC). Unlabeled goat IgG $F(ab')_2$, employed to block non-specific binding of labeled secondary to microspheres employed in flow cytometric analysis and fluorescein isothiocynate (FITC)-labeled goat $F(ab')_2$ anti-mouse IgG Fc-specific polyclonal antibody to detect primary mAbs in the flow cytometric analysis, were both obtained from Jackson Immunoresearch Labs (Westgrove, PA). Peroxidase-conjugated goat anti-mouse (heavy and light chain specific) $F(ab')_2$ polyclonal antibody employed in enzyme-linked immunosorbent assays (ELISA) was from Calbiochem (La Jolla, CA).

Cell culture and substrate preparation for flow assays: Human Umbilical Vein Endothelial Cells (HUVEC) were purchased from Clonetics (San Diego, CA) and cultured as described (45). Cell culture media for culturing HUVEC was prepared by adding heparin (0.05g) and endothelial mitogen (0.025g) to 500 ml Medium 199 containing 10% FBS, 1% L-glutamine and 0.4% penicillin streptomycin. Cryo-preserved

HUVEC were thawed, washed in cell culture media and transferred to gelatin coated-75mm^2 tissue culture flasks (T-flasks). Upon reaching confluence, cells were harvested from confluent T-flasks by washing twice in HBSS$^-$ and treating them with trypsin-versene that facilitates their cleavage from T-flasks. The cells were diluted to a desired concentration in HUVEC culture media and transferred to new gelatin coated T-flasks to maintain passage, or to gelatin coated- 35 mm culture dishes to be employed in adhesion studies. In some instances, HUVEC were also transferred to gelatin coated-96-well plates for enzyme-linked immunosorbent assays (ELISA). E-selectin and ICAM-1 expression on HUVEC monolayers was induced by pre-treating HUVEC with 50 U/mL of IL-1β for four hours prior to being employed in the adhesion studies.

Preparation of native and recombinant Mac-1, and LFA-1 microspheres: The technique for generating ligand (native Mac-1, recombinant Mac-1 or recombinant LFA-1) -coated microspheres was similar to that described previously (45). Briefly, 10 μm microspheres were washed twice in *Tris* buffer (150 mM NaCl, 2mM $MgCl_2$, and 25 mM Trizma base, pH 7.3) and incubated either in native Mac-1 (diluted 1:10 in *Tris* buffer), recombinant Mac-1 (50μg/mL in *Tris* buffer) or recombinant LFA-1 (50μg/mL in *Tris* buffer), overnight at 4^{o}C. The addition volume of native Mac-1 to 10μm microspheres was 1mL per 10^7 microspheres, while recombinant Mac-1 and LFA-1 were added at 5μL per 10^6 microspheres. These addition volumes and reagent dilutions were optimized through titration and flow cytometric analysis to yield significant and equivalent ligand densities of recombinant and native molecules on the ligand-coated microspheres. Following an

overnight incubation at 4^0C, the microspheres were washed and resuspended to $1x10^8$ microspheres/mL in heat-treated HBSS, + 1% BSA (blocking buffer) the next day. Prior to perfusion through the parallel plate flow chamber, ligand-coated microspheres were diluted to $5x10^5$/mL in assay buffer (heat-treated HBSS, + 0.5%BSA).

Monoclonal antibody (mAb) blocking on Mac-1 and LFA-1 coated microspheres and HUVEC monolayers: The specificity of adhesive interactions between native Mac-1, recombinant Mac-1 or recombinant LFA-1 microspheres and HUVEC was determined through a series of monoclonal antibody (mAb) blocking experiments. Native and recombinant Mac-1 coated microspheres were pre-treated, at room temperature, with anti-Mac-1 mAbs, CBRM1/29, TS1/18 and LM2/1 (diluted to 10μg/ml in blocking buffer) while LFA-1 microspheres were pre-treated with an anti-LFA-1 mAb, TS1/22 employed at the same concentration. HUVEC monolayers were separately subjected to mAb blocking treatments and incubated at 37^oC, in anti-E-selectin mAb (HEL3/2), anti-ICAM-1 mAb (R6.5), or anti-ICAM-2 mAb (B-T1) diluted to 20μg/mL in HUVEC culture media. mAbs were either used individually or in conjunction with each other. Note that in every instance, ligand-coated microspheres or HUVEC were incubated in these mAbs for at least 15 minutes prior to employing them in adhesion assays.

Flow cytometric analysis: Aliquots of ~ $2x10^5$ native Mac-1, recombinant Mac-1 or recombinant LFA-1 coated microspheres were washed twice in heat-treated HBSS +, 1% BSA blocking buffer and incubated in 40μL primary antibodies (mAbs 44, CBRM1/5,

TS1/18, TS1/22 and LM2/1) diluted to 20μg/mL in blocking buffer for 20 minutes at room temperature. After one wash, the microspheres were blocked for 10 minutes with unlabeled goat $F(ab')_2$ fragment (1:100), followed by a 20 minute incubation at room temperature with an FITC-labeled polyclonal antibody (1:25) which facilitates detection of bound primary mAbs during flow cytometric analysis. Following this twenty-minute incubation, the microspheres were washed thrice in blocking buffer, and fixed in 1% formaldehyde until further use. Fluorescence levels on these ligand-coated microspheres were quantified via flow cytometry by plotting fluorescence histograms on a four-decade scale.

Enzyme linked immunosorbent assays (ELISA): HUVEC coated on 96 well plates were activated separately for 4 hrs and 24 hrs with 50 U/mL IL-1, which induces expression of a variety of endothelial cell adhesion molecules. Following activation, the cells were washed with $HBSS^+$ and held in HUVEC culture media at 4^0C for at least 30 minutes. The culture media was withdrawn and 40μL primary mAbs (R6.5, TS1/22 and HEL3/2), diluted to 20 μg/mL in culture media were added to HUVEC for 20 minutes at 4^0C. Residual unbound primary mAbs were removed through subsequent HUVEC washes in cell culture media. The cells were then held in 40μL peroxidase-conjugated secondary antibody for 20 minutes at 4^0C. Following a series of washes to remove unbound secondary antibody, HUVEC were incubated in *o*-phenylenediamine (OPD) that enables detection of surface proteins through quantification of absorbance levels at 450nm on a plate reader.

Description of the flow assembly and analysis of adhesion data: The parallel plate flow chamber (Glycotech; Rockville, MD) employed in this study is similar to that used by McIntire, Smith and colleagues (64) and consists of a plexiglass flow deck that fits inside a 35 mm tissue culture dish (Appendix A-2). Our particular flow set-up has been described previously (65). In brief, the flow field is defined by a gasket which sits between the flow deck and the 35 mm dish. The shear stress at the bottom surface of the flow chamber is given by $\tau = 3Q\mu/2wh^2$ where Q is the volumetric flow rate, μ is the viscosity, 2 h is the height (0.2 mm) of the flow field, and w is the width (0.5 cm) of the flow field. The volumetric flow rate was therefore adjusted to obtain the desired shear stress. Experiments were performed either at room temperature (24^oC) or at 37 ^0C (maintained by a heating plate). After assembly, the flow chamber was placed on an inverted microscope connected to a CCD videocamera, VCR and monitor that enable data acquisition for subsequent analysis.

After rinsing the 35 mm culture dish with heat-treated assay buffer (HBSS, + 0.5 % BSA) and allowing the substrate to equilibrate under flow, ligand-coated microspheres ($5x10^5$ /mL) were perfused separately over HUVEC coated culture dishes at requisite shear stresses for 2.5 minutes. Microsphere accumulation over eight fields of view was recorded *at the end of* the perfusion interval to yield total firmly adherent microspheres. In some instances, microspheres that attached from the free stream to HUVEC *during* the 2.5-minute perfusion interval were quantified and only adhesion events in the visible field of view were considered. This enabled an examination of Mac-1 microspheres

undergoing primary attachments over the entire duration of flow. Microspheres that did not display any motion during the entire duration of the flow period were designated as firmly adherent while those that traversed in the direction of flow were marked as rolling. The experiments were repeated at least three times.

Statistics: Statistical differences between experimental data were evaluated using either the one-tailed Student's T-test or analysis of variance (ANOVA) for multiple data sets. ANOVA was used in conjunction with Bonferroni's test to identify differences in the means of multiple data sets. In all instances, comparisons with p values ≤ 0.05 were considered statistically significant. All error bars represent SEM unless otherwise noted.

Results

Characterization of native Mac-1, recombinant Mac-1 and recombinant LFA-1 coated 10mm microspheres

Prior to adhesion studies, we performed flow cytometry on the ligand-coated microspheres. In a previous study reported by our laboratory (45), native Mac-1 microspheres generated using techniques similar to this study, were shown to express surface densities of accessible extracellular Mac-1 similar to that present on neutrophils. In the present study (Figure 3.1), levels of Mac-1 expression on 10μm microspheres coated with native Mac-1 (purified from leukocyte lysates) (panel a) were similar to those observed on native Mac-1 microspheres generated under similar conditions in our previous study. The present study also employed 10μm microspheres coated with recombinant Mac-1 (panel c) and recombinant LFA-1 (panel e). As seen in Figure 3.1, surface density of recombinant Mac-1 on the microspheres (panel c) was found to be similar to that of native Mac-1 (panel a), while surface density of recombinant LFA-1 was slightly higher than that of native and recombinant Mac-1 (panel e). Furthermore, employing a monoclonal antibody to the activation specific neoepitope of CD11b/CD18 (63) showed that the entire surface expressed native Mac-1 (panel b) and recombinant Mac-1 (panel d) on these microspheres, was present in a functionally active conformation.

Characterization of HUVEC

We also performed an enzyme linked immuno-sorbent assay (ELISA) on un-activated, 4 hr. and 24 hr. IL-1 activated HUVEC to characterize expression of endothelial expressed adhesion molecules E-selectin and ICAM-1 on our stock of un-activated and IL-1 activated HUVEC. Several laboratories (66) have previously reported that (a) un-activated HUVEC express a basal level of ICAM-1 but no E-selectin (b) 4 hr treatment of HUVEC with IL-1β elicits the expression of E-selectin and greatly increases the expression of ICAM-1 and (c) the expression of E-selectin peaks around 4 hrs post-activation and returns to near baseline levels 24 hrs post-activation while the expression of ICAM-1 remains elevated 24 hrs post-activation. Figure 3.2 shows that the HUVEC used in the present studies behave in a manner similar to that reported in literature. A low but detectable level of ICAM-1 is present on un-activated HUVEC and the expression of ICAM-1 is increased at 4 and 24 hrs post-treatment with IL-1β. E-selectin was not detected on un-activated HUVEC, detected on 4 hr activated HUVEC and detected on 24 hr. HUVEC, although at a much lower level than that detected on 4 hr activated HUVEC.

10mm microspheres coated with Mac-1 purified from leukocyte lysates (native Mac-1) undergo firm adhesion to 4 hr. IL-1 activated HUVEC, almost entirely via E-selectin and an epitope on Mac-1 mapped by mAb CBRM1/29

Native Mac-1 coated microspheres were perfused over un-activated and 4 hr IL-1 activated HUVEC monolayers at 1.8 dynes/cm^2 and demonstrated significant adhesion to HUVEC monolayers under flow. Their adhesion to HUVEC was characterized by two distinct adhesive events: (1) initial attachment and rolling and (2) firm adhesion. The former microsphere interactions involving microspheres attaching from the free stream to HUVEC monolayers (initial attachment) and translating along the monolayers with low velocities (rolling) were designated as *primary attachments*. Microspheres undergoing *both* adhesive events, namely attachment/rolling and subsequent firm adhesion, were designated as *firmly adherent*. As shown in Figure 3.3, a substantial number of firmly adherent native Mac-1 microspheres were observed over 4 hr IL-1 activated HUVEC. When perfused over un-activated HUVEC and 4 hr IL-1 activated HUVEC pre-treated with a functional blocking monoclonal antibody (mAb) to E-selectin, HEL3/2, the numbers of firmly adherent microspheres were ~70% and ~65% lower than those observed over un-treated 4 hr IL-1 activated HUVEC. Pre-treatment of Mac-1 microspheres with an anti-Mac-1 mAb, CBRM1/29 also caused a major reduction (~85%) in the number of firmly adherent Mac-1 microspheres compared to un-treated Mac-1 microspheres, while pre-treatment with a control anti-Mac-1 mAb, LM2/1 showed no statistically significant effect on the adhesion.

Previous reports have indicated that endothelial adhesion molecules ICAM-1 and ICAM-2 might serve as endothelial counter-receptors for Mac-1 in mediating leukocyte adhesion to the endothelium (56-59). To identify the role of endothelial cell adhesion molecule ICAM-1 in mediating Mac-1 microsphere adhesion to 4 hr. IL-1 activated HUVEC, HUVEC monolayers were pretreated with an anti-ICAM-1 mAb R6.5 (56), which did not appear to have any effect on the adhesion of Mac-1 coated microspheres. Furthermore, 4 hr. IL-1 activated HUVEC pre-treated with both mAbs HEL3/2 and R6.5 displayed firmly adherent native Mac-1 microspheres at adhesion levels similar to those on 4 hr. IL-1 activated HUVEC blocked by mAb HEL3/2 alone. Pre-treatment of Mac-1 microspheres with mAb CBRM1/29, together with the pre-treatment of 4 hr. IL-1 activated HUVEC with anti-E-selectin mAb HEL3/2, abolished nearly all firmly adherent events, implicating both endothelial expressed E-selectin and an epitope on Mac-1 mapped by mAb CBRM1/29 in mediating native Mac-1 microsphere adhesion to 4 hr. IL-1 activated HUVEC.

Pre-treatment of 4 hr. IL-1 activated HUVEC with an anti-E-selectin mAb HEL3/2 significantly inhibited the primary attachment and firm adhesion of native Mac-1 microspheres, while pre-treatment with an anti-Mac-1 mAb CBRM1/29 only affected their firm adhesion

It is clearly evident from Figure 3.3 that 10μm microspheres coated with native Mac-1 become firmly adherent to 4 hr. IL-1 activated HUVEC through both E-selectin

and an epitope on Mac-1 recognized by the mAb CBRM1/29. To further delineate the roles played by either of these two molecular mechanisms, we reanalyzed all experimental data with 4 hr. IL-1 activated HUVEC pre-treated with an anti-E-selectin mAb HEL3/2 and native Mac-1 coated microspheres pre-treated with an anti-Mac-1 mAb CBRM1/29 at 1.8 dynes/cm^2. Native Mac-1 microspheres that attached from the free stream to 4 hr. IL-1 activated HUVEC during the 2.5-minute perfusion interval, were quantified in the visible field of observation to yield overall primary attachments (black bars). The fraction of these attaching microspheres that underwent subsequent firm adhesion were estimated by quantifying the population of firmly adherent microspheres that accumulated over eight fields of view at the end of the perfusion interval (white bars). As shown in Figure 3.4, over 80% of all native Mac-1 microspheres undergoing primary attachments to 4 hr. IL-1 activated HUVEC (i.e. attaching to the substrate from the free stream and rolling) subsequently underwent firm adhesion. Pre-treating 4 hr. IL-1 activated HUVEC with an anti-E-selectin mAb HEL3/2 resulted in a substantial reduction (~70 %) of native Mac-1 primary attachments to HUVEC monolayers. Note however, that 100% of all native Mac-1 microspheres attaching and rolling on 4 hr. IL-1 activated HUVEC pre-treated with mAb HEL3/2, were converted to firmly adherent microspheres. Importantly, while pre-treatment of native Mac-1 microspheres with the anti- Mac-1 mAb CBRM1/29 had no effect on the primary attachment of these microspheres to 4 hr. IL-1 activated HUVEC, blocking with mAb CBRM1/29 severely inhibited, by about 85%, the ability of the attaching and rolling Mac-1 microspheres to convert to firmly adherent microspheres.

10mm microspheres coated with native Mac-1 adhere to un-activated HUVEC at 1.0 dynes/cm^2

To gain further insight into the role of the CBRM1/29 epitope of Mac-1 in mediating Mac-1 adhesion to HUVEC independent of E-selectin, we perfused 10μm microspheres coated with native Mac-1 over un-activated HUVEC at 1.0 dynes/cm^2. This experimental system was ideally suited to explore this mechanism since no E-selectin expression was detected on un-activated HUVEC (Figure 3.2). The justification for using a lower shear stress (1.0 dyne/cm^2) versus the one employed in studies over 4 hr. IL-1 activated HUVEC is mentioned in the discussion.

As shown in Figure 3.5, native Mac-1 coated microspheres displayed quantifiable levels of attachment, rolling and firm adherence on un-activated HUVEC at 1.0 dyne/cm^2. Pre-treatment of native Mac-1 microspheres with function blocking mAbs to Mac-1, mAbs CBRM1/29 and TS1/18, eliminated nearly all firmly adherent Mac-1 microspheres on un-activated HUVEC while a non-function blocking anti-Mac-1 mAb, LM2/1 had no effect on their adhesion. To determine whether the adhesion of native Mac-1 microspheres to un-activated HUVEC in our system was, in fact, occurring through either ICAM-1 or ICAM-2, we pre-treated un-activated HUVEC with mAbs to ICAM-1 (R6.5) and ICAM-2 (B-T1) and examined their ability to support native Mac-1 microsphere adhesion under flow. As shown in Figure 3.5, pre-treatment of un-activated HUVEC with anti-ICAM-2 mAb B-T1 and anti-ICAM-1 mAb R6.5, employed

individually or together, did not inhibit Mac-1 coated microsphere adhesion to un-activated HUVEC at 1.0 dyne/cm^2.

10mm microspheres coated with recombinant Mac-1 adhere to 4 hr. IL-1 activated HUVEC at 1.8 dynes/cm^2 almost entirely through the epitope on Mac-1 mapped by mAb CBRM1/29

Recombinant Mac-1 microspheres were generated at surface densities similar to those coated with native Mac-1 and then perfused over 4 hr. IL-1 activated HUVEC in a parallel plate flow chamber at 1.8 dynes/cm^2. As shown in Figure 3.6, recombinant Mac-1 microspheres adhere to 4 hr. IL-1 activated HUVEC under flow, albeit at adherence levels lower than those observed with the native Mac-1 molecule. A majority, if not all, of recombinant Mac-1 adhesion to 4 hr. IL-1 activated HUVEC was abolished upon pre-treatment of these microspheres with the anti-Mac-1 mAb CBRM1/29. Furthermore, pre-treatment of 4 hr. IL-1 activated HUVEC with a functional blocking mAb to E-selectin, mAb HEL3/2, had no effect on the adhesion of recombinant Mac-1 microspheres, implying that adhesion of recombinant Mac-1 seemed to occur independently of E-selectin and almost entirely, through an epitope on recombinant Mac-1 mapped by the mAb CBRM1/29 (CBRM1/29 epitope).

10mm microspheres coated with recombinant Mac-1 adhere to un-activated HUVEC at 0.6 dynes/cm^2 through the interactions of the CBRM1/29 epitope with a possibly unidentified endothelial counter-receptor

To further examine the adhesion of recombinant Mac-1 coated microspheres to HUVEC via the E-selectin independent mechanism, we perfused them over un-activated HUVEC at 0.6 dynes/cm^2 (Figure 3.7). Microsphere adhesion was studied at this lower shear stress since insignificant amounts of adherence events were observed at 1.8 (~ 2-3 adherence events per field of view) or even at 1.0 dyne/cm^2 (6-7 adherence events per field of view). As mentioned in the discussion, insufficient levels of interaction hardly justify undertaking a series of mAb blocking experiments to convincingly prove the contribution of the CBRM1/29 epitope in mediating adhesion. We therefore performed our studies at 0.6 dynes/cm^2 and found that at this shear stress, recombinant Mac-1 microspheres show a significant level of firm adhesion to un-activated HUVEC (devoid of E-selectin) and a majority, if not all, of the firmly adherent microspheres were ablated by function blocking mAbs to Mac-1, CBRM1/29 and TS1/18 (Figure 3.7). Employing a non-function blocking anti-Mac-1 mAb LM2/1 also seemed to reduce the adherence events on un-activated HUVEC. To examine whether this adhesion occurred through endothelial expressed ICAM-1, we pre-treated HUVEC monolayers with mAb R6.5, known to inhibit Mac-1 interactions with ICAM-1 (56). Pre-treatment with this mAb however, had no effect on the adhesion of recombinant Mac-1 microspheres to un-activated HUVEC. Microspheres coated with recombinant LFA-1 employed as a control,

displayed significant firm adhesion to un-activated HUVEC and nearly all this firm adhesion was blocked upon pre-treatment of recombinant LFA-1 microspheres with an anti-LFA-1 mAb TS1/22 or pre-treatment of un-activated HUVEC with anti-ICAM-1 mAb, R6.5.

Discussion

As argued by Crutchfield et al. (45), using leukocytes to elucidate a detailed understanding of Mac-1 mediated adhesion to E-selectin expressing HUVEC is cumbersome due to the fact that several leukocyte ligands may interact with E-selectin (e.g. PSGL-1 (13, 28), ESL-1 (31, 32, 67), L-selectin (13, 29, 30) and CD44 (35)), and Mac-1 may bind to several endothelial cell adhesion molecules (potentially ICAM-1, and other undefined ligands (56)). There is also a temporal overlap of these molecular interactions in that many of these interactions may occur simultaneously. In addition to these molecular complexities, as the leukocyte is adhering to the endothelium, it may become activated which alters the shape of the leukocyte as well as the quality and quantity of leukocyte ligands present on the surface. These issues lead to difficulties in characterizing the Mac-1 - endothelial cell ligand(s) interactions and in identifying endothelial expressed Mac-1 ligands. A transfection approach is complicated by the fact that co-transfection of the cDNA for Mac-1 along with a fucosyltransferase would most likely be necessary to generate Mac-1 which is similar to native Mac-1, i.e. which contain SLe^X type glycans. This leads to the caveat of potential alteration of other cell surface molecules, via the fucosyltransferase, to the extent that they may be able to interact with E-selectin (38-40, 68).

These considerations have led us to probe Mac-1 interactions with E-selectin expressing HUVEC using Mac-1 coated microspheres as described in a previous study

(45). Note that, full-length integrins immobilized on solid supports have been used extensively to generate insightful data (56, 62, 69). In addition, the ligand coated microsphere approach is becoming a fairly common technique for probing leukocyte adhesion to the endothelium (28, 36, 37, 45, 65, 70-73). Not only does this technique circumvent the above listed issues, but using this approach allows tight control over the conditions under which Mac-1 is brought into contact with the endothelium and the forces exerted on the Mac-1 - endothelial cell bonds subsequent to adhesion. Such control is not only convenient but most likely necessary to elucidate a detailed understanding of Mac-1 mediated adhesion to the endothelium.

In this study, we therefore generated 10μm microspheres coated with native Mac-1 and recombinant Mac-1, and studied their adhesion to HUVEC in an *in vitro* physiologically relevant fluid dynamic environment. We categorized the observed Mac-1 microsphere adhesion to HUVEC into two separate adhesive events: events where microspheres attached to substrates from the free stream (attached) and rolled on substrates were characterized as primary attachments whereas, microspheres that attached, rolled and subsequently firmly adhered to these substrates were designated as firmly adherent. This distinction was crucial to our understanding of the two mechanisms by which leukocyte-sized microspheres coated with Mac-1 (native and recombinant) interact with 4 hr. IL-1 activated HUVEC.

Our data in Figure 3.3 showed a near two-thirds reduction in firmly adhering native Mac-1 microspheres over un-activated HUVEC and 4 hr. IL-1 activated HUVEC monolayers pre-treated with a monoclonal antibody (mAb) to the lectin domain of E-selectin (HEL3/2), compared to un-treated 4 hr. IL-1 activated HUVEC monolayers. The absence of E-selectin expression on un-activated HUVEC seen with ELISA (Figure 3.2), coupled with the known anti-E-selectin function blocking activity of mAb HEL3/2, allowed us to sufficiently conclude that the firmly adherent native Mac-1 microspheres over un-activated HUVEC and HEL3/2-treated 4 hr. IL-1 activated HUVEC were in fact mediated by interactions 'independent of E-selectin'. Note that all native Mac-1 microspheres undergoing primary attachments over 4 hr. IL-1 activated HUVEC pre-treated with HEL3/2, or in other words, via the E-selectin independent mechanism, become firmly adherent (Figure 3.4). Taken together, these data strongly indicate that Mac-1 microspheres interact with 4 hr. IL-1 activated HUVEC via an E-selectin-independent mechanism that is characterized by firmly adherent microspheres.

In addition to the E-selectin independent mechanism, there is also evidence (Figure 3.3) for an additional mechanism through which native Mac-1 coated microspheres might undergo adhesion to 4 hr. IL-1 activated HUVEC. Pre-treatment of native Mac-1 microspheres with a mAb to the I-domain of Mac-1 (CBRM1/29) specifically eliminated a majority of the firmly adherent microspheres over 4 hr. IL-1 activated HUVEC, implying a role for the epitope mapped by CBRM1/29 (henceforth designated as the CBRM1/29 epitope) in mediating Mac-1 adhesion to activated

endothelium (Figure 3.3). Interestingly, pre-treatment of native Mac-1 microspheres with mAb CBRM1/29 had no effect on their primary attachment to 4 hr. IL-1 activated HUVEC but instead, significantly altered their ability to convert to firmly adherent microspheres (Figure 3.4). This explains the observed overall reduction in firmly adherent microspheres over 4 hr. IL-1 activated HUVEC following Mac-1 microsphere treatment with mAb CBRM1/29, seen in Figure 3.3. These data therefore clearly indicate that Mac-1 microspheres undergo significant primary attachment, but minor firm adherence, to 4 hr. IL-1 activated HUVEC via a mechanism mediated 'independently of the CBRM1/29 epitope'.

Furthermore, a near complete removal of all Mac-1 primary attachment and firm adherence to 4 hr. IL-1 activated HUVEC upon Mac-1 microsphere pre-treatment with CBRM1/29 together with 4 hr. IL-1 activated HUVEC pre-treatment with anti-E-selectin mAb HEL3/2 not only indicates that these two mechanisms mediate a majority, if not all, of the Mac-1 adhesion, but that these two mechanisms might in fact be mutually exclusive. In other words, one mechanism is E-selectin independent but CBRM1/29 epitope dependent and characterized by firmly adherent microspheres and the second is CBRM1/29 epitope independent and E-selectin dependent and characterized by attaching and rolling microspheres that do not undergo firm adherence.

This latter mechanism has been previously explored in a study (45) demonstrating that the Mac-1-E-selectin bond has sufficient biophysical properties to mediate adhesion

of leukocyte-sized microspheres to 4 hr. IL-1 activated HUVEC under flow. A common feature of previously proposed ligands for E-selectin is the expression of sialylated fucosylated glycans (SLe^x –type glycans) that appear to be involved in E-selectin recognition (25, 30-35). The fact that β_2 integrins carry SLe^x makes it quite likely that E-selectin recognition by native Mac-1 coated microspheres occurs via SLe^x –type glycans on the molecule. To provide further evidence for the role of these sialylated fucosylated structures in mediating adhesion to E-selectin, we employed recombinant Mac-1 generated without α (1,3) fucosyltransferase (e.g. FucT-VII). This enzyme plays a key regulatory step in ligand biosynthesis (74) and is crucial for the conferral of E-selectin binding activity on potential E-selectin ligands (38-40, 68, 74). Absence of this enzyme and lack of relevant post-translational modifications thereof, would, in theory, render recombinant Mac-1 ineffective in E-selectin recognition. As expected, a majority, if not all, recombinant Mac-1 coated microspheres adhere to 4 hr. IL-1 activated HUVEC at 1.8 dynes/cm^2 only through the CBRM1/29 epitope, with no contribution of E-selectin (Figure 3.6). Not only does this support the requirement of SLe^x structures in E-selectin recognition, but provides indirect proof for the role of these structures in mediating the E-selectin dependent mechanism observed with native Mac-1 coated microspheres under similar assaying conditions. Additional evidence for the role of these structures in E-selectin recognition was provided separately by Crutchfield et al. (45). In their study, pre-treatment of native Mac-1 coated microspheres with neuraminidase, which is known to remove surface sialylation, significantly inhibited their adhesion to E-selectin expressing

cellular monolayers, thus indicating that sialylated glycans on Mac-1, at least in part, play a role in E-selectin mediated adhesion.

Although an in-depth study on the E-selectin dependent mechanism (45) has previously been undertaken, not much is known about the CBRM1/29 epitope mediated (E-selectin independent) mechanism, except that it occurs through a Mac-1 epitope recognized by the mAb CBRM1/29, which maps to the I-domain of Mac-1 (63). Consequently, further studies on the E-selectin independent mechanism were undertaken on un-activated HUVEC devoid of E-selectin, but expressing basal levels of ICAM-1 at 1.0 dynes/cm^2. Note that, our studies over un-activated HUVEC were performed at a lower shear stress versus that employed over 4 hr. IL-1 activated HUVEC (1.8 dynes/cm^2) since at that higher shear stress, we only recorded ~7-8 adherence events per field of observation over un-activated HUVEC, which do not really constitute adhesion levels significant enough to quantify the effect of mAb blocking to further probe this E-selectin independent mechanism. Further evidence for the occurrence of this mechanism was provided with a near complete abrogation of Mac-1 adhesion to un-activated HUVEC (devoid of E-selectin) at 1.0 dyne/cm^2 (Figure 3.5), with mAbs that map to the I-domain on Mac-1 (CBRM1/29 and TS1/18). Similar results were observed with recombinant Mac-1 coated microspheres over un-activated HUVEC (Figure 3.7). The latter study was performed at an even lower shear stress (0.6 dynes/cm^2) in order to achieve quantifiable levels of adhesion via the CBRM1/29 epitope on Mac-1.

Endothelial cell adhesion molecules ICAM-1 and ICAM-2 have previously been touted as possible endothelial counter-receptors for Mac-1 on neutrophils (56-59). We therefore explored the role of these molecules in mediating Mac-1 adhesion to 4 hr. IL-1 activated HUVEC via the E-selectin independent mechanism. Pre-treatment of 4 hr. IL-1 activated HUVEC with an anti-ICAM-1 mAb R6.5 had no effect on Mac-1 microsphere adhesion while pre-treatment with mAbs to both E-selectin and ICAM-1 (HEL3/2 and R6.5 respectively) supported adhesion of Mac-1 microspheres at levels similar to those with HUVEC monolayers blocked by HEL3/2 alone, suggesting that these interactions are not affected by mAb R6.5, and therefore not mediated by ICAM-1 on activated HUVEC (Figure 3.3). Our observations with native and recombinant Mac-1 microspheres over un-activated HUVEC at lower shear stresses (Figures 3.5 and 3.7) strongly suggest that the E-selectin independent mechanism did not occur via either ICAM-1 or ICAM-2, raising the possibility that this mechanism was mediated by the CBRM1/29 epitope interacting with a previously un-identified endothelial Mac-1 counter-receptor(s). Indeed, Springer et al. (56) have previously discussed the possibility of additional counter-receptor(s) for Mac-1, distinct from ICAM-1, on the surface of un-activated and activated endothelial cells. Probing this hypothesis however, was beyond the scope of this study.

As mentioned earlier, the adhesion of native Mac-1 coated microspheres to 4 hr. IL-1 activated HUVEC under flow occurs via at least two mechanisms, each mediating distinct adhesive states, viz. 1. attachment and rolling (primary attachments) via the E-

selectin mechanism and 2. firm adhesion via the CBRM1/29 epitope. The fact that the primary attachments mediated via E-selectin are far more transient than firmly adherent events via the CBRM1/29 epitope, led us to hypothesize that the two mechanisms have different kinetic and/or tensile properties.

In discussing the biophysical attributes of these mechanisms, it is insightful to consider that an adherent microsphere under equilibrium at the substrate is subjected to an intricate balance of forces: a disruptive force and torque exerted by the fluid that is counter-adhesive and an adhesive force mediated by receptor-ligand bonds that is pro-adhesive. In the event that the disruptive force and torque are more dominant compared to the pro-adhesive bond forces, the particle has a tendency to either roll along the substrate or then detach into the free stream. On the other hand, a dominant pro-adhesive force facilitates firmer adhesion of the particle to the substrate.

The disruptive force and torque acting on the particle on account of the fluid dynamic environment are a function of the particle diameter, shear stress and wall correction factors for a spherical particle translating near a plane (65, 75). These correction factors in turn, are a function of the separation distance of the particle from substrate and the particle diameter. Our studies with the two separate mechanisms maintain the same particle diameter (10μm) and are performed under similar shear stresses. Assuming that the bond separation distances for both mechanisms are a similar order of magnitude, we can approximate the wall correction factors as being nearly the

same. Based on this analysis, we could sufficiently conclude for a given shear stress, that microspheres undergoing adhesion to the substrate via either mechanism, are probably subjected to similar magnitudes of force and torque over the range of shear stresses tested under flow.

The fact that for a given shear stress, the force and the torque acting on the particle during either mechanism is of a similar order of magnitude and that the E-selectin mechanism is characterized by transient rolling and detaching microspheres compared to the robust adhesion occurring through CBRM1/29 dependent mechanism, seems to suggest that the microspheres interacting through the latter mechanism are far more likely to withstand the disruptive counter-adhesive forces compared to the former. In other words, microspheres undergoing adhesion via the E-selectin mechanism perhaps have higher apparent kinetic rates of dissociation compared to those firmly adhering via the CBRM1/29 epitope. Quantifying the intrinsic kinetic rates of dissociation (k_{off}) for the Mac-1-E-selectin bond (E-selectin dependent mechanism) and the bond between the CBRM1/29 epitope and the as yet unidentified endothelial ligand (CBRM1/29 epitope mechanism)would however, require knowledge of the surface ligand densities and the receptor number (76). While an estimation of surface ligand densities (expression levels of domains on Mac-1 that mediate the E-selectin mechanism and the CBRM1/29 mechanism) seems rather straightforward, an estimation of the receptor number seems impossible at this point since the endothelial receptor that mediates the CBRM1/29 epitope mechanism is, as yet, undefined in our studies. One way to circumvent this issue

would be to use an alternate technique proposed by Alon et al. (77) for the estimation of intrinsic kinetic rates of dissociation. This technique offers a distinct advantage, in that it takes into consideration the contribution of these disruptive and pro-adhesive forces. This however, constitutes in itself, a whole separate study.

In conclusion, our studies found that native Mac-1 coated microspheres adhere to 4 hr. IL-1 activated HUVEC via two distinct molecular mechanisms: an E-selectin dependent mechanism that mediates attachment and rolling (primary attachment) and a mechanism dependent on the CBRM1/29 epitope that mediates, predominantly, firm adhesion. Since the characteristics of the adhesive states mediated by the two molecular mechanisms differ, we might speculate that the two molecular mechanisms have different kinetic and/or tensile properties (Figure 3.8). Quantification of these biophysical attributes remains a future aim of this study. This data provides evidence for the hypothesis that as leukocytes adhere to the endothelium, leukocyte expressed Mac-1 is interacting with the endothelium via two distinct molecular mechanisms: one interaction occurring during leukocyte tethering and rolling and another interaction occurring during firm adhesion.

References

1. Kansas, G.S. 1996. Selectins and their ligands: current concepts and controversies. *Blood*. 88:3259-3287.

2. Luscinskas, F.W., and M.A. Gimbrone. 1996. Endothelial-dependent mechanisms in chronic inflammatory leukocyte recruitment. *Annu. Rev. Med.* 47:413-421.

3. Carlos, T.M., and J.M. Harlan. 1994. Leukocyte-endothelial adhesion molecules. *Blood*. 84:2068-2101.

4. Springer, T.A. 1994. Traffic signals for lymphocyte recirculation and leukocyte emigration: the multistep paradigm. *Cell*. 76:301-314.

5. Lawrence, M.B., and T.A. Springer. 1991. Leukocytes roll on a selectin at physiologic flow rates: distinction from and prerequisite for adhesion through integrins. *Cell*. 65:859-873.

6. von Andrian, U.H., J.D. Chambers, L.M. McEvoy, R.F. Bargatze, K.E. Arfors, and E.C. Butcher. 1991. Two-step model of leukocyte-endothelial cell interactions in inflammation: distinct roles for LECAM-1 and the leukocyte ß$_2$ integrins in vivo. *Proc. Natl. Acad. Sci. USA*. 88:7538-7542.

7. Lawrence, M.B., C.W. Smith, S.G. Eskin, and L.V. McIntire. 1990. Effect of venous shear stress on CD18-mediated neutrophil adhesion to cultured endothelium. *Blood*. 75:227-237.

8. Ebnet, K., and D. Vestweber. 1999. Molecular mechanisms that control leukocyte extravasation: the selectins and the chemokines. *Histochem. Cell Biol.* 112:1-23.

9. Bevilacqua, M.P., J.S. Pober, D.L. Mendrick, R.S. Cotran, and M.A. Gimbrone Jr. 1987. Identification of an inducible endothelial-leukocyte adhesion molecule. *Proc. Natl. Acad. Sci., USA*. 84:9238-9242.

10. Bevilacqua, M.P., S. Stengelin, M.A. Gimbrone, Jr., and B. Seed. 1989. Endothelial leukocyte adhesion molecule 1: an inducible receptor for neutrophils related to complement regulatory proteins and lectins. *Science*. 243:1160-1164.

11. Bevilacqua, M.P., R.M. Nelson, G. Mannori, and O. Cecconi. 1994. Endothelial-leukocyte adhesion molecules in human disease. *Ann. Rev. Med.* 45:361-378.

12. McEver, R.P., J.H. Beckstead, K.L. Moore, L. Marshall-Carlson, and D.F. Bainton. 1989. GMP-140, a platelet α-granule membrane protein, is also synthesized by vascular endothelial cells and is localized in Weibel-Palade bodies. *J. Clin. Invest.* 84:92-99.

13. Patel, K.D., K.L. Moore, M.U. Nollert, and R.P. McEver. 1995. Neutrophils use both shared and distinct mechanisms to adhere to selectins under static and flow conditions. *J. Clin. Invest.* 96:1887-1896.

14. Lawrence, M.B., and T.A. Springer. 1993. Neutrophils roll on E-selectin. *J. Immunol.* 151:6338-6346.

15. Patel, K.D., and R.P. McEver. 1997. Comparison of tethering and rolling of eosinophils and neutrophils through selectins and P-selectin glycoprotein ligand-1. *J. Immunol.* 159:4555-4565.

16. Abbassi, O., T.K. Kishimoto, L.V. McIntire, D.C. Anderson, and C.W. Smith. 1993. E-selectin supports neutrophil rolling in vitro under conditions of flow. *J. Clin. Invest.* 92:2719-2730.

17. Mayadas, T.N., R.C. Johnson, H. Rayburn, R.O. Hynes, and D.D. Wagner. 1993. Leukocyte rolling and extravasation are severely compromised in P-selectin deficient mice. *Cell*. 74:541-554.

18. Kunkel, E.J., and K. Ley. 1996. Distinct phenotype of E-selectin-deficient mice: E-selectin is required for slow leukocyte rolling in vitro. *Circ. Res.* 79:1196-1204.

19. Walz, G., A. Aruffo, W. Kolanus, M.P. Bevilacqua, and B. Seed. 1990. Recognition by ELAM-1 of the sialyl-Lex determinant on myeloid and tumor cells. *Science*. 250:1132-1135.

20. Handa, K., E. Neudelman, M. Stroud, T. Shiozawa, and S. Hakomori. 1991. Selectin GMP-140 (CD62; PADGEM) binds to sialosyl-Lea and sialosyl-Lex, and sulfated glycans modulate the binding. *Biochem. Biophys. Res. Commun.* 181:1223-1230.

21. Polley, M.J., M.L. Phillips, E. Wayner, E. Nudelman, A.K. Singhal, S. Hakomori, and J.C. Paulson. 1991. CD62 and endothelial cell-leukocyte adhesion molecule 1

(ELAM-1) recognize the same carbohydrate ligand, sialyl-Lewis x. *Proc. Natl. Acad. Sci.* 88:6224-6228.

22. Moore, K.L., K.D. Patel, R.E. Bruehl, L. Fugang, D.A. Johnson, H.S. Lichenstein, R.D. Cummings, D.F. Bainton, and R.P. McEver. 1995. P-selectin glycoprotein ligand-1 mediates rolling of human neutrophils on P-selectin. *J. Cell Biol.* 128:661-671.

23. Sako, D., X.J. Chang, K.M. Barone, G. Vachino, H.M. White, G. Shaw, G.M. Veldman, K.M. Bean, T.J. Ahern, B. Furie, D.A. Cumming, and G.R. Larsen. 1993. Expression cloning of a functional glycoprotein ligand for P-selectin. *Cell*. 75:1179-1186.

24. Somers, W.S., J. Tang, G.D. Shaw, and R.T. Camphausen. 2000. Insights into the molecular basis of leukocyte tethering and rolling revealed by structures of P- and E-selectin bound to SLe(X) and PSGL-1. *Cell*. 103:467-79.

25. Norgard, K.E., K.L. Moore, S. Diaz, N.L. Stults, S. Ushiyama, R.P. McEver, R.D. Cummings, and A. Varki. 1993. Characterization of a specific ligand for P-selectin on myeloid cells. *J. Biol. Chem.* 268:12764-12774.

26. Wilkins, P.P., R.P. McEver, and R.D. Cummings. 1996. Structures of the O-glycans on P-selectin glycoprotein ligand-1 from HL-60 cells. *J. Biol. Chem.* 271:18732-18742.

27. Moore, K.L., S.F. Eaton, D.E. Lyons, H.S. Lichenstein, R.D. Cummings, and R.P. McEver. 1994. The P-selectin glycoprotein ligand from human neutrophils

displays sialylated, fucosylated, O-linked poly-N-acetyllactosamine. *J. Biol. Chem.* 269:23318-23327.

28. Goetz, D.J., D.M. Greif, R.T. Camphausen, S. Howes, K.M. Comess, K.R. Snapp, G.S. Kansas, and F.W. Luscinskas. 1997. Isolated P-selectin glycoprotein-1 dynamic adhesion to P- and E-selectin. *J. Cell Biol.* 137:509-519.

29. Zollner, O., M.C. Lenter, J.E. Blanks, E. Borges, M. Steegmaier, H. Zerwes, and D. Vestweber. 1997. L-selectin from human, but not from mouse neutrophils binds directly to E-selectin. *J. Cell Biol.* 136:707-716.

30. Picker, L.J., R.A. Warnock, A.R. Burns, C.M. Doerschuk, E.L. Berg, and E.C. Butcher. 1991. The neutrophil selectin LECAM-1 presents carbohydrate ligands to the vascular selectin ELAM-1 and GMP-140. *Cell*. 66:921-933.

31. Steegmaier, M., A. Levinovitz, S. Isenmann, E. Borges, M. Lenter, H.P. Kocher, B. Kleuser, and D. Vestweber. 1995. The E-selectin-ligand ESL-1 is a variant of a receptor for fibroblast growth factor. *Nature*. 373:615-620.

32. Levinovitz, A., J. Muhlhoff, S. Isenmann, and D. Vestweber. 1993. Identification of a glycoprotein ligand for E-selectin on mouse myeloid cells. *J. Cell Biol.* 121:449-459.

33. Kuijpers, T.M., M. Hoogerwerf, L.J. van der Laan, G. Nagel, C.E. van der Schoot, F. Grunert, and D. Roos. 1992. CD66 nonspecific cross-reacting antigens are involved in neutrophil adherence to cytokine-activated endothelial cells. *J. Cell Biol.* 118:457-466.

34. Maemura, K., and M. Fukuda. 1992. Poly-N-acetyllactosaminyl O-glycans attached to leukosialin. The presence of sialyl Lex structures in O-glycans. *J. Biol. Chem*. 267:24379-24386.

35. Dimitroff, C.J., J.Y. Lee, S. Rafii, R.C. Fuhlbrigge, and R. Sackstein. 2001. CD44 is a major E-selectin ligand on human hematopoietic progenitor cells. *J Cell Biol*. 153:1277-86.

36. Brunk, D.K., D.J. Goetz, and D.A. Hammer. 1996. Sialyl Lewisx/E-selectin-mediated rolling in a cell-free system. *Biophys. J.* 71:2902-2908.

37. Brunk, D.K., and D.A. Hammer. 1997. Quantifying rolling adhesion using a cell-free assay: E-selectin and its carbohydrate ligands. *Biophys. J.* 72:2820-2833.

38. Wagers, A.J., J.B. Lowe, and G.S. Kansas. 1996. An important role for the α1,3 fucosyltransferase, FucT-VII, in leukocyte adhesion to E-selectin. *Blood*. 88:2125-2132.

39. Lowe, J.B., L.M. Stoolman, R.P. Nair, R.D. Larsen, T.L. Berhend, and R.M. Marks. 1990. ELAM-1-dependent cell adhesion to vascular endothelium determined by a transfected human fucosyltransferase cDNA. *Cell*. 63:475-484.

40. Knibbs, R.N., R.A. Craig, P. Maly, P.L. Smith, F.M. Wolber, N.E. Faulkner, J.B. Lowe, and L.M. Stoolman. 1998. α(1,3)-fucosyltransferase VII-dependent synthesis of P- and E-selectin ligands on cultured T lymphoblasts. *J. Immunol.* 161:6305-6315.

41. Alon, R., T. Feizi, C. Yuen, R.C. Fuhlbrigge, and T.A. Springer. 1995. Glycolipid ligands for selectins support leukocyte tethering and rolling under physiologic flow conditions. *J. Immunol.* 154:5356-5366.

42. Kishimoto, T.K., R.S. Larson, A.L. Corbi, M.L. Dustin, D.E. Stauton, and T.A. Springer. 1989. The leukocyte integrins. *Adv. Immunol.* 46:149-181.

43. Van der Vieren, M., H. Trong, C.L. Wood, P.F. Moore, T. St. John, D.E. Staunton, and W.M. Gallatin. 1995. A novel leukointegrin, αdβ2, binds preferentially to ICAM-3. *Immunity.* 3:683-690.

44. Asada, M., K. Furukawa, C. Kantor, C.G. Gahmberg, and A. Kobata. 1991. Structural study of the sugar chains of human leukocyte cell adhesion molecules CD11/CD18. *Biochemistry*. 30:1561-1571.

45. Crutchfield, K.L., V.R. Shinde Patil, C.J. Campbell, C.A. Parkos, J.R. Allport, and D.J. Goetz. 2000. CD11b/CD18-coated microspheres attach to E-selectin under flow. *J. Leuk. Biol.* 67:196-205.

46. Lawrence, M.B., D.F. Bainton, and T.A. Springer. 1994. Neutrophil tethering to and rolling on E-selectin are separable by requirement for L-selectin. *Immunity.* 1:137-145.

47. Kotovuori, P., E. Tontti, R. Pigott, M. Shepherd, M. Kiso, A. Hasegawa, R. Renkonen, P. Nortamo, D.C. Altieri, and C.G. Gahmberg. 1993. The vascular E-selectin binds to the leukocyte integrins CD11/18. *Glycobiology*. 3:131-136.

48. Jung, U., K.E. Norman, K. Scharffetter-Kochanek, A.L. Beaudet, and K. Ley. 1998. Transit time of leukocytes rolling through venules controls cytokine-induced inflammatory cell recruitment in vivo. *J Clin Invest*. 102:1526-33.

49. Abbassi, O., C.L. Lane, S. Krater, T.K. Kishimoto, D.C. Anderson, L.V. McIntire, and C.W. Smith. 1991. Canine neutrophil margination mediated by lectin adhesion molecule-1 in vitro. *J Immunol*. 147:2107-15.

50. Smith, C.W., R. Rothlein, B.J. Hughes, M.M. Mariscaico, H.E. Rudloff, F.C. Schmalstieg, and D.C. Anderson. 1988. Recognition of an endothelial determinant for CD18-dependent human neutrophil adherence and transendothelial migration. *J. Clin. Invest.* 82:1746-1756.

51. Miller, M.D., and M.S. Krangel. 1992. Biology and biochemistry of the chemokines: a family of chemotactic and inflammatory cytokines. *Crit. Rev. Immunol.* 12:17-46.

52. Smith, C.W. 2000. Possible steps involved in the transition to stationary adhesion of rolling neutrophils: a brief review. *Microcirculation*. 7:385-94.

53. Diamond, M.S., and T.A. Springer. 1994. The dynamic regulation of integrin adhesiveness. *Current Biology*. 4:506-517.

54. Smith, C.W., S.D. Marlien, R. Rothlein, C. Toman, and D.C. Anderson. 1989. Cooperative interactions of LFA-1 and Mac-1 with intercellular adhesion molecule-1 in facilitating adherence and transendothelial migration of human neutrophils in vitro. *J. Clin. Invest.* 83:2008-2017.

55. Lo, S.K., G.A. Van Seventer, S.M. Levin, and S.D. Wright. 1989. Two leukocyte receptors (CD11a/CD18 and CD11b/CD18) mediate transient adhesion to endothelium by binding to different ligands. *J. Immunol.* 143:3325-3329.

56. Diamond, M.S., D.E. Staunton, A.R. de Fougerolles, S.A. Stacker, J. Garcia-Aguilar, M.L. Hibbs, and T.A. Springer. 1990. ICAM-1 (CD54): A counter-receptor for Mac-1 (CD11b/CD18). *J. Cell Biol.* 111:3129-3139.

57. Berton, G., and C.A. Lowell. 1999. Integrin signaling in neutrophils and macrophages. *Cell Signal*. 11:621-35.

58. Diamond, M.S., D.E. Staunton, S.D. Marlin, and T.A. Springer. 1991. Binding of the integrin Mac-1 (CD11b/CD18) to the third immunoglobulin- like domain of ICAM-1 (CD54) and its regulation by glycosylation. *Cell*. 65:961-71.

59. Xie, J.J., R. Li, P. Kotovuori, C. Vermot-Desroches, J. Wijdenes, M.A. Arnaout, P. Nortamo, and C.G. Gahmberg. 1995. Intercellular adhesion molecule-2 (CD102) binds to the leukocyte integrin CD11b/CD18 through the A domain. *J. Immunol.* 155:3619-3628.

60. Shimaoka, M., C. Lu, R.T. Palframan, U.H. von Andrian, A. McCormack, J. Takagi, and T.A. Springer. 2001. Reversibly locking a protein fold in an active conformation with a disulfide bond: Integrin alpha L I domains with high affinity and antagonist activity in vivo. *Proc Natl Acad Sci U S A*. 15:15.

61. Lu, C., M. Shimaoka, Q. Zang, J. Takagi, and T.A. Springer. 2001. Locking in alternate conformations of the integrin alpha Lbeta 2 I domain with disulfide

bonds reveals functional relationships among integrin domains. *Proc Natl Acad Sci U S A*. 98:2393-8.

62. Diamond, M.S., and T.A. Springer. 1993. A subpopulation of Mac-1 (CD11b/CD18) molecules mediates neutrophil adhesion to ICAM-1 and fibrinogen. *J. Cell Biol.* 120:545-556.

63. Diamond, M.S., G.-A. J., J.K. Bickford, A.L. Corbi, and T.A. Springer. 1993. The I domain is a major recognition site on the leukocyte integrin Mac-1 (CD11b/CD18) for four distinct adhesion ligands. *J. Cell Biol.* 120:1031-1043.

64. Gopalan, P.K., D.A. Jones, L.V. McIntire, and C.W. Smith. 1996. Cell adhesion under hydrodynamic flow conditions. *In* Current Protocols in Immunology. J.E. Coligan, A.M. Kruisbeek, D.H. Margulies, E.M. Shevach, and W. Strober, editors. J. Wiley, New York. 7.29.1-7.29.23.

65. Shinde Patil, V.R., C.J. Campbell, Y.H. Yun, S.M. Slack, and D.J. Goetz. 2001. Particle diameter influences adhesion under flow. *Biophys J*. 80:1733-1743.

66. Bevilacqua, M.P. 1993. Endothelial-leukocyte adhesion molecules. *Annu. Rev. Immunol.* 11:767-804.

67. Saad, B., T.D. Hirt, M. Welti, G.K. Uhlschmid, P. Neuenschwander, and U.W. Suter. 1997. Development of degradable polyesterurethanes for medical applications: in vitro and in vivo evaluations. *J Biomed Mater Res*. 36:65-74.

68. Snapp, K.R., A.J. Wagers, R. Craig, L.M. Stoolman, and G.S. Kansas. 1997. P-selectin glycoprotein ligand-1 is essential for adhesion to P- selectin but not E-selectin in stably transfected hematopoietic cell lines. *Blood*. 89:896-901.

69. Parkos, C.A., S.P. Colgan, T.W. Liang, A. Nusrat, A.E. Bacarra, D.K. Carnes, and J.L. Madara. 1996. CD47 mediates post-adhesive events required for neutrophil migration across polarized intestinal epithelia. *J. Cell Biol*. 132:437-450.

70. Norman, K.E., A.G. Katopodis, G. Thoma, F. Kolbinger, A.E. Hicks, M.J. Cotter, A.G. Pockley, and P.G. Hellewell. 2000. P-selectin glycoprotein ligand-1 supports rolling on E- and P-selectin in vivo. *Blood*. 96:3585-91.

71. Hafezi-Moghadam, A., K.L. Thomas, A.J. Prorock, Y. Huo, and K. Ley. 2001. L-selectin shedding regulates leukocyte recruitment. *J Exp Med*. 193:863-72.

72. Burch, E.E., V.R. Shinde Patil, M.F. Kiani, and D.J. Goetz. 2002. The N-terminal PSGL-1 Peptide can Mediate Adhesion to Trauma-activated Endothelium via P-selectin in Vivo. *Blood (In press)*.

73. Shinde Patil, V.R., L.A. Smith, and D.J. Goetz. 2002. PSGL-1 purified from HL-60 cells can support adhesion to IL-1β-activated endothelial cells via E-selectin under flow. *Submitted*.

74. Knibbs, R.N., R.A. Craig, S. Natsuka, A. Chang, C. M., J.B. Lowe, and L.M. Stoolman. 1996. The fucosyltransferase FucT-VII regulated E-selectin ligand synthesis in human T cells. *J. Cell Biol*. 133:911-920.

75. Goldman, A.J., R.G. Cox, and H. Brenner. 1967. Slow viscous motion of a sphere parallel to a plane wall. II. Couette flow. *Chem. Eng. Sci.* 22:635-660.

76. Lauffenburger, D.A., and J.J. Linderman. 1993. Receptors. Oxford University Press, New York.

77. Alon, R., D.A. Hammer, and T.A. Springer. 1995. Lifetime of the P-selectin-carbohydrate bond and its response to tensile force in hydrodynamic flow. *Nature*. 374:539-542.

Figures

Figure 3.1. **Characterization of ligand coated microspheres.** Flow cytometric analysis was performed on 10μm microspheres incubated in native Mac-1, recombinant Mac-1 and recombinant LFA-1 to test levels of ligand expression on each of the respective microsphere types. Levels of extracellular surface Mac-1 expression on native Mac-1 coated microspheres (panel a) and recombinant Mac-1 coated microspheres (panel c) were detected using anti-Mac-1 mAb 44, (shaded histograms) and found to be similar; Functional conformation of native Mac-1 (panel b) and recombinant Mac-1 (panel d) were detected using an mAb to the activation specific neo-epitope of Mac-1, mAb CBRM1/5 (shaded histograms); anti- LFA-1 mAb TS1/22 served as a negative control in all four instances (open histograms). The level of recombinant LFA-1 expression on recombinant LFA-1 coated microspheres (panel e) was detected using anti- LFA-1 mAb TS1/22 (shaded histogram) while anti-Mac-1 mAb 44 served as a negative control (open histogram). Primary mAbs indicated above were detected via FITC labeled secondary antibody through flow cytometry. Relative number vs. mean channel fluorescence (MCF) are plotted on a four-decade scale. Results typical of 2 separate experiments.

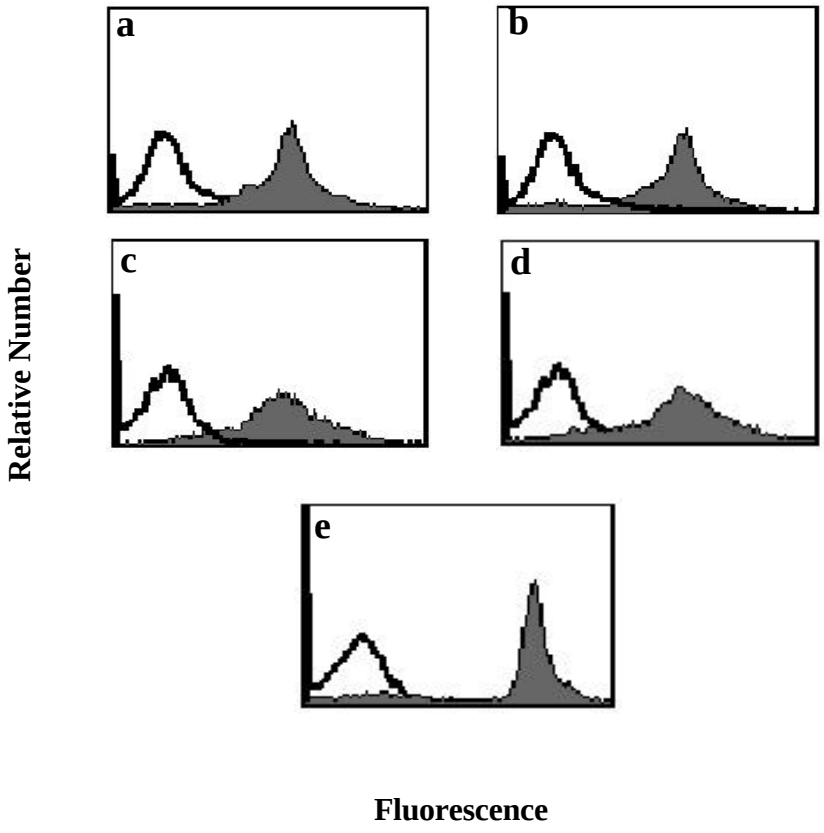
a
b
c
d
e
Relative Number
Fluorescence

Figure 3.2. Characterization of HUVEC. Enzyme linked immunosorbent assay (ELISA) was performed on un-activated (open bars), 4 hr. IL-1 activated (black bars) and 24 hr IL-1 activated HUVEC (gray bars) coated on 96 well plates. Expression of endothelial cell adhesion molecules ICAM-1 and E-selectin was detected using primary mAbs to ICAM-1 (R6.5) and E-selectin (7A9) while anti-LFA-1 mAb (TS1/22) served as a negative control. Relative expression levels of adhesion molecules were detected via HRP conjugated 2^0 Abs through ELISA, by plotting their absorbance at 450 nm. (Legend: 1^0 mAb indicates pre-treatment of HUVEC with anti-LFA-1 mAb TS1/22, anti-ICAM-1 mAb R6.5 and anti-E-selectin mAb 7A9, or no pre-treatment (-). 2^0 Ab indicates the HUVEC treatment with HRP-conjugated secondary antibodies (+) or no treatment(-)). Observations are representative of three treatment wells (n=3). Error bars indicate standard deviation. Experiments were performed on at least two separate occasions.

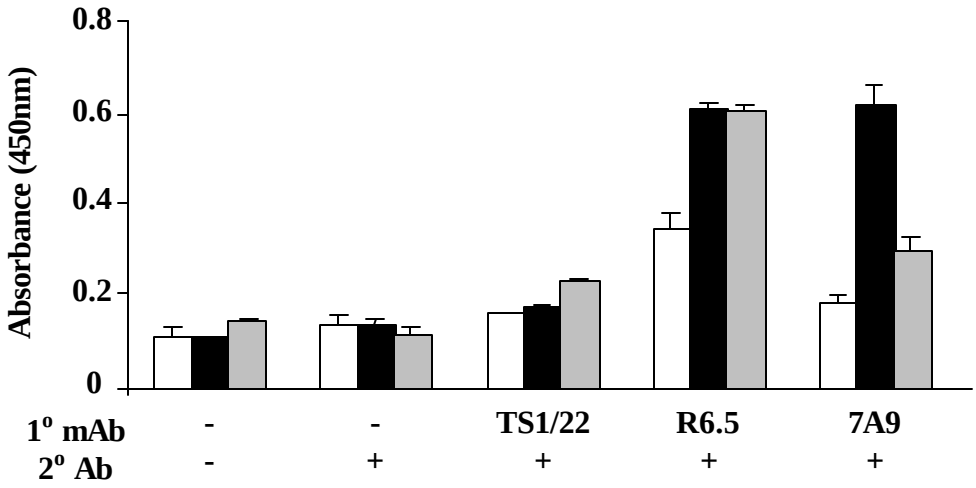
0.8
0.6
0.4
0.2
0
Absorbance (450nm)
1° mAb
2° Ab
-
-
TS1/22
R6.5
7A9
-
+
+
+
+

Figure 3.3. Native Mac-1 coated 10mm microspheres adhere to 4 hr. IL-1 activated HUVEC at 1.8 dynes/cm^2 via at least two distinct mechanisms. Firm adherence (attachment, rolling and firm adhesion) of 10μm microspheres coated with Mac-1 purified from leukocyte lysates (native Mac-1) to 4 hr. IL-1 activated and un-activated HUVEC was studied at 1.8 dynes/cm^2. In certain instances, native Mac-1 coated microspheres and/or HUVEC were pretreated with mAbs prior to use in adhesion assays. (Legend: Activation indicates pretreatment (+) or no pretreatment (-) of HUVEC with IL-1β for 4 hours prior to the assay; μsphere mAb indicates pre-treatment of native Mac-1 microspheres with anti-Mac-1 mAbs (CBRM1/29 and LM2/1) or no pre-treatment (-). HUVEC mAb indicates pre-treatment of HUVEC with mAbs to endothelial expressed E-selectin (HEL3/2), ICAM-1 (R6.5), both E-selectin and ICAM-1 (HEL3/2&R6.5) or no pre-treatment (-). * indicates $p < 0.05$ compared to second (un-treated) bar from left . Error bars indicate SEM. Shear stress = 1.8 dynes/cm^2; $n \geq 3$).

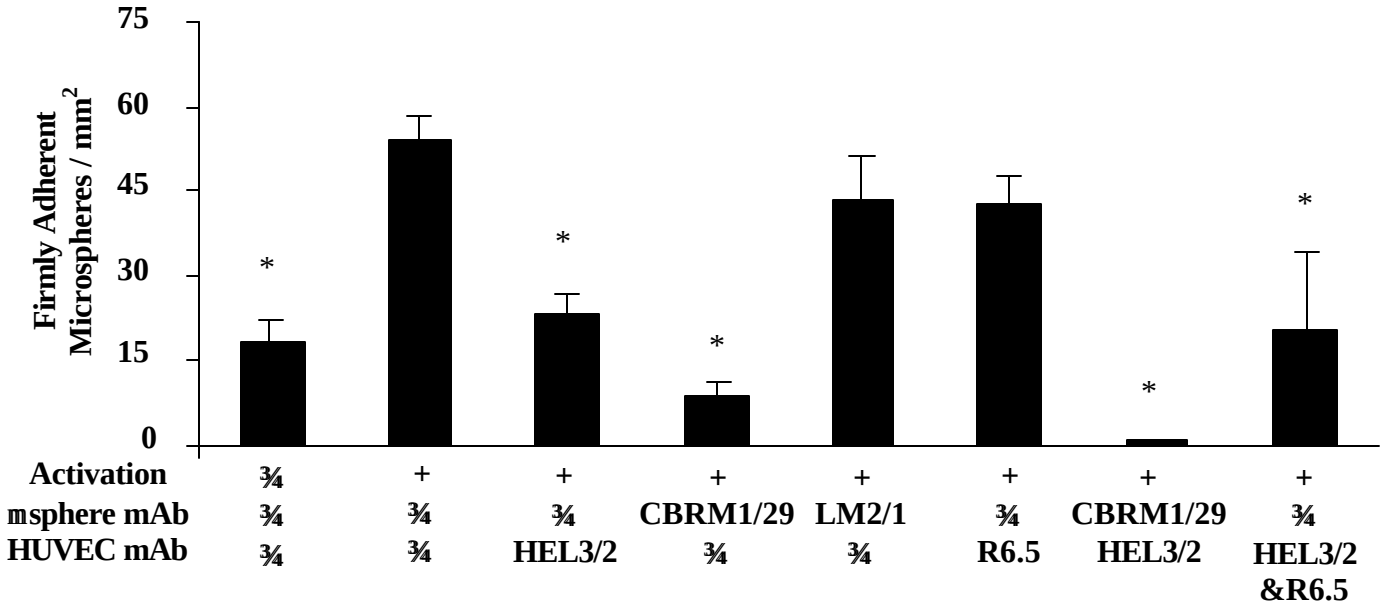
75
60
45
30
15
0
Firmly Adherent Microspheres / mm2
*
*
*
*
*
*
Activation ¾ + + + + + + +
msphere mAb ¾ ¾ ¾ CBRM1/29 LM2/1 ¾ CBRM1/29 ¾
HUVEC mAb ¾ ¾ HEL3/2 ¾ ¾ R6.5 HEL3/2 HEL3/2 &R6.5

Figure 3.4. Effect of anti-Mac-1 and anti-E-selectin mAbs on primary attachment and subsequent firm adhesion of native Mac-1 coated microspheres to 4 hr. IL-1 activated HUVEC at 1.8 dynes/cm^2. Native microspheres attaching and rolling (primary attachments) from the free stream to 4 hr. IL-1 activated HUVEC (black bars) and those adhering firmly, subsequent to primary attachment (open bars) were estimated at 1.8 dynes/cm^2. In certain instances, native Mac-1 coated microspheres and/or HUVEC were pretreated with mAbs prior to use in adhesion assays. (Legend: µsphere mAb indicates pre-treatment of native Mac-1 microspheres with anti-Mac-1 mAb (CBRM1/29) or no pre-treatment (-). HUVEC mAb indicates pre-treatment of HUVEC with an mAb to endothelial expressed E-selectin (HEL3/2) or no pre-treatment (-). Error bars indicate SEM. Shear stress = 1.8 dynes/cm^2; $n \geq 3$).

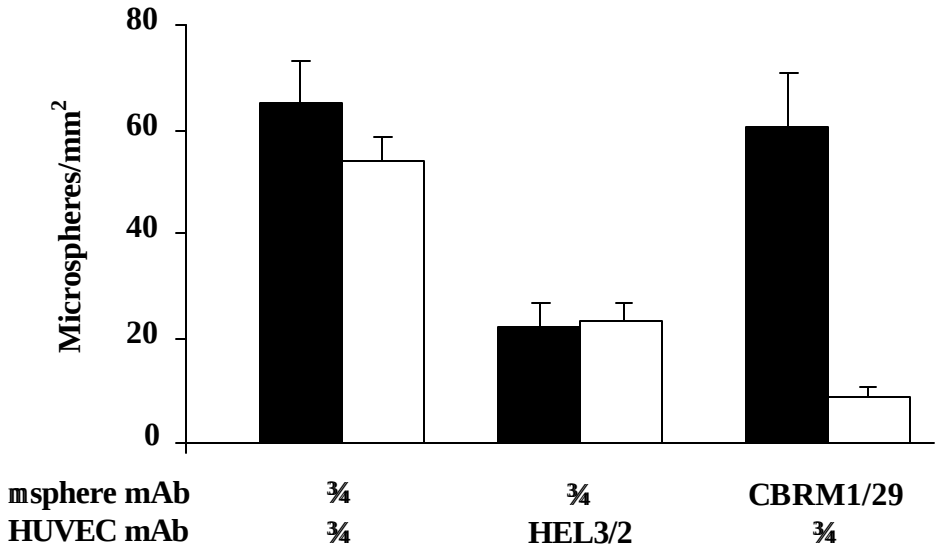
80
60
40
20
0
Microspheres/mm2
msphere mAb
¾
¾
CBRM1/29
HUVEC mAb
¾
HEL3/2
¾

Figure 3.5. Native Mac-1 coated 10mm microspheres adhere to un-activated HUVEC at 1.0 dyne/cm^2 via an epitope on Mac-1 recognized by mAbs CBRM1/29 and TS1/18. Firm adherence (attachment, rolling and firm adhesion) of 10μm microspheres coated with Mac-1 purified from leukocyte lysates (native Mac-1) to un-activated HUVEC was studied at 1.0 dyne/cm^2. In certain instances, native Mac-1 coated microspheres and/or HUVEC were pretreated with mAbs prior to use in adhesion assays. (Legend: μsphere mAb indicates pre-treatment of native Mac-1 microspheres with anti-Mac-1 mAbs (CBRM1/29, TS1/18 and LM2/1) or no pre-treatment (-). HUVEC mAb indicates pre-treatment of HUVEC with mAbs to endothelial expressed ICAM-1 (R6.5), ICAM-2 (B-T1), both ICAM-1 and ICAM-2 (R6.5&B-T1) or no pre-treatment (-). * indicates $p < 0.05$ compared to left most (un-treated) bar. Error bars indicate SEM. Shear stress = 1.0 dyne/cm^2; $n \geq 3$).

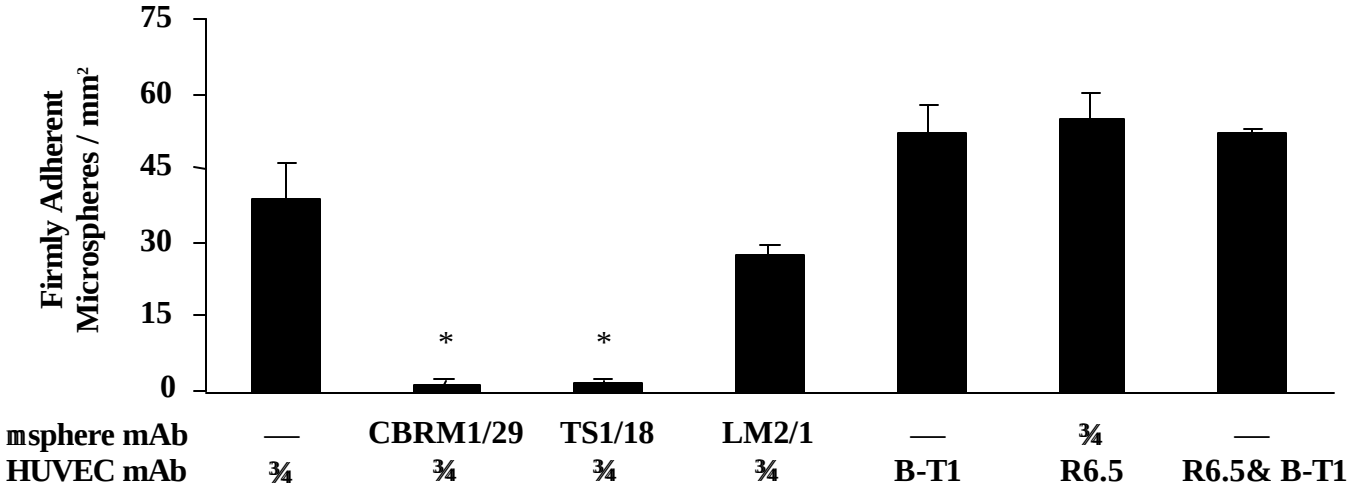
Firmly Adherent Microspheres / mm²
75
60
45
30
15
0
*
*
msphere mAb — CBRM1/29 TS1/18 LM2/1 — ¾ —
HUVEC mAb ¾ ¾ ¾ ¾ B-T1 R6.5 R6.5& B-T1

Figure 3.6. A majority, if not all, recombinant Mac-1 coated 10mm microspheres adhere to 4 hr. IL-1 activated HUVEC via the CBRM1/29 epitope at 1.8 dynes/cm^2. Firm adherence (attachment, rolling and firm adhesion) of 10μm microspheres coated with recombinant Mac-1 to 4 hr. IL-1 activated was studied at 1.8 dynes/cm^2. In certain instances, recombinant Mac-1 coated microspheres and/or HUVEC were pretreated with mAbs prior to use in adhesion assays. (Legend: μsphere mAb indicates pre-treatment of recombinant Mac-1 microspheres with an anti-Mac-1 mAb (CBRM1/29) or no pre-treatment (-). HUVEC mAb indicates pre-treatment of HUVEC with mAbs to endothelial expressed E-selectin (HEL3/2) or no pre-treatment (-). * indicates $p < 0.05$ compared to left most (un-treated) bar . Error bars indicate SEM. Shear stress = 1.8 dynes/cm^2; $n \geq 3$).

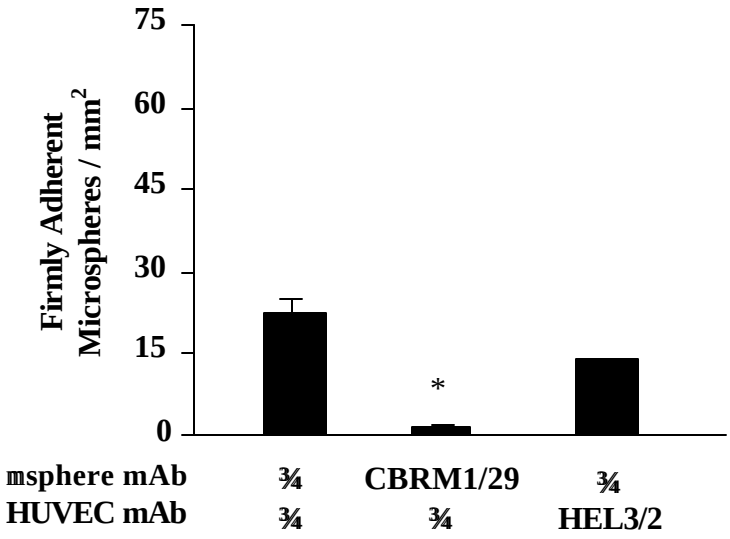
75
60
45
30
15
0
Firmly Adherent
Microspheres / mm2
*
msphere mAb
¾
CBRM1/29
¾
HUVEC mAb
¾
¾
HEL3/2

Figure 3.7. Recombinant Mac-1 coated 10mm microspheres adhere to un-activated HUVEC at 0.6 dynes/cm^2. Firm adherence (attachment, rolling and firm adhesion) of 10μm microspheres coated with recombinant Mac-1 to un-activated HUVEC was studied at 0.6 dynes/cm^2, with recombinant LFA-1 coated microspheres serving as a negative control. In certain instances, recombinant Mac-1 and LFA-1 coated microspheres and/or HUVEC were pretreated with mAbs prior to use in adhesion assays. (Legend: Ligand indicates coating 10μm microspheres with recombinant Mac-1 (R-Mac-1) and recombinant LFA-1 (R-LFA-1). μsphere mAb indicates pre-treatment of recombinant Mac-1 and LFA-1 microspheres with anti-Mac-1 mAbs (CBRM1/29, TS1/18 and LM2/1), anti-LFA-1 mAb (TS1/22) or no pre-treatment (-). HUVEC mAb indicates pre-treatment of HUVEC with mAbs to endothelial expressed ICAM-1 (R6.5) or no pre-treatment (-). * indicates $p < 0.05$ compared to left most (un-treated R-Mac-1) bar. ** indicates $p < 0.05$ compared to third bar from the right (un-treated R-LFA-1) bar. Error bars indicate SEM. Shear stress = 0.6 dynes/cm^2; $n \geq 3$).

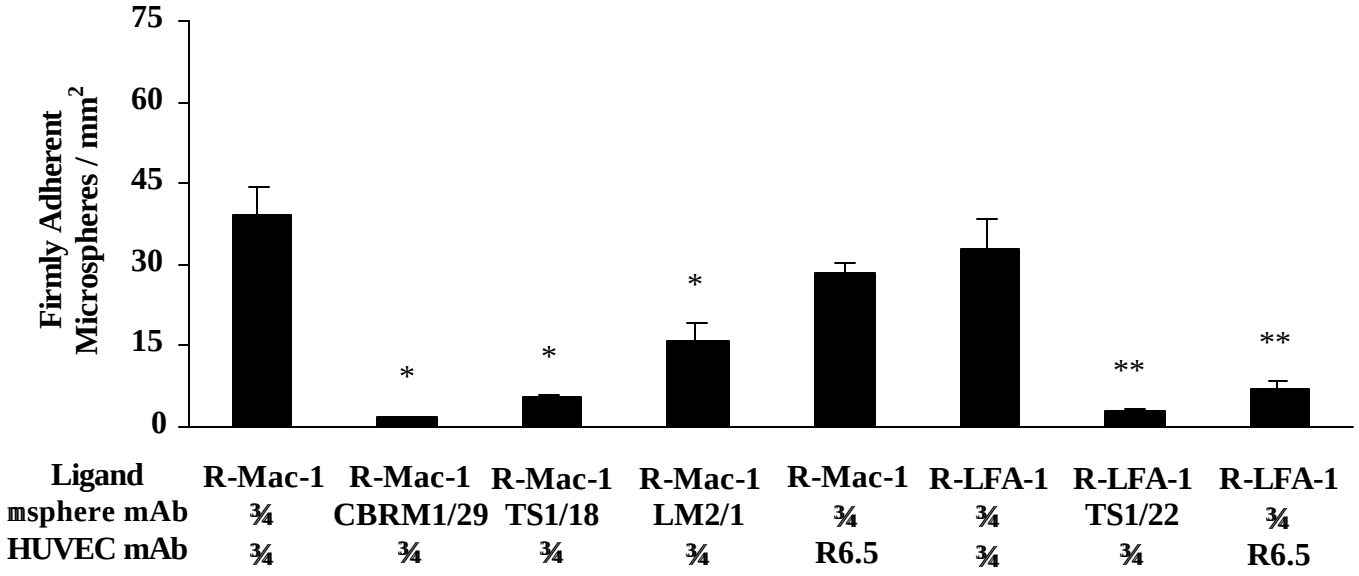
75
60
45
30
15
0
Firmly Adherent Microspheres / mm2
*
*
*
**
**
Ligand
msphere mAb
HUVEC mAb
R-Mac-1 ¾ ¾
R-Mac-1 CBRM1/29 ¾
R-Mac-1 TS1/18 ¾
R-Mac-1 LM2/1 ¾
R-Mac-1 ¾ R6.5
R-LFA-1 ¾ ¾
R-LFA-1 TS1/22 ¾
R-LFA-1 ¾ R6.5

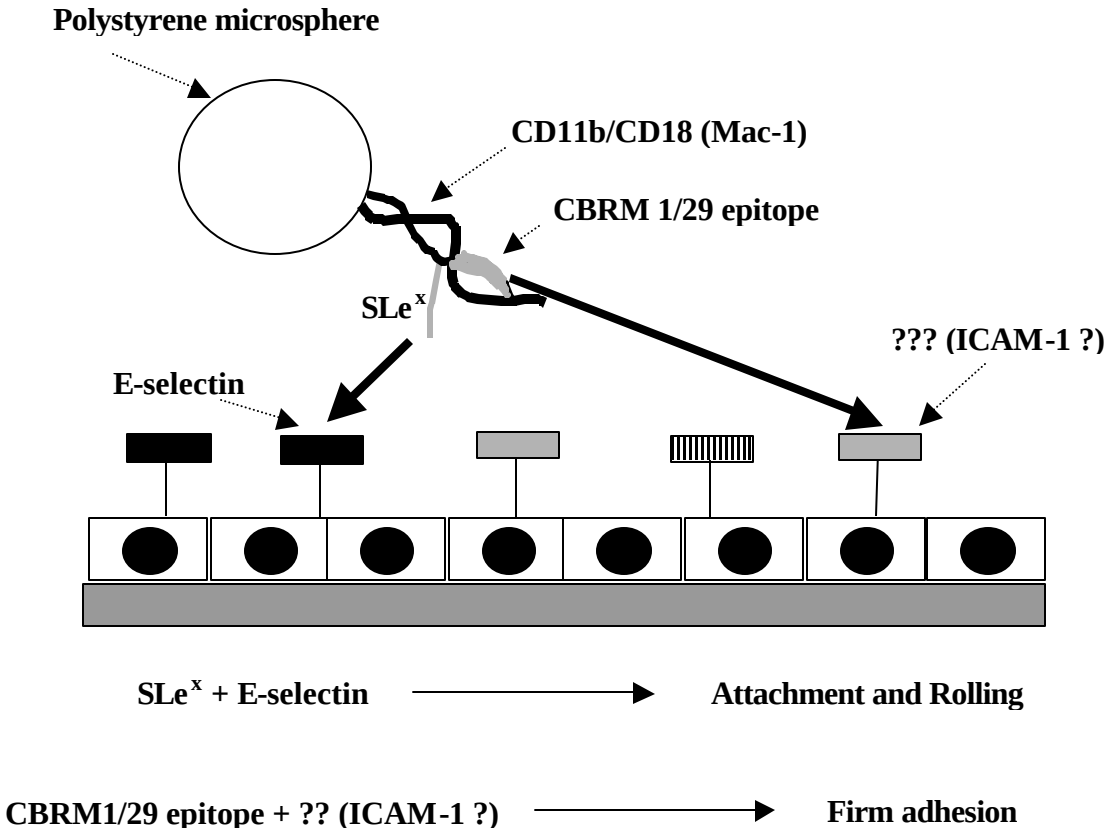

Figure 3. 8 Native Mac-1 coated microspheres adhere to 4 hr. IL-1 activated HUVEC via two distinct mechanisms

CHAPTER 4

PSGL-1 CAN SUPPORT HL60 CELL ATTACHMENT TO ENDOTHELIAL CELL EXPRESSED E-SELECTIN

Introduction

A critical step in a variety of physiological and pathological processes (e.g. leukocyte recruitment to a site of tissue injury, T-cell homing to skin, and hematopoietic progenitor cell (HPC) into bone marrow) is the adhesion of leukocytes to the endothelium. This adhesion process involves a cascade of events including initial attachment of the leukocyte to the endothelium (initial tethering), rolling, spreading, and firm adhesion (1-7). *In vivo* and *in vitro* studies have shown that the inducible endothelial cell adhesion molecule E-selectin (CD62E) is involved in leukocyte initial attachment and rolling on the endothelium (8-10). E-selectin is one of three known selectins, the others being P-selectin (CD62P) and L-selectin (CD62L). A notable feature of the selectins is their NH_2-terminal, lectin-like domain that binds carbohydrate moieties in a Ca^{2+}-dependent manner (11, 12). Thus, several carbohydrate ligands for the selectins have been proposed including the sialyl Lewis x (SLe^x) tetrasaccharide (13, 14) and related glycans such as the cutaneous lymphocyte associated antigen (CLA), first defined by its reactivity with the mAb HECA-452 (15-19).

Although many leukocyte glycoproteins are decorated with SLe^x-type glycans, it appears that P-selectin glycoprotein ligand –1 (PSGL-1) is the major counter-receptor for P-selectin (14, 20-22). PSGL-1 was first isolated from HL60 cells (21) and subsequently cloned from an HL60 cell cDNA library (20). PSGL-1, a homodimer of disulfide-linked subunits with an apparent molecular mass of 120 kD each (21), is present on a variety of leukocytes including neutrophils, monocytes, eosinophils and lymphocytes (22, 23). PSGL-1 is extensively glycosylated with N-linked glycans and closely spaced O-linked glycans, a portion of which are modified by SLe^x (24-26). Recent studies have shown that a variety of leukocytes (i.e. memory T-cells, monocytes, and neutrophils) express PSGL-1 that carries the SLe^x related glycan CLA (27).

While the major counter-receptor for P-selectin appears to be PSGL-1, the issue of what is the major counter-receptor for E-selectin is still subject to debate. There have been a number of studies, motivated by a desire to further the understanding of HPC entry into bone marrow and leukocyte recruitment to a site of tissue injury, focused on identifying the HL60 counter-receptors for E-selectin. This body of work has resulted in data both supporting and refuting the hypothesis that PSGL-1 is involved in HL60 cell adhesion to endothelial expressed E-selectin under flow. Sackstein's group (19) found that Chinese hamster ovary cells stably expressing E-selectin (CHO-E) roll on a broad 140 kDa glycoprotein band (presumably monomeric PSGL-1) isolated from HL-60 cells in a blot rolling assay, suggesting that PSGL-1 is the major E-selectin ligand on HL-60 cells. This study also reported that PSGL-1 is the only HECA-452 reactive epitope

(CLA) on HL60 cells. Patel et al. (28) reported that HL-60 cell adhesion to CHO-E was diminished by ~50% upon pre-treatment of the HL-60 cells with OSGE, a protease that cleaves PSGL-1, and diminished by ~80% upon pretreatment of HL-60 cells with a mAb to PSGL-1, mAb PL-1. Microspheres coated with recombinant PSGL-1 (made in the presence of a fucosyltransferase) attach and roll on E-selectin expressing endothelium *in vitro* and *in vivo*, suggesting that any cell that expresses PSGL-1 and a fucosyltransferase can use PSGL-1 to attach and roll on E-selectin (14, 29).

On the other hand, there are other studies that suggest that PSGL-1 is not involved in HL60 cell adhesion to E-selectin. In particular, Snapp et al. (30), reported that HL-60 cell adhesion to CHO-E under flow is not diminished by pre-treatment of the HL-60 cells with a mAb to PSGL-1, mAb KPL-1. In addition, pre-treatment of HL-60 cells with a variety of proteases has been shown to not diminish HL-60 cell adhesion to CHO-E cells under static conditions. This latter effect may suggest that glycolipids play a role in adhesion to E-selectin, a concept bolstered by a recent study demonstrating that CHO-E cells bind to SLe^x bearing glycosphingolipids under fluid flow (31).

Thus, there is data both supporting and refuting the notion that PSGL-1 plays a role in HL-60 cell adhesion to endothelium via E-selectin. In the present study we have probed the hypothesis that PSGL-1 mediates initial attachment of HL60 cells to endothelial expressed E-selectin. Such a focused hypothesis (i.e. limiting the hypothesis to HL60 cells) is justified by the following: (1) as noted above, HL60 cells have been

used to gain insight into important physiological processes (e.g. HPC entry into bone marrow and leukocyte recruitment to a site of injury); (2) the role of PSGL-1 in HL60 cell adhesion to E-selectin expressing endothelium remains unresolved; and (3) HL60 cells do not express L-selectin, thus making it easier to study PSGL-1 mediated primary attachment (cell attachment from the free stream) to the endothelium in the absence of confounding secondary attachment (cell to cell followed by cell to endothelium attachment) that has been shown to involve L-selectin and PSGL-1.

Materials and Methods

Materials: Medium199, RPMI 1640, Alpha-MEM, FBS, dialyzed FBS, L-glutamine, trypsin-versene, penicillin/streptomycin, HBSS (Hanks Balanced Salt Solution) with Ca^+ and Mg^+ (HBSS+) or without (HBSS-), and HEPES, were obtained from BioWhittaker (Walkersville, MD). Endothelial mitogen was from Biomedical Technologies Inc. (Stoughton, MA). Gelatin was purchased from Difco Labs (Detroit, MI). Heparin, glycophorin, asialoglycophorin, sodium bicarbonate, and human IgG_1 were obtained from Sigma Chemical Co. (St. Louis, MO). Bovine serum albumin, BSA (Sigma) was added to HBSS+ to generate HBSS+, 1%BSA and HBSS+, 0.5% BSA buffers that were heated-treated (60^oC for 25 minutes). These are referred to as blocking and assay buffers respectively. A *Tris* buffer, pH 7.3, containing 150 mM NaCl, 2mM $MgCl_2$, and 25 mM Trizma base (Sigma) was used to dilute purified PSGL-1. PSGL-1 isolated from HL60 cells was generously provided by Dr. Michael B. Lawrence of the University of Virginia. PSGL-1 was purified from HL60 lysates via immunoprecipitation with anti-PSGL-1 mAb KPL-1. 10μm polystyrene microspheres (P (S/2%DVB)) with a standard deviation of 0.10μm were purchased from Bangs Laboratories Inc. (Fishers, IN). Neuraminidase (Boehringer Mannheim Corp., Indianapolis, IN) was from *Vibrio cholerae*; O-sialoglycoprotein endopeptidase (OSGE) was from Cedarlane Laboratories (Hornby, ON). Interleukin–1β (IL -1β) was from Calbiochem (La Jolla, CA).

Antibodies: Function blocking murine mAb to human E-selectin, 7A9 (lectin domain; IgG_1) and non-function blocking mAb to human E-selectin, H4/18 (CR domain; IgG_1) were generously provided by Dr. William Luscinskas (Brigham and Women's Hospital, Boston, MA). Function blocking murine mAb to human-P-selectin, HDG2/3 was a generous gift from Dr. Raymond T. Camphausen (Genetics Institute; Cambridge, MA). Murine mAbs to human PSGL-1 were: KPL-1 (IgG_1; BD Pharmingen, San Diego, CA), PL-1 (IgG_1; Calbiochem), PL2 (IgG_1; Accurate Chemical and Scientific, Westbury, NY) and PSL-275 (IgG_1; Genetics Institute). Murine mAb to sialyl-Le^x (SLe^x), CSLEX (IgM), rat mAb to cutaneous lymphocyte associated antigen (CLA), mAb HECA 452 (IgM) and murine mAb to human MHC Class-I antigens, G46-2.6 (IgG_1), were all from BD Pharmingen. Unlabeled goat IgG $F(ab')_2$, fluorescein isothiocynate (FITC)-labeled goat $F(ab')_2$ anti-mouse IgG Fc-specific and anti-mouse IgM, and FITC-labeled goat $F(ab')_2$ anti-rat IgM, polyclonal antibodies were from Jackson Immunoresearch Labs (Westgrove, PA).

Cell culture: Human umbilical vein endothelial cells (HUVEC) were purchased from Clonetics (San Diego, CA) and cultured as described in Chapter 3 (32). To induce E-selectin expression, HUVEC monolayers were pre-treated with 50 U/ml of IL-1β for 4 hours prior to use in the adhesion studies. Chinese hamster ovary cells stably expressing P-selectin (CHO-P) and untransfected (CHO) cells were provided by Dr. Raymond Camphausen (Genetics Institute). Their generation and characterization has been described previously (32). HL-60 cells were cultured as described previously (33).

Preparation, flow cytometric analysis, and enzymatic treatment of HL60 cells and PSGL-1 microspheres: HL60 cells were withdrawn from culture, washed and resuspended to $1x10^8$ cells/ml in RPMI 1640 and held at 4 ^oC until used in an assay. The HL60 cells were typically used within 4 hrs of harvest. The technique for generating PSGL-1 microspheres was similar to that described previously (32). Briefly, 10 μm microspheres were washed in Tris buffer and incubated ($1x10^7$ microspheres / ml) in PSGL-1 (diluted 1:30 in Tris buffer) overnight at 4 ^oC. The next day the microspheres were washed in blocking buffer and resuspended to $1x10^8$ microspheres/ml in blocking buffer. A similar procedure was used to generate the glycophorin and asialoglycophorin 10μm microspheres. Prior to perfusion through the parallel plate flow chamber, HL60 cells and microspheres were diluted to $5x10^5$ / ml in assay buffer.

Flow cytometric analysis: Aliquots of ~ $2x10^5$ microspheres or HL60 cells were washed with blocking buffer and incubated in 40 μl primary mAbs diluted to 20μg/ml. Subsequently, the microspheres or HL60 cells were washed and incubated with FITC-labeled polyclonal antibodies (1:50). Following this incubation, the microspheres or HL60 cells were washed and fixed in 1% formaldehyde. FITC fluorescence of 10,000 microspheres or HL60 cells was determined using a FACSort^{TM} flow cytometer (Beckon-Dickinson Immunocytometry Sys., Mountain View, CA) and plotted on a four-decade scale. All mAbs were diluted in blocking buffer. Incubations were performed at 4^oC for 20 minutes.

OSGE and sialidase treatment of HL60 cells and PSGL-1 microspheres: PSGL-1 microspheres and HL60 cells were washed and incubated (30 minutes at 37 ^{o}C) in OSGE (160 μg/ml) or neuraminidase (0.1 U /ml) diluted in blocking buffer supplemented with 25mM HEPES. Control PSGL-1 microspheres or HL60 cells were incubated in a similar manner in HEPES supplemented blocking buffer containing no enzymes. Following treatment, the PSGL-1 microspheres or HL60 cells were washed in cold blocking buffer and resuspended to $1x10^{8}$ /ml. For flow cytometric analysis, the HL60 cells and PSGL-1 microspheres were used immediately. PSGL-1 microspheres and HL60 cells were held for up to 2 hours and 1 hour, respectively, prior to use in adhesion assays.

Adhesion Assay: The parallel plate flow chamber (Glycotech; Rockville, MD) employed in this study is similar to that used by McIntire, Smith and colleagues (34) and consists of a plexiglass flow deck that fits inside a 35 mm tissue culture dish (Appendix A-2). Our particular flow set-up has been described previously (Chapters 2 and 3)(35). Temperature was maintained at 37 ^{0}C with a heating plate. HL60 cells or PSGL-1 microspheres ($5x10^{5}$ /ml) were perfused separately over HUVEC, CHO-P or CHO cell monolayers at 1.8 dynes/cm^{2} for 2.5 minutes. For experiments involving CHO-P and CHO, adhesion was quantified by determining the number of HL60 cells or PSGL-1 microspheres adherent to the cellular monolayers in 8 different fields of view after 2.5 minutes of flow. These numbers were averaged to yield one 'n' value. For experiments involving HUVEC, adhesion was quantified by determining the number of HL60 cells or PSGL-1 microspheres that attached from the free stream to the HUVEC monolayers

(primary attachment events) during the 2.5 minutes of flow. Note that secondary attachments and HL60 cells or PSGL-1 microspheres that rolled into the field of observation from an upstream field of view were not counted. This number represented one 'n' value. In certain experiments the HL60 cells, PSGL-1 microspheres, HUVEC or CHO-P were pretreated with mAbs (20 – 40 μg/ml) 15 minutes prior to use in the adhesion assay.

Statistics: Statistical differences between two means were estimated using unpaired Student's T-tests. In case of multiple comparisons against a single control, we performed a single-factor ANOVA coupled with Bonferroni's test. p values ≤ 0.05 were considered statistically significant.

Results

MAbs to PSGL-1 diminish HL60 cell adhesion to 4 hr. IL-1 activated HUVEC

To investigate the role of PSGL-1 in mediating HL60 cell adhesion to 4 hr. IL-1 activated HUVEC, we studied the adhesion of HL60 cells to 4 hr. IL-1 activated HUVEC in a parallel plate flow chamber at 1.8 dynes/cm^2. As shown in Figure 4.1, HL60 cells showed significant attachment to 4 hr. IL-1 activated HUVEC but not to unactivated HUVEC. The majority, if not all, of the adhesion was eliminated upon pre-treatment of the 4 hr. IL-1 HUVEC with a mAb that recognizes the lectin domain of E-selectin, mAb 7A9 (Figure 4.1). In contrast, a mAb that recognizes the CR domain of E-selectin, mAb, H4/18 did not significantly affect the adhesion (Figure 4.1). Combined, this data indicate that the majority, if not all, of the attachment of HL60 cells to 4 hr. IL-1 activated HUVEC occurs via the lectin domain of HUVEC expressed E-selectin.

To probe whether the attachment is mediated by PSGL-1 expressed on the HL60 cells, we pre-treated the HL60 cells with mAbs to PSGL-1 prior to use in the adhesion assay. Pretreatment of HL60 cells with mAbs to PSGL-1 significantly reduced HL60 cell attachment to 4 hr. IL-1 activated HUVEC (Figure 4.1). Specifically, mAbs KPL-1, PL-1 and PSL-275 reduced the adhesion by ~64%, ~54% and ~53% respectively. Pretreatment of HL60 cells with all three mAbs to PSGL-1 reduced adhesion by ~76%. In contrast to the results with the PSGL-1 mAbs, pretreatment of HL60 cells with anti-MHC Class I

mAb G46-2.6 did not have a significant effect on the adhesion. Taken together, the data in Figure 4.1 suggest a role for PSGL-1 in HL60 cell attachment to 4 hr. IL-1 activated HUVEC via E-selectin under flow.

Pretreatment of HL60 cells with OSGE does not diminish HL60 cell adhesion to 4 hr. IL-activated HUVEC

Previous studies have shown that the metalloprotease OSGE cleaves mucin like proteins including PSGL-1. Thus, to further probe the potential role of PSGL-1 in HL60 cell adhesion to 4 hr. IL-1 activated HUVEC, we pretreated the HL60 cells with OSGE prior to use in the adhesion assay. In conjunction with the adhesion studies, we performed flow cytometric analysis to characterize PSGL-1, SLe^x and CLA (HECA-452 reactive epitopes) expression on OSGE treated HL60 cells (Figure 4.2). Pre-treatment of HL60 cells with OSGE removed PSGL-1 (Figure 4.2 panel a vs. panel d), had little effect on SLe^x (panel b vs. panel e) and appeared to increase HECA-452 reactivity (panel c vs. f).

The fact that OSGE removed a significant amount, if not all, of the PSGL-1 from the HL60 cells combined with the data presented in Figure 4.1, led us to expect a significant reduction in adhesion of OSGE treated HL60 cells to 4 hr. IL-1 activated HUVEC. Surprisingly, we found that pre-treatment of HL60 cells with OSGE had no significant effect on HL60 cell attachment to 4 hr. IL-1 activated HUVEC (Figure 4.3A).

It has been shown that PSGL-1 is the primary ligand for P-selectin. Thus, as a positive control for the OSGE, we pretreated the HL60 cells with OSGE and studied their adhesion to Chinese hamster ovary cells transfected with P-selectin (CHO-P). As shown in Figure 4.3B, a significant number of HL60 cells adhere to CHO-P. Pretreatment of the CHO-P with a function blocking mAb to P-selectin (mAb HPDG2/3) or the HL60 cells with anti-PSGL-1 mAb KPL-1 eliminated the majority, if not all, of the HL60 cell adhesion to CHO-P strongly suggesting that the adhesion occurs via PSGL-1 and P-selectin. In agreement with previous studies, pretreatment of the HL60 cells with OSGE eliminated nearly all of the HL60 cell adhesion to CHO-P strongly suggesting that treatment of HL60 cells with OSGE does in fact cleave, at minimum, the N-terminal P-selectin binding site on PSGL-1 from HL60 cells. Thus, while pretreatment of HL60 cells with OSGE removes PSGL-1 to the extent that adhesion to CHO-P is greatly diminished, there is no significant effect on HL60 cell attachment to 4 hr. IL-1 activated HUVEC.

10mm diameter microspheres coated with PSGL-1 purified from HL60 cells attach to 4 hr. IL-1 activated HUVEC via E-selectin under flow

The results with the mAbs (Figure 4.1) suggest that HL60 cell attachment to 4 hr. IL-1 activated HUVEC is mediated, at least in part, by one or more distinct sites on PSGL-1. Our data in Figure 4.3, however, reveals that in spite of removal of PSGL-1 by OSGE, HL60 cells exhibit no significant change in their ability to attach to 4 hr. IL-1

activated HUVEC. To probe these apparently contradictory results, we sought to determine if PSGL-1, by itself, could mediate significant attachment of leukocyte sized particles to 4 hr. IL-1 HUVEC via E-selectin under physiological fluid shear conditions. To do this we coated 10 μm diameter polystyrene with PSGL-1 purified from HL60 cells. Note the justification for using the microsphere approach to study adhesion to E-selectin, as opposed to a transfection approach, has been given in the previous study (Chapter 3).

Prior to the adhesion assays, we used flow cytometric analysis to compare the PSGL-1 microspheres to the HL60 cells. As shown in Figures 4.4a, 4.4c, 4.4e, treating the PSGL-1 microspheres with mAbs to PSGL-1 (KPL-1), SLex (CSLEX) and CLA (HECA 452) resulted in an increase in the fluorescence of the microspheres relative to treatment with isotype-matched control antibodies, demonstrating that PSGL-1, SLe^x and HECA 452 reactive epitopes are present on the PSGL-1 microspheres. In parallel, we treated HL60 cells with the same set of antibodies. Flow cytometric analysis of the HL60 cells (Figures 4.4b, d, f) revealed that the level of PSGL-1 present on the HL60 cells appeared to be about twice that present on the PSGL-1 microspheres and that the level of SLe^x and CLA present on the HL60 cells was significantly greater, ~100 fold and 50-fold respectively, than that present on the PSGL-1 microspheres. These later observations are congruous with results from McEver's lab showing that SLe^x on PSGL-1 is only a small component of the total amount of SLe^x on HL60 cells (26). Although the level of PSGL-1 on the microspheres appeared to be only half that present on HL60

cells, we chose to prepare PSGL-1 microspheres in this fashion for use in the adhesion assays due to material limitations of purified PSGL-1.

We perfused the PSGL-1 microspheres over 4 hr. IL-1 activated HUVEC monolayers at 1.8 dynes/cm^2. As shown in Figure 4.5, the PSGL-1 microspheres exhibited significant attachment to 4 hr. IL-1 activated HUVEC but not to unactivated HUVEC. The majority, if not all, of the attachment was eliminated upon pre-treatment of the 4 hr. IL-1 HUVEC with a mAb that recognizes the lectin domain of E-selectin, mAb 7A9 (Figure 4.5). In contrast, pretreatment of the 4 hr. IL-1 HUVEC with a function blocking mAb to P-selectin, mAb HPDG2/3, did not significantly affect the adhesion. The result with mAb HPDG2/3 is consistent with the fact that we have been unable to detect P-selectin on the 4 hr. IL-1 activated HUVEC we used for this study (n=3 assayed via ELISA; data not shown). Microspheres not coated with PSGL-1, coated with trans-membrane proteins glycophorin or asioaloglycophorin purified from red blood cells did not attach to 4 hr. IL-1 activated HUVEC. Pre-treatment of the PSGL-1 microspheres with a mAb to PSGL-1, mAb KPL-1, significantly reduced the attachment to 4 hr. IL-1 activated HUVEC, but clearly not all of it. In summary, the data presented in Figure 4.5 strongly suggest that PSGL-1 microspheres attach to 4 hr. IL-1 activated HUVEC under physiologically relevant flow conditions via interactions between E-selectin and one or more binding sites on PSGL-1, including the epitope mapped by the anti-PSGL-1 mAb, KPL-1.

Pre-treatment of PSGL-1 microspheres with OSGE or neuraminidase significantly reduces attachment to 4 hr. IL-1 activated HUVEC

PSGL-1 appears to have more than one binding site for E-selectin. Thus we used an enzymatic approach, as opposed to mAbs, to further probe the specificity of PSGL-1 microsphere adhesion to 4 hr. IL-1 activated HUVEC. As stated above, previous studies have shown that the metalloprotease OSGE cleaves mucin like proteins including PSGL-1. Additionally, it has been shown that SLe^x-mediated adhesion to E-selectin can be diminished by pretreatment with neuraminidase. Thus, if PSGL-1 microsphere attachment to 4 hr. IL-1 activated HUVEC is occurring via SLe^x glycans on PSGL-1, pretreatment of the PSGL-1 microspheres with OSGE or neuraminidase should diminish the attachment.

We first characterized the effect of neuraminidase and OSGE treatment of the PSGL-1 microspheres via flow cytometric analysis (Figure 4.6). As shown, treatment of PSGL-1 microspheres with OSGE removed the majority, if not all, of the mAb KPL-1 (anti-PSGL-1) binding sites on the PSGL-1 microspheres, suggesting that the majority, if not all, of the PSGL-1 was removed from the PSGL-1 microspheres by OSGE treatment. Treatment with OSGE also removed the majority, if not all, of the HECA 452 reactive epitopes and SLe^x on the PSGL-1 microspheres. Treatment of the PSGL-1 microspheres with neuraminidase removed the majority, if not all, of the HECA 452 reactive epitopes and SLe^x on the PSGL-1 microspheres. Interestingly, treatment of the PSGL-1

microspheres with neuraminidase appeared to increase the binding of mAb KPL-1 to the PSGL-1 microspheres.

With these findings, we next tested the adhesion of OSGE and neuraminidase pretreated PSGL-1 microspheres to 4 hr. IL-1 activated HUVEC. As shown in Figure 4.7, pretreatment of the PSGL-1 microspheres with OSGE or neuraminidase significantly diminished (~86% and ~93% respectively) the attachment of the PSGL-1 microspheres to 4 hr. IL-1 activated HUVEC. Thus, combined, the data presented in Figures 4.5, 4.6 and 4.7 strongly suggest that microspheres coated with PSGL-1 purified from HL60 cells attach to 4 hr. IL-1 activated HUVEC under physiologically relevant fluid shear conditions via E-selectin on the HUVEC and PSGL-1 on the microspheres.

Discussion

Previous studies have both supported and refuted a role for P-selectin glycoprotein-1 (PSGL-1) expressed on HL60 cells to support adhesive interactions with E-selectin (14,19,28 29-31). In the present study, we probed the hypothesis that PSGL-1 mediates initial attachment of the hematopoietic progenitor cell (HPC) line HL60 to endothelial expressed E-selectin. Such a focused hypothesis (i.e. limiting the hypothesis to HL60 cells) is justified by the following: (1) HL60 cells have been widely used to gain insight into important physiological processes (e.g. HPC entry into bone marrow and leukocyte recruitment to a site of injury); (2) the role of PSGL-1 in HL60 cell adhesion to E-selectin expressing endothelium remains unresolved; and (3) HL60 cells do not express L-selectin, thus making it easier to study PSGL-1 mediated primary attachment (cell attachment from the free stream) to the endothelium in the absence of confounding secondary attachment (cell to cell followed by cell to endothelium attachment) that has been shown to involve L-selectin and PSGL-1.

As seen in Figure 4.1, primary attachments of HL60 cells to 4 hr. IL-1 activated HUVEC at 1.8 dynes/cm^2 were almost completely abolished with a functional blocking mAb to E-selectin (7A9), clearly implying a role for E-selectin in mediating these adhesive interactions. Previous reports have indicated that HPCs roll on bone marrow endothelium through adhesive interactions between VLA-4 on the HPCs and VCAM-1 on the endothelium (36-38). Despite high levels of VLA-4 expression on HL60 cells

(39), the adhesion of these cells to HUVEC in our studies were mediated primarily through E-selectin since the anti-E-selectin mAb 7A9 abrogated nearly all of the adhesive interactions. The residual level of adhesion following treatment with mAb 7A9 could be attributed to the VLA-4/VCAM-1 pathway since 4 hr. IL-1 activated HUVEC employed in our studies, were found to display basal expression levels of VCAM-1(42).

Anti-PSGL-1 mAbs PL-1, KPL-1 and PSL-275 when employed separately, caused a partial reduction in HL60 cell adhesion to E-selectin. Employing all three mAbs simultaneously, caused an overall 80% reduction in the adhesion of HL60 cells to activated HUVEC under flow. These data seem to suggest that HL60 cell primary attachments to E-selectin occur predominantly through PSGL-1, via sites recognized by mAbs PL-1, KPL-1 and PSL-275 in addition to other potential binding sites on the molecule. Note that, mAbs PL-1 and KPL-1 map to amino acids 5-11 and 13-17 on PSGL-1 respectively, while PSL275 binds to a later region on the molecule. This interpretation seems consistent with a previous study using recombinant PSGL-1 that suggests the presence of one E-selectin binding site in first 19 amino acids and one or more additional E-selectin binding sites in later amino acids 19-148 (14).

It is important to recognize however, that the observed inhibition of HL60 cell adhesion to IL-1 activated HUVEC by anti-PSGL-1 mAbs could be due to one or more reasons. Firstly, this inhibition in HL60 cell adhesion could be attributed to the mapping of these anti-PSGL-1 mAbs to their specific recognition sites or neighboring regions,

consequently blocking the ability of their specific sites to bind to E-selectin. This seems to be the case in our studies, since the inhibitory effects of the set of mAbs employed to the N-terminal region of PSGL-1 (mAbs KPL-1 and PL-1) and the mAb to a later region of the molecule (PSL275) seem to be additive, suggesting specific recognition of their respective sites. Secondly, these anti-PSGL-1 mAbs could, in theory, sterically recognize molecule(s) distinct from PSGL-1, thus blocking its interactions with E-selectin and resulting in a reduction of the overall level of HL60 adhesion. Our adhesion studies with native PSGL-1 coated microspheres however, discount this possibility since the anti-PSGL-1 mAb KPL-1 specifically recognizes the P-selectin binding site on PSGL-1 as expected and blocks adhesion of these microspheres to E-selectin (Figure 4.5) and P-selectin (data not shown) under flow. Thirdly, this inhibition could attributed to the ability of just about any mAb to non-specifically inhibit PSGL-1 binding to HL60 cell adhesion. This does not seem to be the case in our studies, since the use of an anti-MHC Class I mAb had no effect on the adhesion of these HL60 cells to E-selectin.

A major presence of clustered O-glycans on the PSGL-1 molecule renders it susceptible to cleavage by the metalloprotease O-sialoglycoprotein endopeptidase (OSGE). Consequently, treatment of HL60 cells with OSGE was found to completely remove regions of surface PSGL-1 recognized by the anti-PSGL-1 mAb KPL-1 (Figure 4.2) as detected by flow cytometry. If PSGL-1 was indeed a predominant ligand for E-selectin on HL60 cells, removal of all surface PSGL-1 would therefore be expected to cause a significant reduction in adhesion of HL60 cells to E-selectin expressing HUVEC.

On the contrary, our data shows that pre-treatment of HL60 cells with OSGE had no qualitative or quantitative effect on the overall adhesion of these cells to HUVEC (Figure 4.3A). This observation contradicts a previous study showing a near 50% reduction in adhesion of HL60 cells to CHO-E upon pre-treatment with OSGE under similar conditions (28), and could be due to the use of different substrates in these studies (CHO-E in that study versus HUVEC in ours).

On the other hand, our experimental observations are in complete agreement with previous observations showing no difference in HL60 cell adhesion to E-selectin in spite of pre-treatments with O-sialoglycoprotease or OSGE (19, 40). We speculate that the unchanged levels of HL60 cell adhesion following OSGE treatment, might be attributed to E-selectin interactions *independent* of PSGL-1 or for that matter, any other sialomucin on these cells. Flow cytometry data on HL60 cells clearly shows significant levels of SLe^x and HECA-452 reactive epitopes on these cells, which remain unchanged in spite of OSGE pre-treatment. While SLe^x type glycans have been found to be sufficient to mediate attachment and rolling on E-selectin (13, 14), presence of HECA-452 reactive epitopes/CLA has previously been correlated with E-selectin binding activity (41). It is therefore quite likely that the adhesion of OSGE treated cells might be occurring in a PSGL-1/sialomucin independent manner, and mediated by SLe^x glycans and HECA-452 reactive epitopes on these cells.

Combined with our initial observations in Figure 4.1, these data suggest that HL60 cell adhesion to E-selectin occurs predominantly via PSGL-1 with secondary contributions from other possible E-selectin ligand(s). Furthermore, pre-treatment of these cells with OSGE might not only result in complete removal of PSGL-1 but also, a probable unmasking of these less dominant structures or other potential E-selectin binding sites that upon becoming more accessible to E-selectin, makes them more predominant E-selectin counter-receptors in the absence of PSGL-1. Identification of these alternate physiological E-selectin ligands was beyond the scope of this study.

To investigate the E-selectin binding activity of HL60 cell PSGL-1, independent of these other possible E-selectin counter-receptors on HL60 cells, we decided to employ a cell-free experimental system consisting uniquely of PSGL-1, and devoid of any other possible E-selectin ligands. In other words, we generated leukocyte sized polystyrene microspheres coated with purified HL60 cell-derived PSGL-1 at site densities slightly lower than those expressed on HL60 cells (Figure 4.4). Although, this technique was previously employed to study the adhesion of recombinant PSGL-1 coated microspheres to E- and P-selectin under flow (14), that study differs from ours in three respects. Firstly, our study employs microspheres coated with native PSGL-1 (purified from HL60 cells) rather than a recombinant molecule. Secondly, unlike the previous study, levels of native PSGL-1 on our microspheres were known and correlated with those expressed on HL60 cells.

As shown in Figure 4.4, expression of SLe^x and HECA-452 reactive epitopes correlated well with PSGL-1 expression levels on PSGL-1-coated microspheres. SLe^x and CLA expression on HL60 cells however, was far greater than levels of PSGL-1 on these cells, suggesting that a significant percentage of these two structures were not associated with PSGL-1. Interestingly, in a previous study (19), investigators found that all of the HECA-452 reactivity on HL60 cells was associated with a 140 kD monomeric form of PSGL-1/CLA. Our data however seems to indicate otherwise, reinforcing our hypothesis that these structures might in fact play a dominant role in E-selectin binding in the absence of PSGL-1 and/or a secondary role in its presence.

As shown in Figure 4.5, attachment of PSGL-1 coated microspheres was lower than that observed with HL60 cells, and might be due to lower levels of PSGL-1 on these microspheres. The attachment and rolling of PSGL-1 microspheres to 4 hr. IL-1 activated HUVEC occurred entirely through E-selectin expressed on activated HUVEC monolayers. A majority of this adhesion seems to be mediated via sites on PSGL-1 that are independent from that mapped by KPL-1 since mAb blocking using this anti-PSGL-1 mAb reduced only 40% of the microsphere adhesion. To further probe the structures on PSGL-1 that might be involved in binding to E-selectin, we subjected these microspheres to sialidase and protease treatments. As shown in Figure 4.6 and 4.7, OSGE treatment of PSGL-1 coated microspheres completely cleaves, at minimum, regions of PSGL-1 bearing the KPL-1 recognition site, and results in a major reduction of microsphere adhesion to E-selectin under flow, as expected. In spite of unchanged levels of PSGL-1

expression on the microspheres following sialidase treatment, a complete removal of all SLe^x and HECA-452 immuno-reactivity from these microspheres is observed. Sialidase treatment of PSGL-1 microspheres also completely inhibits their attachment and rolling to E-selectin, clearly identifying a role for these structures in mediating PSGL-1 binding to E-selectin. This is consistent with our hypothesis that E-selectin binding occurs through one or more distinct sites on the molecule. It is therefore quite likely that the additional binding sites might be associated with these structures.

In summary, our studies provide evidence for the role of PSGL-1 as a pre-dominant ligand for E-selectin on HL60 cells. Our experimental data also suggests that PSGL-1 binds to E-selectin through more than one site on the molecule, consistent with previous reports. These studies also demonstrate a role for other possible E-selectin counter-receptor(s) on HL60 cells that, in the absence of PSGL-1, assume a more predominant role in mediating adhesion to E-selectin.

References

1. Kansas, G.S. 1996. Selectins and their ligands: current concepts and controversies. *Blood*. 88:3259-3287.

2. Luscinskas, F.W., and M.A. Gimbrone. 1996. Endothelial-dependent mechanisms in chronic inflammatory leukocyte recruitment. *Annu. Rev. Med.* 47:413-421.

3. Springer, T.A. 1994. Traffic signals for lymphocyte recirculation and leukocyte emigration: the multistep paradigm. *Cell*. 76:301-314.

4. Carlos, T.M., and J.M. Harlan. 1994. Leukocyte-endothelial adhesion molecules. *Blood*. 84:2068-2101.

5. von Andrian, U.H., J.D. Chambers, L.M. McEvoy, R.F. Bargatze, K.E. Arfors, and E.C. Butcher. 1991. Two-step model of leukocyte-endothelial cell interactions in inflammation: distinct roles for LECAM-1 and the leukocyte ß$_2$ integrins in vivo. *Proc. Natl. Acad. Sci. USA*. 88:7538-7542.

6. Lawrence, M.B., C.W. Smith, S.G. Eskin, and L.V. McIntire. 1990. Effect of venous shear stress on CD18-mediated neutrophil adhesion to cultured endothelium. *Blood*. 75:227-237.

7. Lawrence, M.B., and T.A. Springer. 1991. Leukocytes roll on a selectin at physiologic flow rates: distinction from and prerequisite for adhesion through integrins. *Cell*. 65:859-873.

8. Lawrence, M.B., and T.A. Springer. 1993. Neutrophils roll on E-selectin. *J. Immunol.* 151:6338-6346.

9. Bevilacqua, M.P., J.S. Pober, D.L. Mendrick, R.S. Cotran, and M.A. Gimbrone Jr. 1987. Identification of an inducible endothelial-leukocyte adhesion molecule. *Proc. Natl. Acad. Sci., USA*. 84:9238-9242.

10. Abbassi, O., T.K. Kishimoto, L.V. McIntire, D.C. Anderson, and C.W. Smith. 1993. E-selectin supports neutrophil rolling in vitro under conditions of flow. *J. Clin. Invest*. 92:2719-2730.

11. Bevilacqua, M.P. 1993. Endothelial-leukocyte adhesion molecules. *Annu. Rev. Immunol.* 11:767-804.

12. Bevilacqua, M.P., and R.M. Nelson. 1993. Selectins. *J. Clin. Invest*. 91:379-387.

13. Brunk, D.K., D.J. Goetz, and D.A. Hammer. 1996. Sialyl Lewisx/E-selectin-mediated rolling in a cell-free system. *Biophys. J.* 71:2902-2908.

14. Goetz, D.J., D.M. Greif, R.T. Camphausen, S. Howes, K.M. Comess, K.R. Snapp, G.S. Kansas, and F.W. Luscinskas. 1997. Isolated P-selectin glycoprotein-1 dynamic adhesion to P- and E-selectin. *J. Cell Biol.* 137:509-519.

15. Picker, L.J., S.A. Michie, L.S. Rott, and E.C. Butcher. 1990. A unique phenotype of skin-associated lymphocytes in humans. Preferential expression of the HECA-

452 epitope by benign and malignant T cells at cutaneous sites. *Am J Pathol*. 136:1053-68.

16. Picker, L.J., T.K. Kishimoto, C.W. Smith, R.A. Warnock, and E.C. Butcher. 1991. ELAM-1 is an adhesion molecule for skin-homing T cells. *Nature*. 349:796-9.

17. Fuhlbrigge, R.C., J.D. Kieffer, D. Armerding, and T.S. Kupper. 1997. Cutaneous lymphocyte antigen is a specialized form of PSGL-1 expressed on skin-homing T cells. *Nature*. 389:978-81.

18. Rossiter, H., F. van Reijsen, G.C. Mudde, F. Kalthoff, C.A. Bruijnzeel-Koomen, L.J. Picker, and T.S. Kupper. 1994. Skin disease-related T cells bind to endothelial selectins: expression of cutaneous lymphocyte antigen (CLA) predicts E-selectin but not P- selectin binding. *Eur J Immunol*. 24:205-10.

19. Dimitroff, C.J., J.Y. Lee, S. Rafii, R.C. Fuhlbrigge, and R. Sackstein. 2001. CD44 is a major E-selectin ligand on human hematopoietic progenitor cells. *J Cell Biol*. 153:1277-86.

20. Sako, D., X.J. Chang, K.M. Barone, G. Vachino, H.M. White, G. Shaw, G.M. Veldman, K.M. Bean, T.J. Ahern, B. Furie, D.A. Cumming, and G.R. Larsen. 1993. Expression cloning of a functional glycoprotein ligand for P-selectin. *Cell*. 75:1179-1186.

21. Moore, K.L., N.L. Stults, S. Diaz, D.F. Smith, R.D. Cummings, A. Varki, and R.P. McEver. 1992. Identification of a specific glycoprotein ligand for P-selectin (CD62) on myeloid cells. *J. Cell Biol.* 118:445-456.

22. Moore, K.L., K.D. Patel, R.E. Bruehl, L. Fugang, D.A. Johnson, H.S. Lichenstein, R.D. Cummings, D.F. Bainton, and R.P. McEver. 1995. P-selectin glycoprotein ligand-1 mediates rolling of human neutrophils on P-selectin. *J. Cell Biol.* 128:661-671.

23. Laszik, Z., P.J. Jansen, R.D. Cummings, T.F. Tedder, R.P. McEver, and K.L. Moore. 1996. P-selectin Glycoprotein Ligand-1 is broadly expressed on cells of myeloid, lymphoid, and dendritic lineage and in some nonhematopoietic cells. *Blood*. 88:3010-3021.

24. Moore, K.L., S.F. Eaton, D.E. Lyons, H.S. Lichenstein, R.D. Cummings, and R.P. McEver. 1994. The P-selectin glycoprotein ligand from human neutrophils displays sialylated, fucosylated, O-linked poly-N-acetyllactosamine. *J. Biol. Chem*. 269:23318-23327.

25. Norgard, K.E., K.L. Moore, S. Diaz, N.L. Stults, S. Ushiyama, R.P. McEver, R.D. Cummings, and A. Varki. 1993. Characterization of a specific ligand for P-selectin on myeloid cells. *J. Biol. Chem.* 268:12764-12774.

26. Wilkins, P.P., R.P. McEver, and R.D. Cummings. 1996. Structures of the O-glycans on P-selectin glycoprotein ligand-1 from HL-60 cells. *J. Biol. Chem.* 271:18732-18742.

27. Kieffer, J.D., R.C. Fuhlbrigge, D. Armerding, C. Robert, K. Ferenczi, R.T. Camphausen, and T.S. Kupper. 2001. Neutrophils, monocytes, and dendritic cells express the same specialized form of PSGL-1 as do skin-homing memory T cells: cutaneous lymphocyte antigen. *Biochem Biophys Res Commun*. 285:577-87.

28. Patel, K.D., K.L. Moore, M.U. Nollert, and R.P. McEver. 1995. Neutrophils use both shared and distinct mechanisms to adhere to selectins under static and flow conditions. *J. Clin. Invest*. 96:1887-1896.

29. Norman, K.E., A.G. Katopodis, G. Thoma, F. Kolbinger, A.E. Hicks, M.J. Cotter, A.G. Pockley, and P.G. Hellewell. 2000. P-selectin glycoprotein ligand-1 supports rolling on E- and P-selectin in vivo. *Blood*. 96:3585-91.

30. Snapp, K.R., H. Ding, K. Atkins, R. Warnke, F.W. Luscinskas, and G.S. Kansas. 1998. A novel P-selectin glycoprotein ligand-1 monoclonal antibody recognizes an epitope within the tyrosine sulfate motif of human PSGL-1 and blocks recognition of both P- and L-selectin. *Blood*. 91:154-164.

31. Burdick, M.M., B.S. Bochner, B.E. Collins, R.L. Schnaar, and K. Konstantopoulos. 2001. Glycolipids support E-selectin-specific strong cell tethering under flow. *Biochem Biophys Res Commun*. 284:42-9.

32. Crutchfield, K.L., V.R. Shinde Patil, C.J. Campbell, C.A. Parkos, J.R. Allport, and D.J. Goetz. 2000. CD11b/CD18-coated microspheres attach to E-selectin under flow. *J. Leuk. Biol.* 67:196-205.

33. Goetz, D.J., H. Ding, W.J. Atkinson, G. Vachino, R.T. Camphausen, D.A. Cumming, and F.W. Luscinskas. 1996. A human colon carcinoma cell line exhibits adhesive interactions with P-selectin under fluid flow via a PSGL-1-Independent mechanism. *Am. J. Path.* 149:1661-1673.

34. Gopalan, P.K., D.A. Jones, L.V. McIntire, and C.W. Smith. 1996. Cell adhesion under hydrodynamic flow conditions. *In* Current Protocols in Immunology. J.E. Coligan, A.M. Kruisbeek, D.H. Margulies, E.M. Shevach, and W. Strober, editors. J. Wiley, New York. 7.29.1-7.29.23.

35. Shinde Patil, V.R., C.J. Campbell, Y.H. Yun, S.M. Slack, and D.J. Goetz. 2001. Particle diameter influences adhesion under flow. *Biophys J*. 80:1733-1743.

36. Leavesley, D.I., J.M. Oliver, B.W. Swart, M.C. Berndt, D.N. Haylock, and P.J. Simmons. 1994. Signals from platelet/endothelial cell adhesion molecule enhance the adhesive activity of the very late antigen-4 integrin of human CD34+ hemopoietic progenitor cells. *J Immunol*. 153:4673-83.

37. Liesveld, J.L., K.E. Frediani, A.W. Harbol, J.F. DiPersio, and C.N. Abboud. 1994. Characterization of the adherence of normal and leukemic CD34+ cells to endothelial monolayers. *Leukemia*. 8:2111-7.

38. Mazo, I.B., J.C. Gutierrez-Ramos, P.S. Frenette, R.O. Hynes, D.D. Wagner, and U.H. von Andrian. 1998. Hematopoietic progenitor cell rolling in bone marrow microvessels: parallel contributions by endothelial selectins and vascular cell adhesion molecule 1. *J Exp Med*. 188:465-74.

39. Oxley, S.M., and R. Sackstein. 1994. Detection of an L-selectin ligand on a hematopoietic progenitor cell line. *Blood*. 84:3299-306.

40. Alon, R., H. Rossitier, X. Wang, T.A. Springer, and T.S. Kupper. 1994. Distinct cell surface ligands mediate T lymphocyte attachment and rolling on P- and E-selectin under physiological flow. *J. Cell Biol*. 127:1485-1495.

41. Borges, E., G. Pendl, R. Eytner, M. Steegmaier, O. Zollner, and D. Vestweber. 1997. The binding of T cell-expressed P-selectin glycoprotein ligand-1 to E- and P-selectin is differentially regulated. *J Biol Chem*. 272:28786-92.

42. Dagia, N.M. and Goetz, D.J. Lactacystin inhibits myeloid cell adhesion to endothelium elicited by hetero-cytokine activation. *(Manuscript in preparation)*

Figures

Figure 4.1. Pretreatment of HL60 cells with mAbs to PSGL-1 diminishes HL60 cell attachment to 4 hr. IL-1 activated HUVEC. HL60 cell attachment from the free stream (primary attachment) to 4 hr. IL-1 activated and unactivated HUVEC was determined. In certain instances, HL60 cells or HUVEC were pretreated with mAbs prior to use in adhesion assays. (Legend: Activation indicates pretreatment (+) or no pretreatment (-) of HUVEC with IL-1β 4 hr. prior to the assay; HL60 mAb indicates pre-treatment of HL60 cells with anti-PSGL-1 mAbs, KPL-1, PL-1, PSL275, All (all three mAbs KPL-1, PL-1 and PSL-275), with anti-MHC Class I (mAb G46-2.6), or no pre-treatment (-). HUVEC mAb indicates pre-treatment of HUVEC with mAbs to E-selectin, (7A9 and H4/18) or no pre-treatment (-). * indicates $p < 0.05$ compared to left most bar. Shear stress = 1.8 dynes/cm^2.

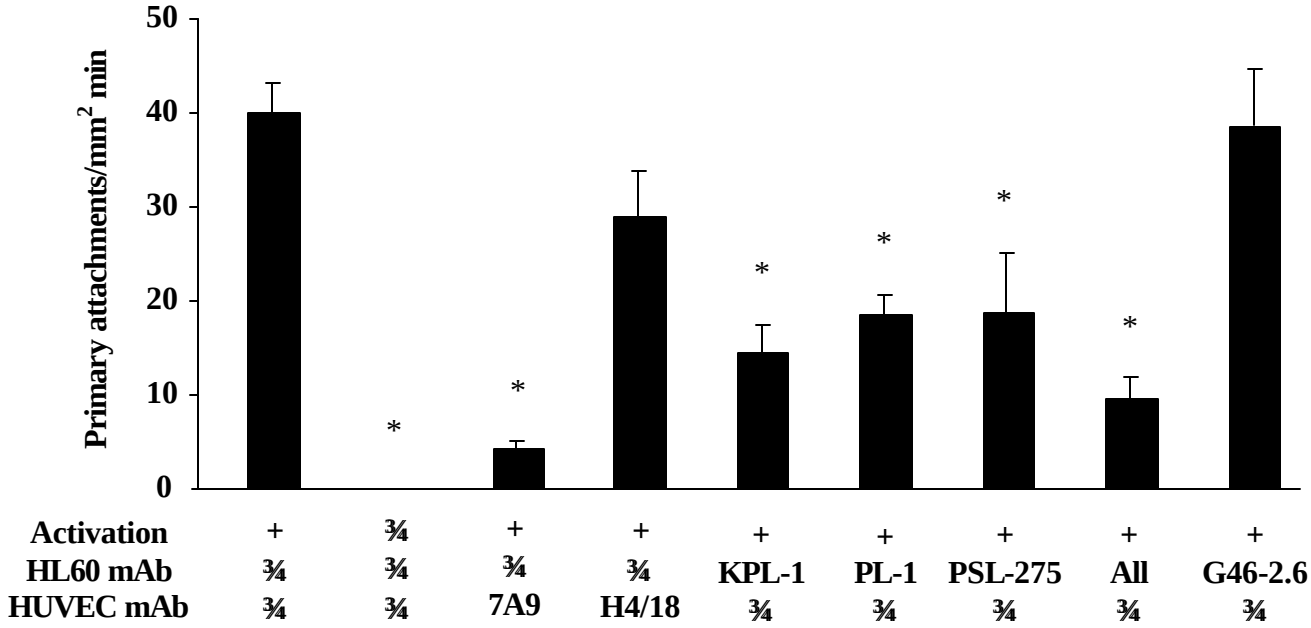
Primary attachments/mm2 min
50
40
30
20
10
0
*
*
*
*
*
*
Activation + ¾ + + + + + + +
HL60 mAb ¾ ¾ ¾ ¾ KPL-1 PL-1 PSL-275 All G46-2.6
HUVEC mAb ¾ ¾ 7A9 H4/18 ¾ ¾ ¾ ¾ ¾

Figure 4.2. OSGE removes the majority, if not all, of the PSGL-1 from HL60 cells but has little effect on SLe^x and CLA. Levels of PSGL-1, SLe^x and HECA-452 reactive epitopes (CLA) on untreated (top row) and OSGE treated HL60 cells (bottom row) were determined by flow cytometric analysis. Panels a and d: PSGL-1 on untreated (Panel a) and OSGE treated (Panel d) HL60 cells were detected using anti-PSGL-1 mAb KPL-1 (shaded histograms); mAb HPDG2/3 served as a negative control (open histograms). Panels b and e: SLe^x on untreated (Panel b) and OSGE treated (Panel e) HL60 cells were detected using anti-SLe^x mAb, CSLEX (shaded histograms); mouse IgM served as a negative control (open histograms). Panels c and f: CLA levels on untreated (Panel c) and OSGE treated (Panel f) HL60 cells were detected using mAb HECA-452 (shaded histograms); rat IgM served as a negative control (open histograms). Primary mAbs indicated above were detected via a FITC labeled secondary antibody and flow cytometry. Cell number vs. mean channel fluorescence (MCF) plotted on a four decade scale. Results typical of 3 separate experiments.

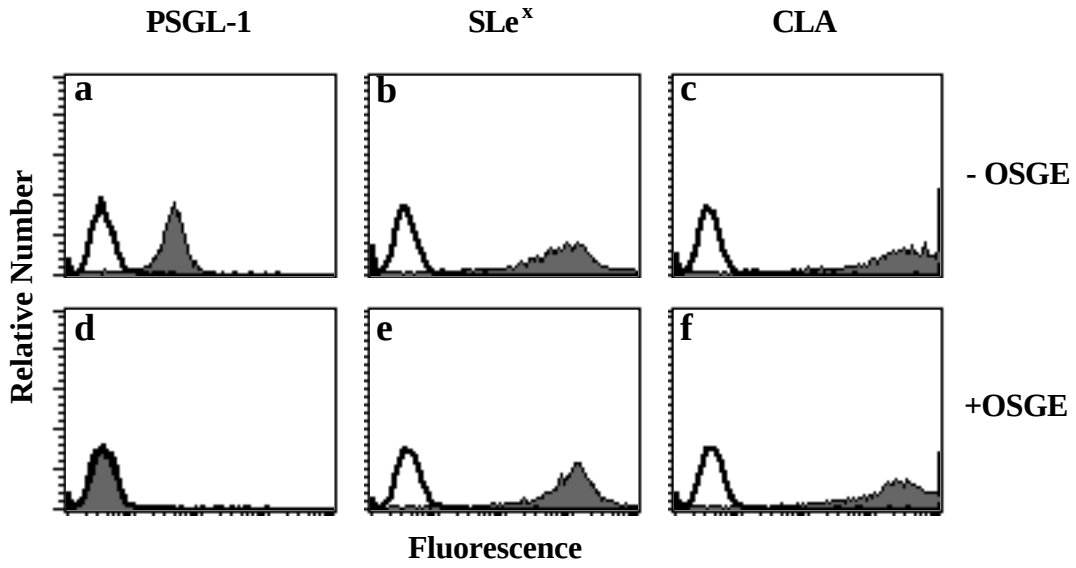
PSGL-1
SLe x
CLA
a
b
c
d
e
f
- OSGE
+OSGE
Relative Number
Fluorescence

Figure 4.3. Pretreatment of HL60 cells with OSGE has no significant effect on HL60 cell attachment to 4 hr. IL-1 activated HUVEC. (a) HL60 cells were pretreated with OSGE (+OSGE) or buffer only (-OSGE) and subsequently perfused over 4 hr. IL-1 activated HUVEC. Pretreatment of HL60 cells with OSGE had no effect on their attachment to 4 hr. IL-1 activated HUVEC. (n = 7; shear stress = 1.8 dynes/cm^2). (B) HL60 cells were perfused over CHO-P and the number of adherent HL60 cells at the end of 2.5 minutes of flow was determined. HL60 mAb indicates pre-treatment of HL60 cells with anti-PSGL-1 mAb (KPL-1) or no pre-treatment (-). CHO-P mAb indicates treatment of CHO-P substrates with anti-P-selectin mAb, HPDG2/3 (2/3) or no treatment (-). Treatment indicates HL60 cells incubated in OSGE (+OSGE), in control buffer only (-OSGE) or no treatment (-). (n =2-3; * $p < 0.05$ compared the left most bar). Error bars indicate standard deviation.

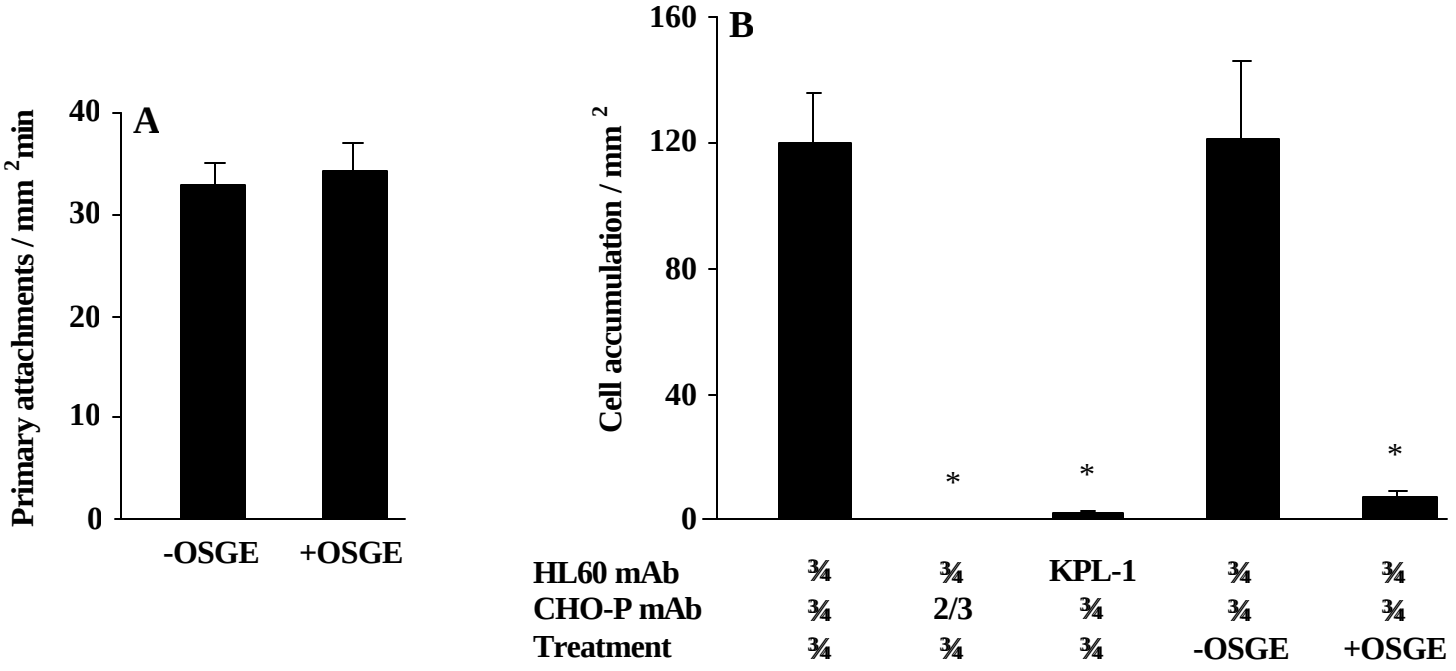
A
Primary attachments / mm 2min
40
30
20
10
0
-OSGE
+OSGE
B
Cell accumulation / mm 2
160
120
80
40
0
*
*
*
HL60 mAb ¾ ¾ KPL-1 ¾ ¾
CHO-P mAb ¾ 2/3 ¾ ¾ ¾
Treatment ¾ ¾ ¾ -OSGE +OSGE

Figure 4.4. Comparison of PSGL-1, SLe^x and CLA on PSGL-1 microspheres and HL60 cells. Levels of PSGL-1, SLe^x and HECA-452 reactive epitopes (CLA) on PSGL-1 microspheres (top row) and HL60 cells (bottom row) were determined by flow cytometric analysis. Panels a and b: PSGL-1 on PSGL-1 microspheres (Panel a) and HL60 cells (Panel b) was detected using mAb KPL-1 (shaded histograms); anti-MHC Class-I mAb G46-2.6 and anti-P-selectin mAb HPDG2/3 served as negative controls (open histograms) on the PSGL-1 microspheres and HL60 cells respectively. Panels c and d: SLe^x on PSGL-1 microspheres (Panel c) and HL60 cells (Panel d) were detected using an anti-SLe^x mAb CSLEX (shaded histograms); mouse IgM served as a negative control (open histograms). Panels e and f: CLA levels on PSGL-1 microspheres (Panel e) and HL60 cells (Panel f) were detected using an mAb HECA-452 (shaded histograms); rat IgM served as a negative control (open histograms). Primary mAbs indicated above were detected via a FITC labeled secondary antibody and flow cytometry. Cell number vs. mean channel fluorescence (MCF) plotted on a four decade scale. Results shown are typical of 3 separate experiments.

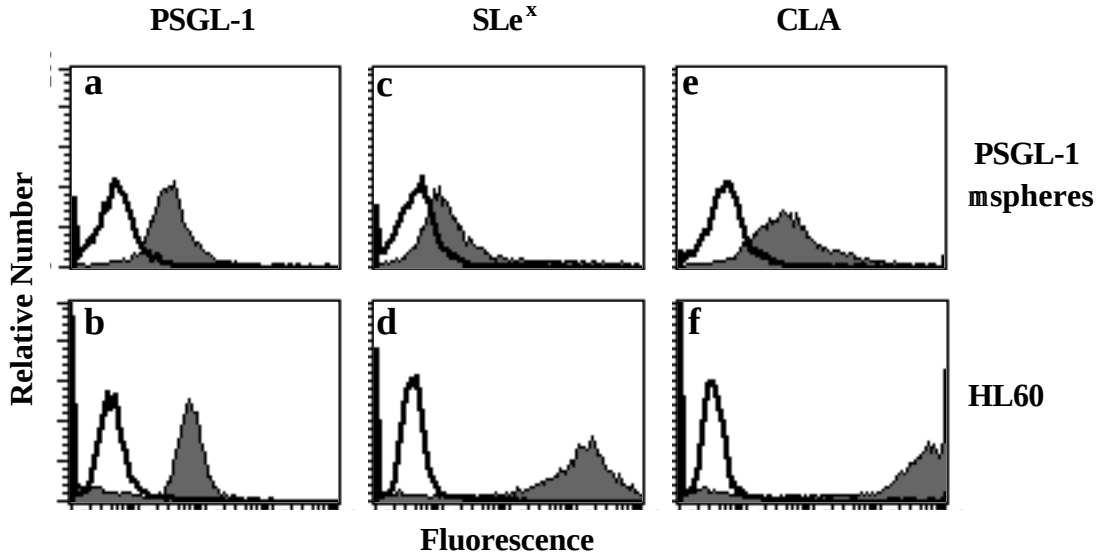
PSGL-1
SLe x
CLA
a
c
e
b
d
f
Relative Number
PSGL-1 mspheres
HL60
Fluorescence

Figure 4.5. Microspheres coated with PSGL-1 purified from HL60 cells attach to 4 hr. IL-1 activated HUVEC under flow. PSGL-1 microsphere attachment from the free stream (primary attachment) to 4 hr. IL-1 activated and unactivated HUVEC was determined. In certain instances, HL60 cells or HUVEC were pretreated with mAbs prior to use in adhesion assays. (Legend: Ligand indicates microspheres coated with PSGL-1 purified from HL60 cells (PSGL-1), Glycophorin (Glycop) or Asialoglycophorin (AsialoG) purified from red blood cells, or not coated with a ligand (-); μsphere mAb indicates pretreatment of PSGL-1 microspheres with anti-PSGL-1 mAb KPL-1 or no pretreatment (-); HUVEC mAb indicates pretreatment of HUVEC with a mAb to E-selectin, (mAb 7A9) or P-selectin (mAb HPDG2/3) or no pretreatment (-). Activation indicates pretreatment (+) or no pretreatment (-) of HUVEC with IL-1β 4 hr. prior to the assay; * indicates $p < 0.05$ compared to left most bar. Shear stress = 1.8 dynes/cm^2.

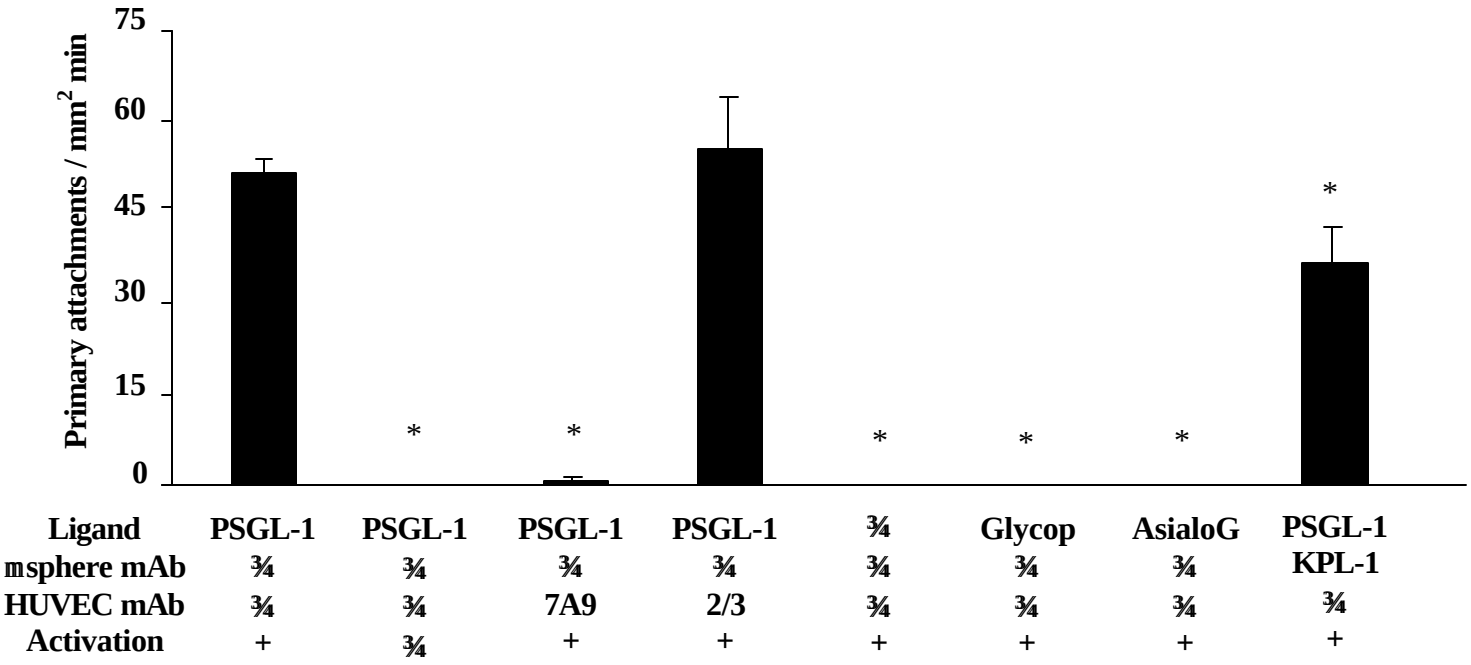
Primary attachments / mm2 min
75
60
45
30
15
0
*
*
*
*
*
*
Ligand
PSGL-1
PSGL-1
PSGL-1
PSGL-1
¾
Glycop
AsialoG
PSGL-1
msphere mAb
¾
¾
¾
¾
¾
¾
¾
KPL-1
HUVEC mAb
¾
¾
7A9
2/3
¾
¾
¾
¾
Activation
+
¾
+
+
+
+
+
+

Figure 4.6. Pre-treatment of PSGL-1 microspheres with OSGE or neuraminidase significantly diminishes PSGL-1 microsphere adhesion to 4 hr. IL-1 activated HUVEC. Levels of PSGL-1, SLe^x and HECA-452 reactive epitopes (CLA) on untreated (top row) OSGE treated (middle row) or neuraminidase treated PSGL-1 microspheres (bottom row) were determined by flow cytometric analysis. Panels a, b, c: PSGL-1 on untreated (Panel a) OSGE treated (Panel b) and neuraminidase treated PSGL-1 microspheres was detected using anti-PSGL-1 mAb KPL-1 (shaded histograms); mAb HPDG2/3 served as a negative control (open histograms). Panels d, e, f: SLe^x on untreated (Panel d) OSGE treated (Panel e) and neuraminidase treated (Panel f) PSGL-1 microspheres was detected using anti-SLe^x mAb, CSLEX (shaded histograms); mouse IgM served as a negative control (open histograms). Panels g, h, i: CLA levels on untreated (Panel g) OSGE treated (Panel h) and neuraminidase treated (Panel i) PSGL-1 microspheres was detected using mAb HECA-452 (shaded histograms); rat IgM served as a negative control (open histograms). Primary mAbs indicated above were detected via a FITC labeled secondary antibody and flow cytometry. Cell number vs. mean channel fluorescence (MCF) plotted on a four decade scale. Results typical of 3 separate experiments.

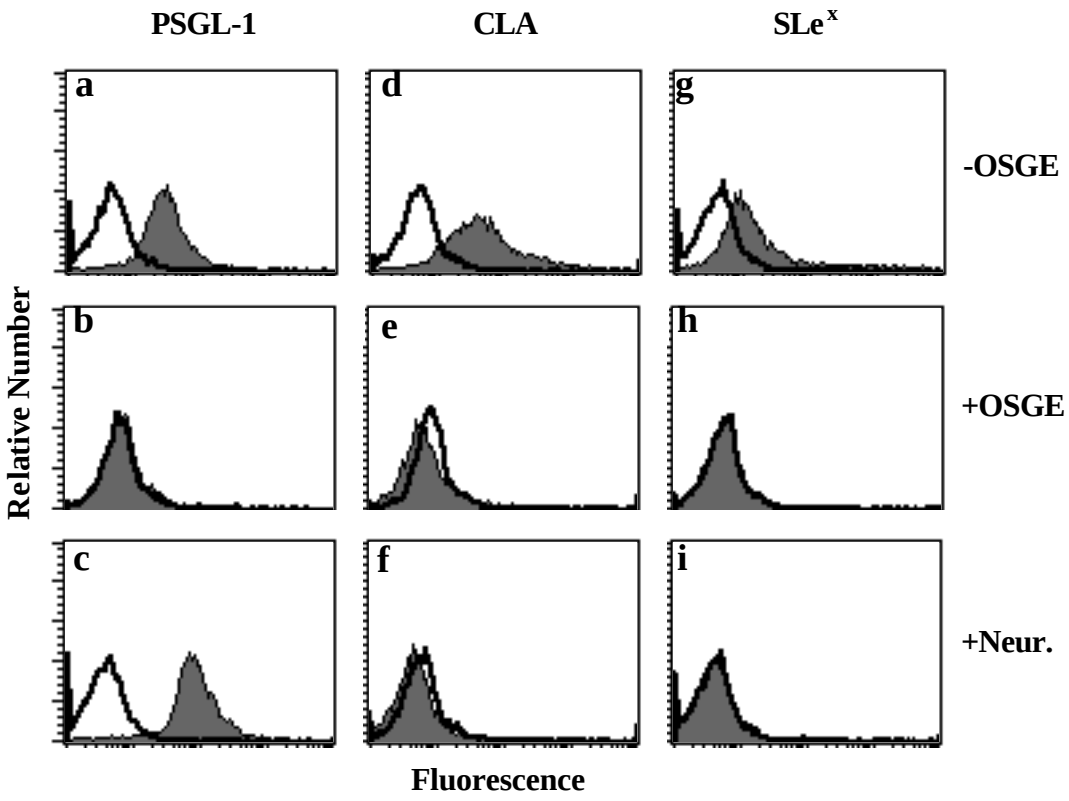
PSGL-1
CLA
SLe x
a
d
g
-OSGE
b
e
h
+OSGE
c
f
i
+Neur.
Relative Number
Fluorescence

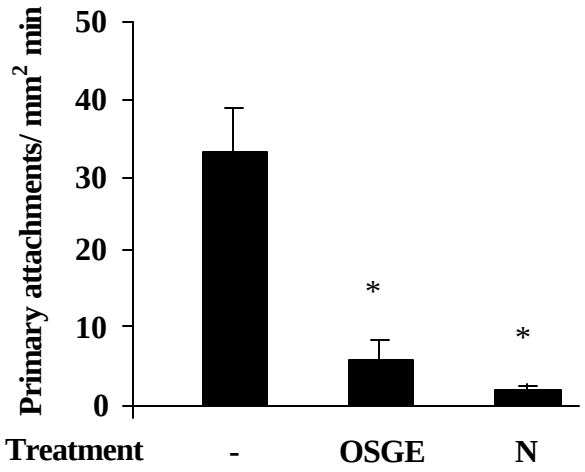

Figure 4.7. Pretreatment of PSGL-1 microspheres with OSGE or neuraminidase significantly diminishes PSGL-1 microsphere attachment to 4 hr. IL-1 activated HUVEC. PSGL-1 microspheres were incubated in buffer alone (-), OSGE (OSGE) or neuraminidase (N) and subsequently perfused over 4 hr. IL-1 activated HUVEC. PSGL-1 microsphere attachment to 4 hr. IL-1 activated HUVEC was determined for each condition. (n= 2-3; * indicates $p < 0.05$ compared to left most bar. Shear stress = 1.8 dynes/cm^2.)

CHAPTER 5

CONCLUSIONS AND RECOMMENDATIONS FOR FUTURE STUDIES

This doctoral study had two specific aims: (1). To explore the role of one biophysical parameter, namely particle size, on receptor-ligand mediated adhesion under flow, and (2). To gain insight into the roles played by two key molecules in the recruitment of neutrophils and homing of hematopoietic progenitor cells under physiological flow. These two issues were investigated in great detail in studies outlined in Chapters 2, 3 and 4.

The first study described in Chapter 2, explored the dependence of receptor-ligand mediated adhesion on particle diameter. An *in vitro* study on the adhesion of 5μm, 10μm, 15μm and 20μm diameter 19.ek.Fc (PSGL-1) coated microspheres to P-selectin substrates under flow revealed that: (a) at relatively high shear, the attachment rate of 19.ek.Fc coated microspheres decreased with increasing microsphere diameter while the rate of attachment remained unaffected by the microsphere diameter at a lower shear, (b) the shear stress required to set in motion a firmly adherent 19.ek.Fc microsphere decreased with increasing microsphere diameter and (c) the rolling velocity of the 19.ek.Fc microspheres was directly proportional to microsphere diameter for the entire range of shear stresses tested. These results strongly indicate a functional dependence for attachment, rolling and firm adhesion on particle diameter and provide experimental proof for theoretical models that indicate a role for cell diameter in adhesion.

Through this study, we have made a first step towards elucidating the role of particle size in adhesion under flow. As noted previously (1), several future investigations are quite evident from this study. First, as we noted in the results section, the *in vitro* model we used in this study does not capture all of the complexities of the *in vivo* environment. *In vivo*, adhesion occurs in a tube of finite size and the ratio of the tube diameter to the particle diameter can influence the drag force on a particle near the tube wall (2-4). It might be possible to investigate this issue with the *in vitro* model described here. For example, one could systematically alter the height of the flow chamber and the microsphere diameter to determine if the ratio of the gap size to particle diameter affects the resulting adhesion. A second study of interest would be to apply pause time analysis (5, 6) to the system described in the present study. Our data suggests that the kinetic rate of dissociation increases with increasing particle diameter (Figures 2.3, 2.4 and 2.5). One could test this hypothesis using pause time analysis. In addition, by varying the particle size in pause time experiments, one could gain insight into the tensile properties of ligand – receptor bonds. Such studies would be an excellent complement to existing data that has probed the tensile properties of ligand – receptor bonds by varying the shear stress. Finally, while we have given a plausible explanation of the attachment data (Figure 2.2), other explanations could also be put forward. Notably, the scenario we outlined in the first part of the discussion, did not directly address the issue of bond strength. The interplay between bond strength, attachment and particle size is likely quite complex given the fact that Evan's group (7, 8) has

demonstrated that increasing the rate of loading of a receptor-ligand bond may increase the strength of the bond. Obtaining a complete understanding of the role of particle size in attachment will clearly require several additional studies.

The second study described in Chapter 3, explored the adhesion of leukocyte-sized microspheres coated with the β_2 integrin Mac-1 (purified from leukocyte lysates) to 4 hr. IL-1 activated human umbilical vein endothelial cells (HUVEC) *in vitro* fluid dynamic environment. Our studies revealed that native Mac-1 coated microspheres adhere to 4 hr. IL-1 activated HUVEC via two distinct molecular mechanisms: an E-selectin dependent mechanism that mediates attachment and rolling of Mac-1 microspheres (primary attachment) and a mechanism dependent on the CBRM1/29 epitope that mediates, predominantly, firm adhesion. The results of our study provide insights into the physiological role of Mac-1 in mediating leukocyte adhesion to the endothelium under flow. There is a distinct possibility that Mac-1 on these cells interacts with the endothelium via two distinct mechanisms: one interaction occurring during leukocyte tethering and rolling and the other occurring during their firm adhesion to the endothelium.

Although we have clearly demonstrated the presence of two distinct mechanisms via which Mac-1 adheres to HUVEC, our interpretation of these observations are clearly speculative. This warrants future studies to account for differences in the two mechanisms. Indeed, we believe that the differences in the adhesive states mediated by

either mechanism can perhaps be attributed to distinct differences in the kinetic and tensile properties of the bonds mediating these mechanisms. One way to resolve this issue, would be to employ a modified version of a technique described by Alon et al. (5) to estimate kinetic rates of dissociation for either mechanism and the effect of the fluid disruptive force and torque on these kinetic rates. This technique has previously been employed to estimate kinetic rates of dissociation and bond responses to fluid shear.

Our studies have also indicated a role for a previously undefined endothelial ligand in mediating firm adhesion of Mac-1 coated microspheres via interactions with the CBRM1/29 epitope. Identification of this ligand would, in itself, constitute a whole separate study involving techniques in engineering, biochemistry and molecular biology. If and when this ligand is identified, it would be insightful to determine its relative abundance on HUVEC in comparison to levels of E-selectin expression. This answer, coupled with results of the kinetic studies would help account for the difference in properties of E-selectin and non-E-selectin mediated adhesion of the Mac-1 microspheres.

The third study described in Chapter 4, focused on highlighting a role for HL60 cell P-selectin glycoprotein ligand-1 (PSGL-1) to serve as a physiological ligand for E-selectin. We undertook *in vitro* fluid dynamic assays to specifically probe the adhesion of a HPC cell line (HL60) to E-selectin expressing HUVEC under physiological shear conditions. Our observations with HL60 cells, coupled with our observations with

leukocyte-sized microspheres coated with purified native PSGL-1 isolated from these cells, provide evidence for the role of PSGL-1 in serving as a pre-dominant ligand for E-selectin on HL60 cells. Our data also suggest that the adhesion of HL60 cells and PSGL-1 microspheres seems to occur through multiple sites on PSGL-1, consistent with previous reports (9, 10). In addition, these studies highlight a role for other possible E-selectin counter-receptor(s) on HL60 cells that, in the absence of PSGL-1, assume a more predominant role in mediating adhesion to E-selectin. Based on these observations, an interesting future study would be the identification of these additional E-selectin counter-receptor(s) and their role(s) in mediating HL60 cell adhesion to the endothelium. A good place to start would be to highlight the contributions of HL60 cell expressed SLe^x and HECA-452 reactive structures in mediating adhesion of these cells to HUVEC.

An interesting parallel among the studies undertaken in this dissertation is the ability of both PSGL-1 and the integrin CD18 (Mac-1) to mediate attachment and rolling of ligand coated microspheres through interactions with selectins (E- and P-selectin) under flow. Our results lay the foundation for a future study exploring the biophysical properties of the Mac-1-E-selectin, PSGL-1- E-selectin and/or PSGL-1-P-selectin bonds in mediating attachment and rolling of leukocyte-sized microspheres under flow. Leukocyte-sized microspheres expressing equal surface densities of PSGL-1 and Mac-1 could then be employed in pause time analysis studies over E-selectin to quantify the kinetic and tensile attributes of these respective bonds. These future studies, in their entirety, would address what are arguably, the two most important issues in

understanding cell adhesion under flow: 1. Identifying key molecular players involved in various physiological and pathological phenomena and, 2. Highlighting the biochemical and biophysical properties underlying the adhesive interactions mediated by these molecules.

References

1. Shinde Patil, V.R., C.J. Campbell, Y.H. Yun, S.M. Slack, and D.J. Goetz. 2001. Particle diameter influences adhesion under flow. *Biophys J*. 80:1733-1743.

2. Schmid-Schoenbein, G.W., Y.C. Fung, and B.W. Zweifach. 1975. Vascular endothelium-leukocyte interaction; sticking shear force in venules. *Circ Res*. 36:173-84.

3. House, S.D., and H.H. Lipowsky. 1988. In vivo determination of the force of leukocyte-endothelium adhesion in the mesenteric microvasculature of the cat. *Circ Res*. 63:658-68.

4. Chapman, G.B., and G.R. Cokelet. 1998. Flow resistance and drag forces due to multiple adherent leukocytes in postcapillary vessels. *Biophys J*. 74:3292-301.

5. Alon, R., D.A. Hammer, and T.A. Springer. 1995. Lifetime of the P-selectin-carbohydrate bond and its response to tensile force in hydrodynamic flow. *Nature*. 374:539-542.

6. Smith, M.J., E.L. Berg, and M.B. Lawrence. 1999. A direct comparison of selectin-mediated transient, adhesive events using high temporal resolution. *Biophys J*. 77:3371-83.

7. Evans, E. 1998. Energy landscapes of biomolecular adhesion and receptor anchoring at interfaces explored with dynamic force spectroscopy. *Faraday Discuss*. 111:1-16.

8. Evans, E., and K. Ritchie. 1997. Dynamic strength of molecular adhesion bonds. *Biophys J*. 72:1541-55.

9. Patel, K.D., K.L. Moore, M.U. Nollert, and R.P. McEver. 1995. Neutrophils use both shared and distinct mechanisms to adhere to selectins under static and flow conditions. *J. Clin. Invest*. 96:1887-1896.

10. Goetz, D.J., D.M. Greif, R.T. Camphausen, S. Howes, K.M. Comess, K.R. Snapp, G.S. Kansas, and F.W. Luscinskas. 1997. Isolated P-selectin glycoprotein-1 dynamic adhesion to P- and E-selectin. *J. Cell Biol*. 137:509-519.

A-1 Estimation of critical shear stress values for microspheres with different diameters based on a model by Cozens-Roberts et al. (1)

In discussing results of the firm adhesion data described in Chapter 2 (Figures 2.3 and 2.4), it is insightful to consider the analysis of Cozens-Roberts et al. (1) with respect to the role of particle diameter in adhesion. While experimental critical shear stress values (black squares) in Figure 2.4 were calculated by estimating the shear stress required to detach 50% of a population of adherent 5μm, 10μm, 15μm and 20μm diameter microspheres, the theoretical curve of critical shear stress values was calculated based on a model proposed by Cozens-Roberts et al. (1). Calculation of theoretical S_c values is outlined below.

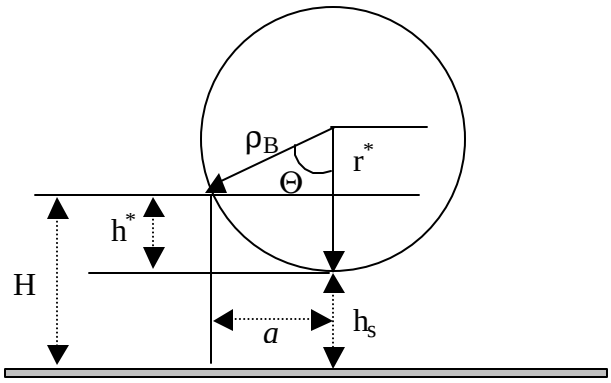

Figure A-1.1 Schematic of a solid sphere in contact with the surface

The above schematic (not drawn to scale) represents a solid sphere in contact with a substrate. ρ_B and a are the radii of the microsphere and the contact area respectively.

H represents the maximum separation distance for receptor-ligand binding, approximated from the relative dimensions of each molecule forming the bond. h_s represents the minimum separation distance between the microsphere and the surface. Cozens-Roberts et al. define the relationship between h^*, H and *a* as follows:

$$h^* = H - h_s \qquad \text{……(Eq. A-1)}$$

$$r^* = \rho_B - h^* \qquad \text{……(Eq. A-2)}$$

From simple geometry, Θ turns out to be,

$$\Theta = \cos^{-1}(r^*/\rho_B) \qquad \text{……(Eq. A-3)}$$

and the radius of the contact area:

$$a = \rho_B \sin \Theta \qquad \text{……(Eq. A-4)}$$

Based on their estimates, H and h_s were assigned values of 40 nm and 10 nm respectively. This allows calculation of all parameters listed above.

Particle diameter (μm)	h^* (nm)	ρ_B (nm)	r^* (nm)	Θ	*a* (nm)
5	30	2500	2470	0.155	2087.31
10	30	5000	4970	0.109	4191.07
15	30	7500	7470	0.0894	6294.77
20	30	10000	9970	0.0774	8398.46

Table A.1-1. Estimation of critical model parameters

Expression for the critical shear stress S_c defined by Cozens-Roberts et al. (1) is:

$$S_c = (K^o/ 33e)(k_bT/\gamma)(N_R N_L)(a/\rho_B)^3 \quad \text{.....(Eq. A-5)}$$

where,

K^o is the receptor-ligand affinity constant (cm^2)

k_b is the Boltzman constant (J/molecule-^oK)

T is the temperature (^oK)

γ is the range of bond interaction (~$5x10^{-8}$ cm for an antigen-antibody bond)

N_R and N_L represent the receptor (P-selectin) and ligand (19.ek.Fc) densities (cm^{-2}) respectively.

Since these last six parameters are constant for all four different sized particles, we treat them as an overall constant $\boldsymbol{K}$

$$\boldsymbol{K} = (K^o/ 33e)(k_bT/\gamma)(N_R N_L) \quad \text{.....(Eq. A-6)}$$

Equation A-5 may then be rewritten as,

$S_c = \boldsymbol{K}(a/\rho_B)^3$ ……(Eq. A-7)

or

$S_c = \boldsymbol{K}\sin\Theta^3$ ……(Eq. A-8)

The estimation of parameter $\boldsymbol{K}$ is complicated by the fact that the receptor density (N_R) in our system is unknown. We therefore indirectly approximated this value of $\boldsymbol{K}$ by equating the theoretical and experimental critical shear stress values for the 5 μm diameter particle. Note that, this simplification represents an attempt to circumvent the complexities associated with N_R and N_L estimation. It also allows us to approximate the parameter $\boldsymbol{K}$, which can then be employed in future calculations of theoretical critical shear stress values for other microsphere diameters.

In other words, assuming

$S_{c\ (theoretical)} = S_{c\ (experimental)} = 5$ dynes/cm^2

Substituting values for a and ρ_B in equation A-7, yields $\boldsymbol{K}$=1356.9

This value of $\boldsymbol{K}$ when employed with other microsphere diameters in equation A-7 yields theoretical S_c values for a wide range of particle diameters and generates the curve shown in Figure 2.4. The numerical values on the next page are tabulated for reference.

Table A-1.2: **Tabulation of theoretical and experimental critical shear stress values** ($S_{c\ (experimental)}$ and $S_{c\ (theoretical)}$). $S_{c\ (experimental)}$ were estimated from adhesion studies with 5μm, 10μm, 15μm and 20μm diameter ligand coated microspheres, while $S_{c\ (theoretical)}$ were calculated from the model described in the preceding pages

Particle diameter (μm)	$\rho_{B\ (\mu m)}$	$S_{c\ (experimental)}$ (dynes/cm^2)	$S_{c\ (theoretical)}$ (dynes/cm^2)
5.00	2.50	5.00	5.00
5.50	2.75		4.34
6.00	3.00		3.81
6.50	3.25		3.38
7.00	3.50		3.03
7.50	3.75		2.73
8.00	4.00		2.48
8.50	4.25		2.26
9.00	4.50		2.08
9.50	4.75		1.92
10.00	5.00	2.00	1.78
10.50	5.25		1.65
11.00	5.50		1.54
11.50	5.75		1.44
12.00	6.00		1.35
12.50	6.25		1.27
13.00	6.50		1.20
13.50	6.75		1.13
14.00	7.00		1.07
14.50	7.25		1.02
15.00	7.50	1.20	0.97
15.50	7.75		0.92
16.00	8.00		0.88
16.50	8.25		0.84
17.00	8.50		0.80
17.50	8.75		0.77
18.00	9.00		0.74
18.50	9.25		0.71
19.00	9.50		0.68
19.50	9.75		0.65
20.00	10.00	0.90	0.63

References

1. Cozens-Roberts, C., J.A. Quinn, and D.A. Lauffenburger. 1990. Receptor-mediated adhesion phenomena: model studies with the radial flow detachment assay. Biophys. J. 58:107-125.

A-2. Flow Setup

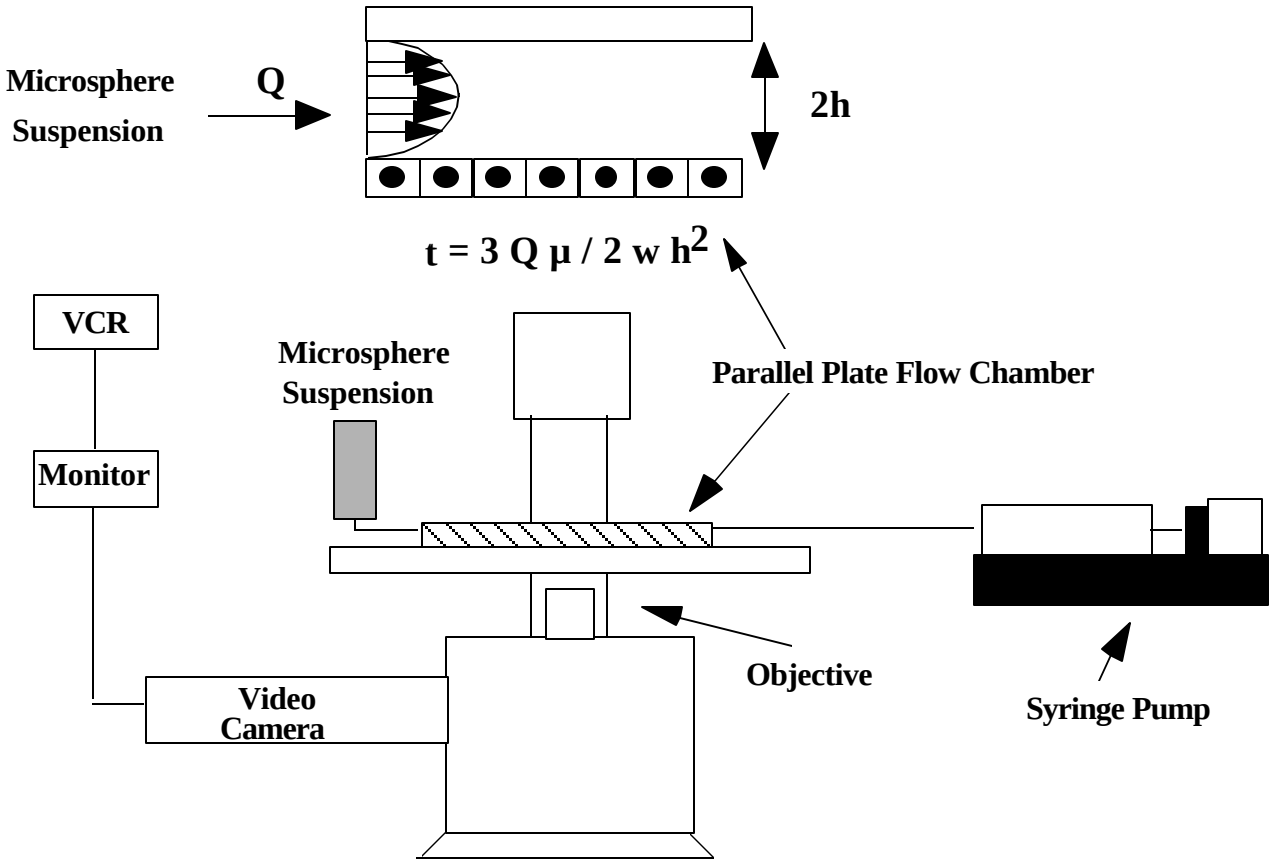

Figure A-2.1 Schematic of a parallel plate flow chamber and flow setup